



Proteomic profiling of exudates from diabetic foot ulcers and acute wounds using mass spectrometry

Christoph Krisp

Bachelor of Chemistry, Ruhr University Bochum

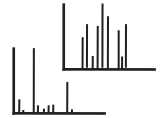
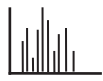
Master of Chemistry, Ruhr University Bochum

A thesis presented for the degree of
Doctor of Philosophy

Ruhr University Bochum
Faculty of Chemistry and Biochemistry
Department of Analytical Chemistry

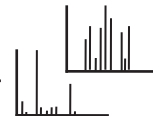
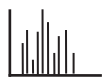
Macquarie University
Faculty of Science
Department of Chemistry and
Biomolecular Sciences

November 2013



Declaration

The work presented in this thesis titled “Proteomic profiling of exudates from diabetic foot ulcers and acute wounds using mass spectrometry” has not been submitted for a higher degree to any other university or institution other than Macquarie University, Sydney, Australia and Ruhr University Bochum, Bochum, Germany under the Cotutelle Agreement.



Acknowledgement

First of all I would like to thank my two magnificent supervisors Mark Molloy and Dirk Wolters.

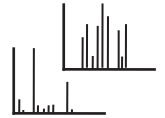
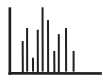
Dirk, you gave me the opportunity to develop into an independent and self-confident scientist, able to assume responsibility for myself and critically reflect upon the work I am doing. You gave me the space I needed to accomplish my work and challenge myself, but were around when I needed your help. I acknowledge your advisedly allocation of additional projects, which taught me to think outside of the box and be open-minded for new ideas.

Mark, I would like to thank you for the fantastic time I had working with your group. You are calm, thoughtful, focused and well organized. The way you supervised me let me transcend my own boundaries which made me succeed in ways I had never dreamed of. You have a special way to motivate people with perfect timing. Your motivation always reached me when I needed it most. You were the person who proposed the Cotutelle program to me and who believed in me to get chosen for this program. For that I will always be deeply grateful. The time with your group increased my passion for science and made me to the scientist I am today. Thank you.

Further, I would like to thank Matthew McKay for the knowledge and expertise he shared with me and the support he gave me during all the challenges I came across. Matthew you helped me keep my patience with the instruments and taught me fundamental skills. I appreciate the thrust you put in me.

This continues with my gratitude to past and present students and staffs at Macquarie University, APAF, and Ruhr University Bochum, especially my colleagues and friends at the Molloy work group, the biomarker discovery Laboratory, and the Wolters work group. You made my PhD studies a memorable time in my life.

I want to express my thanks to Ruhr University Bochum and Macquarie University to allow me to conduct my studies under a joint project acknowledged by both universities. The Cotutelle program is a wonderful program that not only gave me the opportunity to expand my expertise in my research field, but in my whole life. Only because of this program I was able to get to know many wonderful people who became an important part of my life. Further, I would like to thank Macquarie University for granting me a



Macquarie University Research Excellence Scholarships (MQRES) to support me while I worked at Macquarie University.

I thank the laboratory for Molecular Oncology and Wound Repair located in the department of Plastic Surgery at the Ruhr University Hospital “Bergmansheil” especially Lars Steinsträßer and Frank Jacobsen for liberally providing the wound fluids.

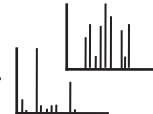
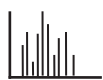
Further, I want to acknowledge BBraun Melsungen AG in particular Andreas Gmerek for supporting the haemodialysis work and Luciano Pedrini at the Nephrology and Dialysis Units at the Bolognini Hospital in Italy who provided the haemodialysis samples.

Finally my thanks go to my family and friends around the world who have always been supportive und sympathetic particularly in busy times. You helped me maintain my work-life balance and made every moment enjoyable.

I am eminently grateful to have such wonderful and loving parents who were always there for me and made me to the person I am today. I love you.

Therefore, I would like to address some words in German to you

Liebe Eltern, ich danke Euch für Eure immerwährende Unterstützung die ihr mir über all die Jahre gegeben habt und dafür, dass ihr immer für mich da gewesen seid und auch weiterhin für mich da seid werdet. Ohne Eure Motivation hätte ich es niemals soweit geschafft. Ihr habt mir gezeigt, was im Leben wichtig ist und dass man für seine Überzeugungen eintreten soll. Ihr habt mich zu dem Menschen gemacht, der ich heute bin. Mit Eurer lebenswerten und fürsorglichen Art habt ihr mir ein Zuhause geboten, das sich jeder nur wünschen kann. Für all dies und noch viel, viel mehr möchte ich mich bei Euch bedanken. Ich habe Euch lieb.



Parts of this work have been published or are submitted for publication in scientific journals (Appendix 2).

[1] Christoph Krisp; Caroline Kubutat; Andreas Kyas; Lars Steinsträßer; Frank Jacobsen; Dirk A. Wolters, Boric acid gel enrichment of glycosylated proteins in human wound fluids. *Journal of Proteomics* 2010, 74, (4), 502-509.

[2] Christoph Krisp; Matthew J McKay; Dirk A. Wolters; Mark P. Molloy, Multidimensional protein identification technology-selected reaction monitoring improving detection and quantification for protein biomarker studies. *Analytical Chemistry* 2012, 84, (3), 1592-1600.

This manuscript was selected by the faculty of thousand as one of the top 2% of published articles in biology and medicine

Further this manuscript was awarded the Macquarie University, Biomolecular Frontiers Research Postgraduate Prize for the best internationally peer-reviewed paper by a postgraduate student as first author accepted for publication

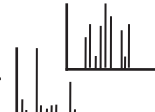
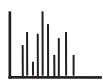
[3] Christoph Krisp; Frank Jacobsen; Lars Steinsträßer; Matthew J McKay; Mark P Molloy; and Dirk A. Wolters, Proteome analysis reveals anti-angiogenic environments in chronic wounds of diabetes mellitus type 2 patients, *Proteomics* 2013, 13, (17), 2670-2681.

Publications achieved during the period of the doctoral studies which are not included in this thesis.

[4] Lars Steinsträßer; Frank Jacobsen; Tobias Hirsch; Marco Kesting; Caroline Chojnacki; Christoph Krisp; Dirk A. Wolters, Immunodepletion of high-abundant proteins from acute and chronic wound fluids to elucidate low-abundant regulators in wound healing. *BMC Research Notes* 2010, 3, (1), 335.

[5] Christoph Krisp; Sarah A. Randall; Matthew J. McKay; Mark P. Molloy, Towards clinical applications of selected reaction monitoring for plasma protein biomarker studies. *Proteomics – Clinical Applications* 2011, 6, (1-2), 42-59. (Appendix A4)

[6] Peter Lüdi; Ulrike B. Hendgen-Cotta; Julia Sobierajski; Matthias Totzeck; Marcel Reeh; Manfred Dewor; Hongqi Lue; Christoph Krisp; Dirk A. Wolters; Malte Kelm; Jürgen Bernhagen, Tienush Rassaf, Cardioprotection Through S-Nitros(yl)ation of Macrophage Migration Inhibitory Factor. *Circulation* 2012, 125, (15), 1880-1889.



[7] Miriam M. Cortese-Krott; Ana Rodriguez-Mateos; Roberto Sansone; Gunter G. C. Kuhnle; Sivatharsini Thasian-Sivarajah; Thomas Krenz; Patrik Horn; Christoph Krisp; Dirk A. Wolters; Christian Heiß; Klaus-Dietrich Kröncke; Neil Hogg; Martin Feelisch; Malte Kelm, Human red blood cells at work: identification and visualization of erythrocytic eNOS activity in health and disease, *Blood* 2012, 120, (20), 4229-4237.

[8] Jessica Jacob; Christina Marx; Vera Kock; Olga Reifschneider; Benjamin Fränzel; Christoph Krisp; Dirk A. Wolters; Ulrich Kück, Identification of a Chloroplast Ribonucleoprotein Complex Containing Trans-splicing Factors, Intron RNA and Novel Components, *Molecular and Cellular Proteomics* accepted for publication

Additionally, parts of this were presented as posters at international scientific conferences

[1] Christoph Krisp; Dirk A. Wolters. Immunodepletion of human wound fluids - always the best way to go? 9th annual meeting of the Human Protein Organization (HUPO), 2010, Sydney, Australia.

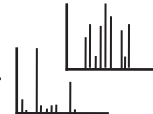
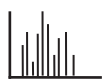
[2] Christoph Krisp; Matthew J. McKay; Dirk A. Woltets; Mark P. Molloy, From SHOTGUN to SNIPER – Proteomic analysis of human wound fluids. 16th Proteomics symposium of the Australasian Proteomics Society (APS), 2011, Lorne, Australia.

[3] Christoph Krisp; Matthew J. McKay; Dirk A. Woltets; Mark P. Molloy, From SHOTGUN to SNIPER – Pipeline for discovery and validation of human wound fluid biomarkers. 59th annual meeting of the American Society of Mass Spectrometry (ASMS), 2011 Denver, Colorado, USA

[4] Christoph Krisp; Andreas Gmerek; Jürgen Wagner; Dirk A. Wolters, The Way to In-Vivo cut-off Profiles: Protein Removal Efficiency of two different haemodialysis membranes using MudPIT-Analysis. 48th annual meeting of the European Renal Association - European Dialysis and Transplant Association (ERA-EDTA), 2011, Prague, Czech Republic.

[5] Christoph Krisp; Matthew J. McKay; Dirk A. Woltets; Mark P. Molloy, MudPIT-SRM – a highly multiplexed strategy for low abundant protein biomarker identification. 10th annual meeting of HUPO, 2011, Geneva, Switzerland.

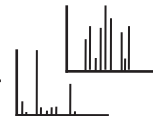
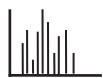
[6] Christoph Krisp; Matthew J. McKay; Mark P. Molloy; Dirk A. Woltets, Proteome Analysis of Human Wound Fluids - MudPIT-FTMS and MudPIT-SRM as strategies of choice for reliable Biomarker identification and validation. 60th annual meeting of ASMS, 2012, Vancouver, Canada.



[7] Christoph Krisp; Andreas Gmerek; Jürgen Wagner; Dirk A. Wolters, MudPIT analysis as a proteomic tool for novel potential uremic toxin identification in haemodialysis filtrates 49th annual meeting of ERA-EDTA, 2012, Paris, France.

The biomarker discovery study of human wound fluids of patients with chronic foot ulcers (Chapter 5), the study of proteins in spent dialysates to estimate the elimination efficiency of dialysis membranes applied to chronic haemodialysis patients (Chapter 8), and the development of a glycoprotein enrichment strategy using a boric acid derivate (Chapter 4) were conducted at the bio molecular mass spectrometry work group of Dr. Dirk Wolters located in the Faculty of Chemistry and Biochemistry, Department of Analytical Chemistry at the Ruhr University Bochum, Bochum, Germany.

The SRM validation of identified regulation differences of proteins in human wound fluids (Chapter 6), and the development of the MudPIT-SRM strategy for improved bio marker detection (Chapter 7) were carried out at the work group of Associate Professor Mark Molloy located in the Faculty of Science, Department of Chemistry and Biomolecular Sciences at Macquarie University, Sydney, Australia.



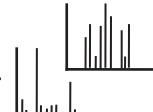
Awards

Macquarie University Research Scholarship (MQRES)

Macquarie University Postgraduate Research Fund (PGRF), June 2011

Macquarie University Faculty of Science Biomolecular Frontiers Research Postgraduate Prize

Awarded for the best internationally peer-reviewed paper by a postgraduate student as first author accepted for publication



Abstract

Poor healing, chronic wounds at the lower extremities of diabetes mellitus patients are a debilitating condition. Numerous studies have revealed dramatic differences in several repair regulation steps with these chronic wounds, but additional information is needed to understand the role of specific proteins in these processes.

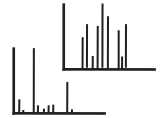
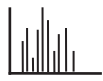
In this study, mass spectrometry (MS) was employed to investigate proteins in exudates from type 2 diabetes mellitus foot ulcers and they were compared to proteins found in acute wound exudates of burn victims that were otherwise healthy.

Initial experiments were conducted to investigate strategies to reduce sample complexity using high abundant protein depletion or post-translational modification based enrichments. High abundant protein depletion was proven to be not applicable to the exudates, as MS investigation revealed substantial co-elimination of important proteins involved in healing processes. The enrichment of glycosylated proteins was demonstrated but found to be unsuitable for large-scale comparative studies as needed for wound exudates. Therefore, liquid-chromatography-tandem mass spectrometry (LC-MS/MS) was performed on undepleted and unenriched wound exudates.

Multi-dimensional protein identification technology-MS/MS (MudPIT-MS/MS) using high resolution MS of 10 chronic and 6 acute wounds revealed expression level differences of proteins in inflammation signalling, predominately S100 proteins, impairment of pro- and anti-inflammatory signalling, elevated matrix metalloproteinase (MMP) activity, anti-angiogenic environment, and elevated cell death with apoptotic and necrotic motifs. The expression level differences of selected proteins were confirmed by selected reaction monitoring (SRM) conducted on 9 chronic and 9 acute wounds. Further, S100A8 and S100A9 elevation was confirmed by western blot. The enzyme activity of MMP2 and MMP9 were investigated with gelatin zymography, confirming higher MMP2 expression in chronic wounds.

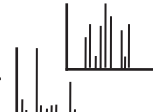
A novel MudPIT-SRM workflow was developed to enable the SRM validation study. The combination of high resolving liquid chromatography with highly sensitive SRM demonstrated significant detection improvement (90%) in peptide quantitation on human plasma proteins and human wound fluids.

Finally, the membrane dependent protein elimination efficiencies of two high-flux haemodialysis filters were investigated in a MudPIT-MS/MS study closely related to diabetes mellitus induces angiopathy in the kidney, leading the nephropathy. Protein profiling revealed crucial insights into the middle molecular mass range of human plasma



and demonstrated better protein elimination of Xevonta Hi23 membrane if compared to Polyflux 210H. Ultimately this method enables the patient-specific assessment of treatment response, which especially in diabetic nephropathy patients could be used to identify the degree of oxidative stress, a known initiator of angiopathy

In summary this thesis has revealed new insight into specific proteins regulating chronic wounds in diabetes mellitus patients, developed a novel MS workflow by combining MudPIT with SRM and investigated the optimum haemodialysis filter to eliminate uremic toxins in chronic haemodialysis patients.



Common abbreviations

AA	acryl amide
ACN	acetonitril
BAGAC	boric acid gel affinity chromatography
BisAA	bis-acryl amide
cps	counts per second
DTT	dithiothreitol
ESI	electro spray ionisation
FA	formic acid
HPLC	high pressure liquid chromatography
IAA	iodoacetamide
LC	liquid chromatography
LLOD	lower limit of detection
LLOQ	lower limit of quantitation
LTQ	linear ion trap
MS	mass spectrometry
MS/MS	tandem mass spectrometry
MudPIT	multidimensional protein identification technology
m/z	mass to charge ratio
NHW	normal healing wound
NSC	normalised spectrum count
PAGE	polyacrylamide gel electrophoresis
PHW:	poor healing wound
PSM	positive spectrum match
P/X	Polyflux 210H/Xevonta Hi23
RP	reverse phase
SCX:	strong cation exchange
SDS	sodium dodecyl sulfate
SRM	selected reaction monitoring
T2DM	type 2 diabetes mellitus
TEMED	N,N,N,N Tetramethylethylenediamine
UPLC	ultra performance liquid chromatography
XIC	extracted ion chromatogram
X/P	Xevonta Hi23/Polyflux 210H

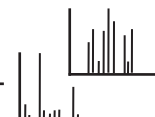
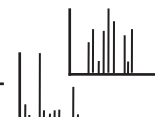
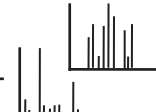
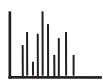


Table of Contents

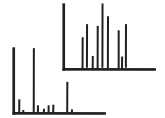
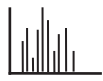
1. Introduction	1
1.1. The skin	1
1.2. Injury to the skin.....	3
1.2.1. Wound repair	3
1.3. Complications in wound repair	6
1.3.1. Diabetes mellitus derived wound repair complications.....	7
1.4. Proteomic based investigation strategies.....	8
1.4.1. Multi-dimensional protein identification technology.....	11
1.4.2. Quantification of LC-MS/MS results	12
1.4.3. Targeted mass spectrometry	14
1.5. Proteomic applications in wound healing processes	14
1.6. Aims and scope of this thesis	16
2. Motivation	17
3. Material and methods	18
3.1. Chemicals and consumables.....	18
3.2. Instruments and processing software.....	20
3.3. Sample cohorts	21
3.3.1. Human wound fluids	21
3.3.2. Haemodialysis samples	22
3.3.3. Ethics	23
3.4. Protein enrichment.....	23
3.4.1. Immunodepletion of highly abundant proteins.....	23
3.4.2. BAGAC affinity chromatography	24
3.5. Sample specific properties and protein visualization	24
3.5.1. Protein concentration.....	24
3.5.2. SDS-PAGE	24
3.5.3. Zymography	25



3.5.4. Western blot.....	26
3.6. Sample preparation.....	27
3.6.1. Trypsin digestion.....	27
3.6.2. In-Gel trypsin digestion.....	27
3.6.3. PNGase F digestion.....	27
3.7. Mass spectrometric characterisation.....	28
3.7.1. Column preparation.....	28
3.7.2. Liquid chromatography.....	28
3.7.3. Tandem MS on LTQ Orbitrap velos.....	29
3.7.4. SRM on 4000 QTrap.....	29
3.7.5. SRM on 5500 QTrap.....	30
3.7.6. Tandem MS on LTQ XL.....	30
3.8. Data Analysis and Statistics.....	30
3.8.1. Database searches.....	30
3.8.2. SRM transition integration.....	31
3.8.3. GO-Term analysis and protein localization.....	31
3.8.4. Statistics.....	31
4. Enrichment of lower abundant proteins.....	32
4.1. Enrichment of glycosylated proteins.....	32
4.1.1. Boric acid gel affinity chromatography of glycoproteins.....	35
4.1.2. Boric acid gel affinity chromatography of N-glycosylated peptides.....	40
4.2. Immunodepletion of high abundant proteins.....	42
4.3. Concluding aspects of protein enrichment.....	44
5. Molecular healing processes.....	45
5.1. General assessment of wound fluids.....	47
5.2. Coagulation.....	49
5.3. Inflammation signalling.....	51
5.4. Vascularisation.....	54



5.4.1. MMP mediated angiogenesis	54
5.4.2. Angiogenesis regulation	61
5.5. Cell death promoting environment	66
6. SRM Investigation of proteins found at differing expression level	68
6.1. SRM validation of differentially expressed proteins in human wound fluids...	68
6.2. Chronic inflammation.....	71
6.3. Angiogenic regulation	73
6.3.1. SRM investigation of MMPs.....	73
6.3.2. SRM-MS of selected proteins involved in angiogenic processes and cell death	75
7. Targeted mass spectrometry with advanced multiplexing potential	77
7.1. Automated MudPIT-SRM.....	78
7.1.1. MudPIT-SRM of high abundant plasma proteins	80
7.1.2. MudPIT-SRM of target proteins in human wound fluids	87
7.2. Concluding aspects.....	89
8. Membrane specific protein elimination in haemodialysis patients	90
8.1. Protein clearance of high flux HD membranes	93
9. Conclusion.....	99
10. References	104
11. Appendix 1: Supporting Tables.....	123
12. Appendix 2: Publications	132
13. Appendix 3: Ethics approval	179
14. Appendix 4: Curriculum Vitae	181



1. Introduction

1.1. The skin

Skin describes the soft outer layer covering the entire body of all vertebrates and is the biggest human organ. The skin is divided into three major regions, the epidermis, the basement membrane, and the dermis (figure 1.1). Each region consists of different cell types and tissue enabling different purposes and functions. First of all it is a two-way barrier protecting underlying organs. Therefore, it has a central role in pathogen defence and water supply to the body. The semi-impermeable nature of the skin serves as a barrier to external water, prevents nutrition loss and controls water loss derived by evaporation. Further, the skin serves as a reservoir for water and lipids, regulates the body temperature and is involved in the respiratory functions allowing oxygen, nitrogen, and carbon dioxide diffusion through the skin. Additionally, imbedded nerve ends in the skin allow sensing of heat, cold, pressure and most importantly, the injury to tissue [1, 2].

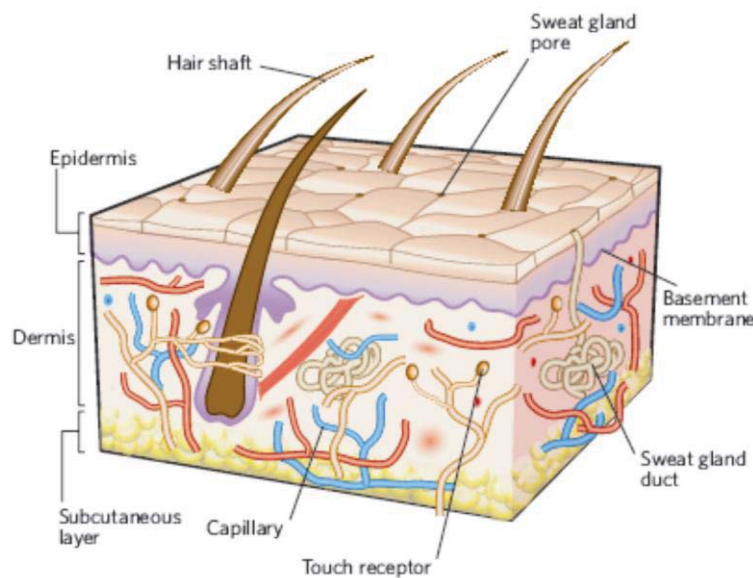
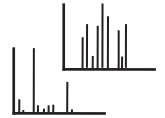
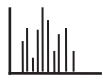


Figure 1.1: organisation of the human skin [3]

The epidermis is the outer most layer of skin. This avascular layer mainly contains keratinocytes (>95%) but also melanocytes, Merkel cells, Langerhans cells and other immune system cells organised in 4 layers (5 layers in palms and soles) with different stages of proliferating or differentiating cells. In ascending order the epidermis is composed of the basal layer, spinous layer, granular layer, translucent layer (palm/sole), and the cornified layer (figure 1.2). The basal layer (stratum basale) is dominated by proliferating and non-proliferating keratinocytes attached to the basement membrane. Keratinocyte differentiation signalling stimulates keratinocyte movement through the



different layers towards the cornified layer (stratum corneum). Keratinocyte differentiation towards corneocytes, terminal differentiated keratinocytes, involves degradation of intracellular material. The production of the lamellar body, an impermeable membrane containing lipids, enzymes, and structural proteins, starts when keratinocytes enter the spinous layer (stratum spinosum) which arranges the needed conditions for nucleus and cytoplasm degradation in the granular layer (stratum granulosum). This leads to the final differentiation of keratinocytes to corneocytes, which are characterised by nucleus and cytoplasm free cells incapable of further differentiation. Therefore, cornification is an alternative pathway to apoptosis. This cornified layer is enveloped by corneodesmosomes, keratins, and lipids which is the main reason for the barrier function of the skin [1, 2].

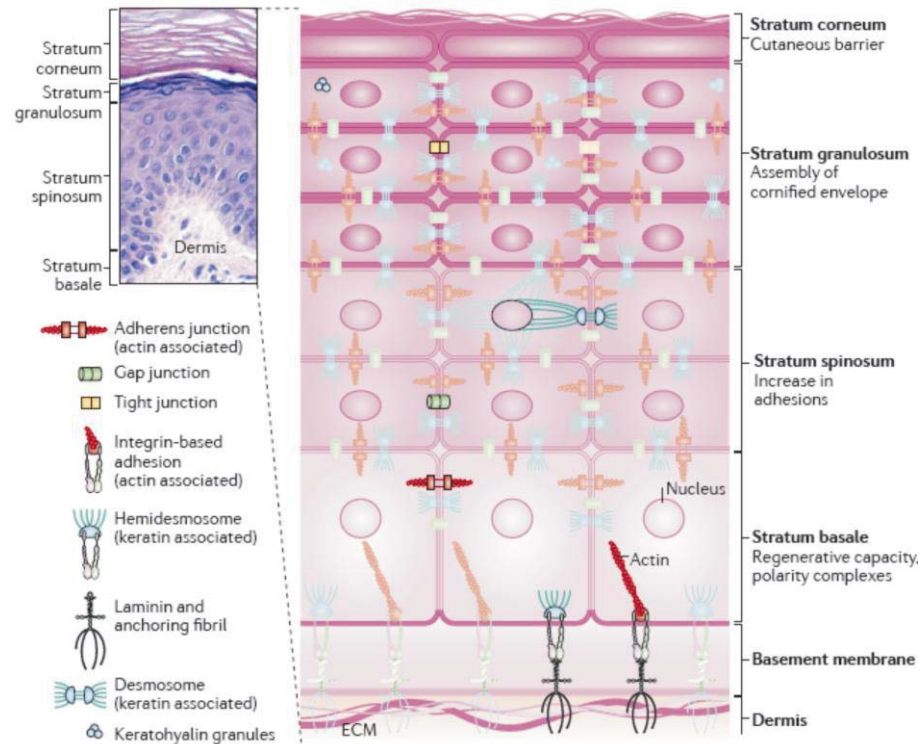
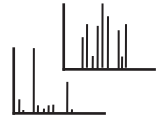
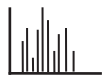


Figure 1.2: layer of diversely differentiated keratinocytes in the epidermis [4]

The epidermis is attached to the basement membrane that connects but also separates the epidermis from the underlying dermis. The basement membrane is surrounding epithelia along organs including the skin and blood vessels and borders them from other tissue types. However, the basement membrane is not only bordering or anchoring the epithelium to the underlying tissue, it comprises important stimulating properties. The basement membrane predominately composes of structural proteins such as collagens, laminins, fibrillin, integrins, perlecan, and nidogens. Several growth factors and cytokines are imbedded in this network of structural proteins which are released after damage to the



basement membrane. Therefore, the basement membrane plays an important role in angiogenesis stimulation and other processes essential in repair mechanisms [5].

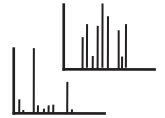
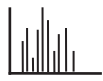
The inner layer of the skin is the dermis, a connective tissue composed of fibroblasts, macrophages, adipocytes and the extracellular components collagen and elastin. Further, hair follicles, nerves, glands (sweat, sebaceous), lymphatic and blood vessels are located in the dermis (figure 1.1). As the epidermis is a capillary free region, the blood and lymphatic vessels in the dermis supply both the dermis and the epidermis with water and nutrition. The dermis is divided in to two regions, the papillary region of loose connective tissue with integrated nerve endings, and capillaries to connect the dermis to the basement membrane and the reticular dermis, a much thicker region than the papillary region, providing strength and elasticity. Blood and lymphatic vessels, hair roots and glands are located in this region. Ultimately, the dermis is connected to the subcutaneous tissue (hypodermis) which attaches the skin to bones and muscles [2].

1.2. Injury to the skin

In the evolution of heterogeneous multi-cell organisms, the repair of damaged cells or injured tissue was one of the most crucial steps in organism survival, to prevent severe organ damage and to defeat invading microorganisms. Depending on the severity of an injury and the location, spontaneous wound healing is either accomplished by tissue regeneration or tissue repair. Regenerated tissue retains physiological integrity, whereas wound repair replaces lost tissue by scar tissue, which is non-physiologic [6]. Regeneration is possible if injuries occur to the epithelial cell layer or the basement membrane. Thus, these layers are regeneratively active. When damage occurs to the underlying, regeneratively inactive tissue, wound repair is the driving activity. Regeneration is commonly non-inflammatory. Wound repair on the other hand involves inflammation under recruitment of the immune system. The skin functions as a barrier to pathogens and other environmental hazards to the organism, e. g. UV radiation, or toxins and prevents dehydration. Therefore, the skin requires fast healing to maintain these functions. Severe damage to the skin predominantly initiates wound repair mechanisms involving multiple highly time dependent cell recruitment steps and cell type interactions. [6-10]

1.2.1. Wound repair

Wound repair processes are directly initiated after injury occurrence. It requires an optimal interaction of macrophages, platelets, monocytes, neutrophils, fibroblasts, lymphocytes, mast cells, and endothelial cells and the regulated expression or inhibition of numerous proteins. In general, wound repair can be divided in three major phases



differentiated by cell type recruitment and protein signalling. The clotting and inflammation phase, granulation phase and the tissue remodelling phase are timely differentiated but show some overlap (figure 1.3) [7].

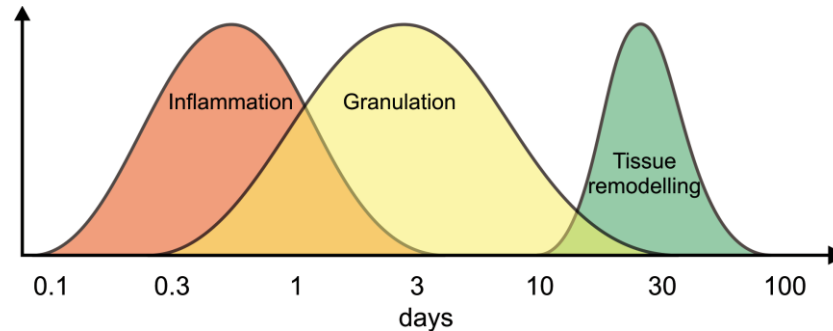
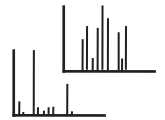
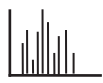


Figure 1.3: schematic of the wound healing time line

Skin injuries with damaged capillaries or blood vessels rapidly activate the coagulation cascades to prevent extensive blood loss. Vasoactive factors provoke high permeability of blood vessels allowing fibrinogen to migrate into the wounded area. Exposed collagens and the tissue factor (coagulation factor 3) further activate the coagulation factor cascade leading to fibrinogen degradation and the generation of a fibrin clot as a temporal wound closure. Endocrine derived cells such as platelets and leukocytes are imbedded into the clot stimulating further cell attraction, proliferation, and defence mechanisms. The Platelet derived growth factor (PDGF) is released from the platelets and macrophages in the fibrin clot to attract fibroblasts. Stimulation by transforming growth factor beta ($TGF\beta$) activates macrophages, which then secrete matrix metalloproteinases (MMP) to degrade the extracellular matrix (ECM). Substrates for MMPs are structural proteins such as collagens, which are highly abundant in the ECM. Cleavage of collagens and other linkage proteins in the ECM release growth factors and cytokines stored in the ECM to attract several cells to remove cell debris and damaged tissue, and to defend the fragile tissue against pathogen invasion. MMPs are predominantly inhibited by tissue inhibitor of metalloproteinases (TIMP) regulating the activity of MMPs [7, 11, 12].

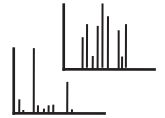
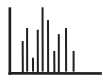
First initiators of the inflammatory response are residing mast cells, macrophages and T-lymphocytes in the wounded skin adjacency, but also keratinocytes are believed to play a role in the early immune response. These cell types release signal proteins to stimulate endothelial cells to express cell adhesion proteins such as vascular cell adhesion molecules (VCAM), intracellular adhesion molecules (ICAM) or selectins to attract leukocytes from the blood stream. Cell invasion is assisted by the provisional matrix, as the fibrin clot is referred to. The most abundant cells during the early inflammatory phase are neutrophils



which degrade foreign material or necrotic cells. Neutrophil invasion is stopped quickly after successful degradation of targeted material. These and other phagocytic leukocytes and lymphocytes release growth factors which accelerate macrophage activation in addition to autocrine derived macrophage activation. Active macrophages take the lead in wound healing as they are involved in crucial regulation processes based on their protein secretion [7].

Cell surface located receptor of advanced glycation end products (RAGE) and the toll-like receptors (TLR) are the major outside-in inflammatory signalling proteins. TLRs are expressed at the cell surface of macrophages and dendritic cells [13], RAGE is expressed at the cell surface of endothelial cells [14]. TLR signalling is stimulated by binding to foreign material such as DNA, RNA, lipoproteins, lipopolysaccharides, or flagella but also to endogenous ligands such as host DNA, RNA, heat shock proteins (HSP), high mobility group protein B (HMGB) or proteins of the S100 protein family [13]. RAGE was first described as a receptor for advanced glycation end products (AGE) derived from non-enzyme controlled reaction of free glucose or metabolites of glucose with functional groups of proteins in the plasma [14]. Especially untreated diabetes mellitus (DM) patients commonly suffer from episodes of high free glucose level in the plasma and thereby increased AGE derived inflammation signalling [15]. Nonetheless, RAGE is a multi-ligand receptor for various endogenous ligands including those stimulating TLRs but also other intracellular proteins derived from unconventional cell death. A highly potent stimulator is the heterodimer complex of S100A8 and A9. Stimulation of TLRs and RAGE always lead to the release of pro-inflammatory cytokines, or other inflammation signalling proteins which mediate cell proliferation and extend the inflammatory response [14, 16].

With decreasing inflammation, commonly after three to four days after injury, the provisional matrix will be replaced by granulation tissue. This more permanent matrix is cell rich and highly vascularised and is generated by fibroblasts, endothelial cells and macrophages. This process is dominated by fibroplasia and angiogenesis. Fibroplasia describes the process of collagen, laminin, and proteoglycan accumulation. Angiogenesis is the process of vascularisation of the tissue either from existing capillaries in the connective tissue (revasculogenesis) or new synthesis of capillaries (neovasculogenesis) for appropriate nutrition supply of the differentiating and proliferating cells. The granulation tissue enables keratinocyte migration to the surface of the wounded area to cover the granulation tissue and start regenerating the epidermis. This is mediated by connective tissue degrading proteases secreted by basal keratinocytes and the release of



keratinocyte growth factors FGF7 and FGF10 who belong to the fibroblast growth factor superfamily [7, 11].

Angiogenic processes during granulation tissue formation generate a high density of capillaries in this tissue derived from several growth factor, cell-cell and cell-ECM interactions. However, the whole process is a highly balanced regulation of vascular growth and vascular regression. In healed wounds the density of capillaries is therefore only slightly higher than normal tissue. Pro- or anti-angiogenic stimulation only depends on the expression of positive and negative mediators and the correlation of those to each other. FGF2 and the vascular endothelial growth factor (VEGF) are two key pro-angiogenic mediators [7, 17-20].

The final step in wound repair is the scar formation. This tissue remodelling process describes the formation of the cell rich and vascularised granulation tissue to a collagen rich tissue with a normal density of capillaries. Further, scar formation leads to wound contraction to decrease the gap between the wound edges. Therefore, fibroblast and specialised myofibroblasts produce cytoskeletal actin to generate contraction of the ECM via integrin receptor interaction of cells with the ECM. The scar formation is a slowly proceeding process that could take up to 6 months [7, 11].

1.3. Complications in wound repair

Wound healing involves highly complex processes with temporal protein regulation. Disturbances of these processes could lead to dysregulated protein expression causing healing delays or stagnation. Several events can influence the healing conditions. Extra corporal events such as intoxication with bacteria or viruses, venomous intoxication by animal bite, severe fractions or continuous pressure are known complications generating poor healing or non-healing wounds (figure 1.4). The decubitus ulcer at the lower back or the heel of bedridden patients is a prominent example of extra corporal derived pressure ulcer. Intra corporal influences mainly originate from underlying diseases, especially those who affect the supply of essential material needed by tissues. Therefore, patients suffering from artery diseases such as coronary artery disease (CAD) are susceptible for developing chronic wounds after injury or chirurgical intervention. Venous and artery diseases are the major causes of complications in wound healing. These ischemic conditions lead to elevated death of tissue due to artery blockage further up the blood stream and thereby generate a critical shortage of nutrition in a specific area.

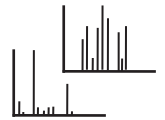
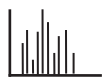
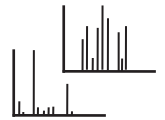
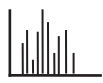


Figure 1.4: examples of chronic wound phenotypes a) stage IV decubitus (pressure ulcer) [21], b) foot ulcer [22], c) leg ulcer [21]

1.3.1. Diabetes mellitus derived wound repair complications

Another disease dramatically influencing wound healing is diabetes mellitus (DM). Patients commonly develop chronic wounds at the legs and feet in consequence to disturbances in the blood flow creating diminished nutrition supply. Diabetes mellitus describes a condition of altered glucose metabolism. Intake of glucose into the cells is limited either by insulin resistance of the cells or diminished insulin production in the pancreas. As a consequence, patients demonstrate elevated free glucose level in the blood bearing the risk of excessive AGE generation. Besides measuring free circulating glucose in the blood, a glycated haemoglobin species (HbA_{1c}) is used as a diagnostic marker for diabetes mellitus indicating long term hyper glycaemic episodes in poorly or non-treated DM patients. Further, it is an important prognostic marker in the treatment of DM indicating if oral medication is satisfying or insulin substitution is necessary. Glucose modified proteins in the circulation can in combination with lipids and lipoproteins produce clots provoking artery blockages, thus favourable conditions for poor healing wounds.

Type 1 DM is a condition of DM where patients lack the ability to produce insulin in the pancreas. In T1DM patients, insulin secreting islet β – cells in the pancreas are destroyed by autoimmune mediated processes [23]. This absolute insulin deficiency requires exogenous insulin application to prevent ketoacidosis to guarantee survival of T1DM patients. T1DM is most commonly developing in the childhood and is either inherited or viral infection derived. Less than 5% of all DM patients suffer from T1DM, the majority (> 90 %) are T2DM patients. T2DM most frequently develop in overweight adults living a so called modern lifestyle with abundant nutrition intake and reduced physical exercise. T2DM is a non-insulin dependent condition of DM. Cells normally dependent on glucose become insulin resistant due to reduced insulin receptor expression at the cell surface. Adipocytes were identified to play an important role in this resistance.



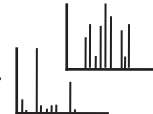
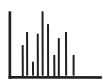
In obese individuals, adipocytes are highly abundant in various tissues secreting fatty acids. An elevated fatty acid environment replaces glucose as the main energy source and is bypassing the insulin receptor pathway, which reduces its expression. In turn, the glucose metabolism is reduced and the blood glucose level increases. In the early phase of T2DM development, the pancreas reacts with increased insulin production to overcome the insulin resistance. This can be assisted with oral medication of biguanides. However, long term overproduction of insulin causes islet β – cell dysfunction and thereby reduced insulin production. Thus, patients that are non-responsive to oral medication indirectly indicate reduced insulin production and exogenous insulin injection is necessary in order to remove the excess of glucose [24].

Although more common in poorly or non-treated T2DM patients, these patients experience reduction in the quality of life, due to elevated AGE and thereby mediated organ damage and inflammation. DM patients are prone to heart diseases, artery diseases, stroke, renal diseases, blindness, chronic wounds and amputation. All of these complications are vascular-borne. It has been shown that T2DM patients have reduced vascularised tissue and an elevated vascular permeability. Especially chronic wounds demonstrate altered microcirculation. Vasodilatation and nerve-axon related dysfunctions of microvascular reactivity are believed to be the major causes of chronic wounds in DM patients. Inadequate healing of wounds and prolonged inflammation generates necrotic tissue exacerbating the status of the wound. Amputation is than the usual consequence to prevent life threatening sepsis. More than any other disease which causes chronic wounds, T2DM patients are highly susceptible to amputations [17].

The number of patients diagnosed with diabetes mellitus globally is continuously increasing. It was estimated that the worldwide number of people diagnosed with DM would be roughly 285 million in 2010 and is believed to increase to 439 million in 2030 [25], especially in the younger generation [26]. Therefore, a dramatic increase in required treatment of diabetes mellitus derived complications including chronic wounds is expected. Although significant progress in the treatment of chronic wounds in diabetics has been made, which is extensively reviewed in chapter 5, further investigation are needed to understand the biological processes necessary in wound healing.

1.4. Proteomic based investigation strategies

Information about molecular processes in wound healing is predominantly derived from immunohistochemistry or enzyme-linked immunosorbent assay (ELISA) protein investigations. Protein analyses using such strategies commonly require highly specific



antibodies allowing for reliable detection and high sensitivity with detection limits below 1 pg/mL, depending on the application and employed antibodies. Although these strategies comprise advantages in analyte detection, they are restricted by the number of biological molecules able to be simultaneously analysed. Further, immuno-based strategies depend on the availability of antibodies for the desired target molecules. Antibody development can be time and cost intensive. For some molecules of interest, antibody generation is not even possible. A strategy enabling multiple protein identification and allowing flexibility in specimens suitable for analysis is the proteomics approach. This can either involve 2D gel electrophoresis or mass spectrometry (MS). In most cases, mass spectrometry is coupled to liquid chromatography (LC). As intact protein investigation using LC-MS is still developing and is extensively challenging due to chromatographic behaviour of large proteins and the limitation in the accessible mass range, commonly applied investigations of complex protein mixtures are performed in the so called bottom-up strategy. In the bottom-up approach proteins are enzymatically digested to generate peptides prior analysis. Trypsin is the enzyme of choice as it specifically hydrolyses the basic amino acids arginine and lysine at the C-terminus side. Arginine and lysine are fairly abundant in proteins, facilitating the ability of protein detections in LC coupled tandem mass spectrometry (LC-MS/MS) applications. For optimal peptide behaviour on octadecyl chains (C18) reverse phase (RP) material (figure 1.7a), generated peptides should consist of 6 – 25 amino acids. Separation of peptides on the RP material is based on hydrophobic interaction between the C18 chains immobilised on silica particles (stationary phase) and the peptides in a mobile phase. The more hydrophobic a peptide is, the stronger the interaction with the stationary phase, and the greater the retention of the peptide. In conventional high performance liquid chromatography (HPLC) RP experiments, peptide elution is achieved by a two-buffer gradient system with low organic solvent concentration in the equilibrating buffer and a high organic solvent concentration in the eluting buffer. Depending on initial equilibration conditions and the steepness of the selected linear increasing eluting buffer gradient, separation of less hydrophobic peptides with high percentage of amino acids with polar or charged residues and hydrophobic peptides with high percentage of amino acids with aliphatic or aromatic residues, as common to transmembrane domains of membrane proteins, is possible.

For mass spectrometric peptide detection, the eluting peptides need to be transferred into the mass spectrometry. Therefore, peptides will be ionised by electro spray ionisation (ESI) through applying a voltage between the RP column and the mass spectrometer 9

(figure 1.5). Excess capacity of protons or electron, depending on the polarity selected, at the column tip resolves in a coulomb explosion leading to ionisation of the peptides in the drop. ESI is a method perfectly serving the needs of LC-MS systems. ESI is a mild ionising strategy generating singly to multiply charged precursor ion (positively or negatively charged version of a peptide by adding or removing protons) without causing extensive fragmentation of the precursor [27, 28].

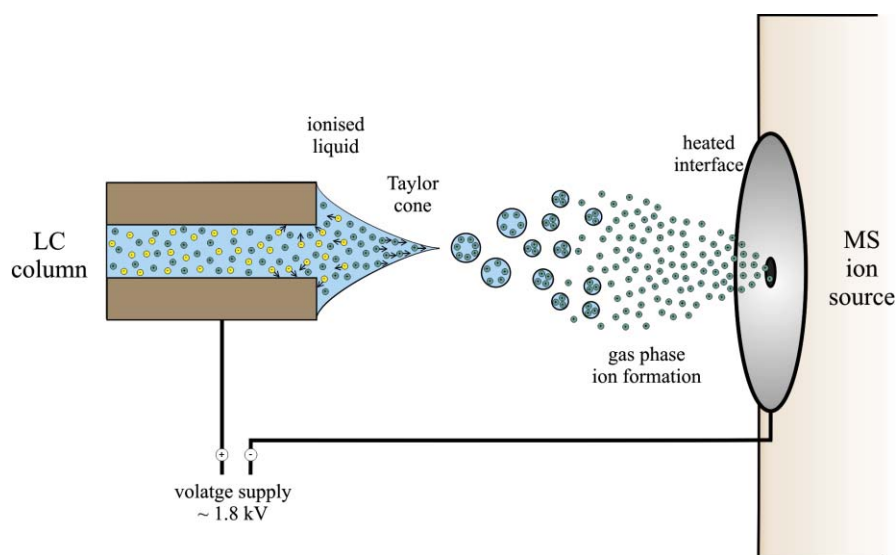


Figure 1.5: processes during electro spray ionisation

Progress in mass spectrometer development to fast scanning, highly accurate, and precise instruments with high resolving potential, enables highly specific precursor selection which is important for peptide sequencing. The LTQ Orbitrap *velos* mass spectrometer for instance is a highly advanced hybrid instrument combining accurate Fourier transformation mass spectrometry (FTMS) with fast analyte fragmentation and detection of linear ion trap mass spectrometry (ITMS). High accurate FTMS on Orbitrap mass analyser is established by generating a balance of electrostatic interaction of ions with a rotating electrode and their centrifugal force. The ion trajectories then correlate to the mass to charge (m/z) of an ion. This type of mass analyser allows ion mass detection with accuracy in the low to sub ppm range and a selectable resolution [29].

Collision induced dissociation (CID) is predominately used in peptide sequencing applications. CID fragmented peptides show specific bond breakages at the amide bond of peptides. Mass shifts between fragments thereby correlate to the mass of amino acids with the loss of water or an amine depending on the side of peptide the fragment was generated from. Peptide fragments with the positive charge remaining at the C-terminus side are termed y-ions, whereas b-ions represent peptide fragments with the positive charge at the N-terminus (figure 1.6).

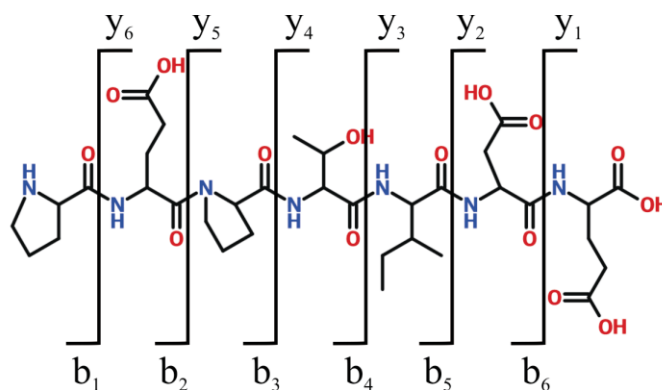
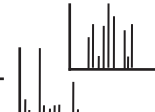
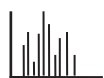


Figure 1.6: exemplified y- and b-ion annotation of the peptide PEPTIDE

Manual annotation of peptide MS/MS spectra in a data set of several thousand MS/MS spectra is not accomplishable in an appropriate amount of time. Thus, computer-based search engines have to be used to generate lists of identified proteins and peptides in an individual LC-MS analysis. De novo peptide sequencing of so far unknown proteins is rarely applied to highly complex samples but is more applicable to purified protein samples excised from 1D or 2D gel electrophoresis experiments. Therefore, LC-MS investigation of highly complex specimens is commonly conducted to organisms with known protein sequences, since they are used as a reference data base for search engine processing. The Sequest algorithm and the Mascot algorithm are example search algorithms that are commonly integrated into search engines. Both search engines use protein sequence databases as a reference to compare the empirical MS/MS spectra to possible fragment pattern of tryptic peptides generated from the database. The greater the matching in the empirical MS/MS spectrum with the theoretical fragment masses of a virtual peptide, the higher the search algorithm specific score. Based on the score, peptides can be filtered and only peptides with a high score, indicative of high probability peptide identities are shown in the final result list. Since most peptide sequences are unique to a protein or a protein group, the presence of a unique peptide can be used to determine protein presence in a certain specimen [30].

1.4.1. Multi-dimensional protein identification technology

Although RP-LC-MS/MS enables the identification of hundreds of peptides within a single analysis, sometimes purification or enrichment of target proteins is necessary for satisfying mass spectrometric identification. Approaches and draw backs of those strategies are discussed in more detail in chapter 4 and 7. Briefly, integration of an additional chromatographic phase into the LC-MS workflow can dramatically increase the detection of peptides contained in a complex sample. The multi-dimensional protein



identification technology (MudPIT) combines strong cation exchange (SCX) chromatography with RP chromatography (figure 1.7c) extensively improving the detection limitation [31].

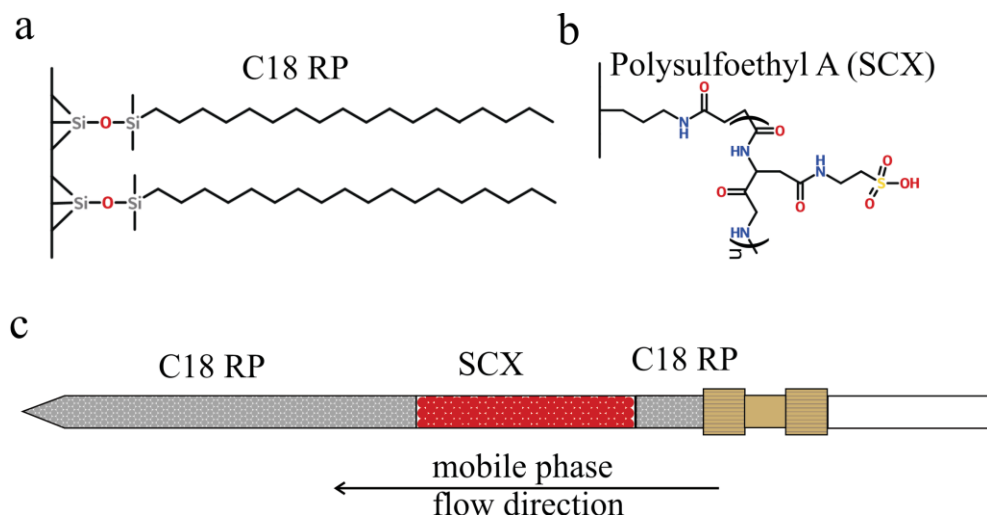
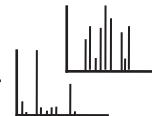
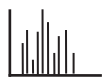


Figure 1.7:a) C18 RP material; b) SCX material, $n = 17 - 18$; c) MudPIT column

Immobilized poly sulfonic acid derivatives are commonly used as stationary phases (figure 1.7b). Requirements for SCX chromatography perfectly matches the conditions of samples submitted to RP-LC-MS. They are acidic in pH and low in salt contamination. Therefore, additional sample handling is not necessary. Similar to conventional SCX separation, the peptides which are retained on the resin based on their charge, are eluted by increasing salt concentration. The cations then replace the positively charged peptides depending on the binding strength. Instead of salt gradient elution, in MudPIT experiments peptide elution is achieved by consecutive salt injection steps of increasing concentrations with RP gradients following each salt injection step. According to this, the higher the salt concentration needed to elute a peptide, the higher the binding strength of this peptide to the stationary phase, which correlates to the number of amino acids carrying amine or amide groups in their side chains usually protonated at $\text{pH} = 3$. The retained peptides on the SCX resin are not influenced by ACN gradients, therefore each consecutive ACN gradient functions as conventional RP-LC-MS analysis without peptide leakage from the SCX material.

1.4.2. Quantification of LC-MS/MS results

Mass spectrometry analyses of molecules comprise a variety of strategies for quantification. In peptide based quantitation, relative and absolute quantitation is applicable. Absolute quantitation involves isotopically labelled reference peptides which are compared to the targeted peptides in a complex solution. Reference peptides have to be



identical to the target peptide to guarantee similar performance on the chromatography material and in the mass spectrometer in terms of the ability to ionise and fragment. Concentration to peak AUC intensity regression of reference peptides allows direct correlation of targeted peptide concentration in a complex solution. This type of quantitation is commonly employed by targeted mass spectrometric approaches. Another strategy is isobaric tag for relative and absolute quantitation (iTRAQ). Analysis of a mixture of n different samples labelled with n different isobaric tags, where each tag is specific for one sample, enables similar chromatographic and mass spectrometric performance of each labelled peptide. Acquired MS/MS spectra of those peptides contain abundance specific intensities of the isobaric tags in the low m/z mass range which can be used for quantitation. Although iTRAQ is applicable for absolute quantitation, it is more dominantly used for relative quantitation.

Relative quantitation can either be performed using labelling strategies or label free strategies. Predominantly used labelling strategies are iTRAQ and stable isotope labelling by amino acids in cell culture (SILAC). iTRAQ is mainly used for *in vivo* derived specimens and SILAC, where ^{13}C and ^{15}N labelled arginines and/or lysines are integrated into proteins during protein synthesis, is applicable to *in vitro* derived specimens. Another labelling strategy more often used for bacteria is metabolic labelling. Here, organisms are grown on ^{15}N media to incorporate ^{15}N into the amino acid synthesis pathway generating an organism entirely labelled with the heavier isotope [32].

Isotopic labelled strategies for relative quantitation in general use chromatographic properties and employ the MS as a detector to monitor precursor elution visualised in extracted ion chromatograms (XIC) and to verify the specific precursor in tandem MS experiments. Label-free strategies on the other hand are based on mass spectrometric properties. In the spectral counting approach for instance, the number of identified peptide spectra assigned to a protein is used. These numbers can be compared between different samples derived from the same specimen demonstrating similar protein compositions to estimate regulation differences. Liu et al [33] have proven a linear correlation of the spectrum counts of a protein to its abundance. Normalising of spectrum counts by the overall spectrum count of a sample, enables comparison of proteins between samples. Additional values e.g. protein length, molecular weight, or sequence coverage enables comparison of protein abundance within a sample. Spectral counting is applicable to biomarker discovery studies of large sample cohorts. However, proteins suspected to

function as biomarkers in a specific specimen have to be validated. Besides ELISA or western blotting, targeted mass spectrometry can be a promising tool.

1.4.3. Targeted mass spectrometry

Instrument development towards targeted proteomics enables highly sensitive and specific analysis of selected target analyte molecules. Selected reaction monitoring (SRM) is the strategy used. SRM is mainly performed on triple quadrupole instruments, but ion-trap instrument implementation have been described as well [34, 35].

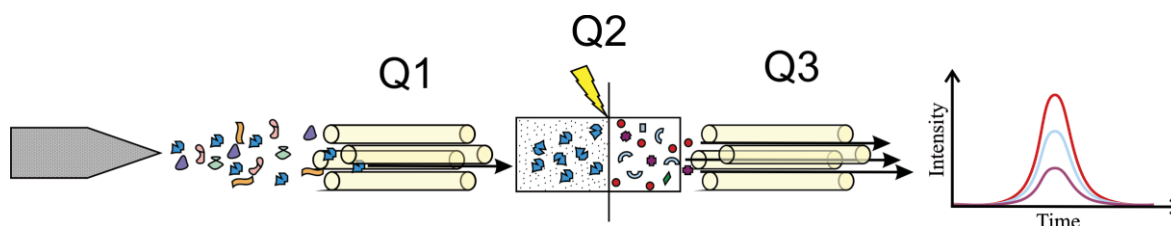
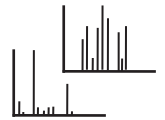
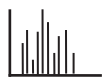


Figure 1.8: schematic of ESI-SRM-MS on triple quadrupole instruments

In triple quadrupole mass spectrometer the high accurate m/z filtering of quadrupole one dramatically increases the instrument sensitivity needed for high specificity analyte molecules detection based on transition monitoring. A transition refers to the transformation of a precursor ion selected in quadrupole one to a product ion detected in quadrupole three, generated by fragmentation in quadrupole two (figure 1.8). Usually the two to three most intense fragments are chosen for each targeted molecule for reliable detection [34]. Therefore, triple quadrupole instruments comprise the advantage of fast ion scanning to facilitate simultaneous and quantitative monitoring of multiple molecules within a single run with reliable analyte identification. These benefits are the key aspects for targeted proteomic implementation into clinical analysis routines. So far this field is dominated by immunohistochemistry-based analyte quantification since SRM is still lacking rapid sample analysis without excessive sample preparation. Nonetheless, besides the multiplexing potential of SRM, it enables investigation and quantitation of substances not accessible by immunohistochemistry or ELISA, as antibody generation is not possible or several different isoforms of a substance is targeted. In recent years improvements in the accessible dynamic range and the instrument speed further increased the sensitivity, facilitating the use of SRM in clinical laboratory routines [36-40].

1.5. Proteomic applications in wound healing processes

Wound fluid investigation is an emerging field of proteomics application with astonishing potential in the wound status assessment, and the detection of diagnostic and prognostic markers [41, 42]. Although this field is still dominated by immuno-based and

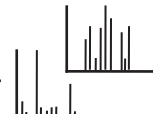
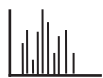


RNA-based investigations, proteomics may be seen as the future application in wound healing investigations [43, 44]. Especially, detailed investigations of specific cell types involved in healing processes or the influence of specialised dressing material on these cells are subject areas for proteomic profiling [45-50]. Groessl et al. for instance, investigated the secretome of monocytes by label-free MS and revealed specific protein secretion based on the proinflammatory stimuli [45].

Several large-scale analyses have been conducted with the focus on the identification of proteins differentially expressed in specific wound types which could serve as potential marker proteins [51-56]. Most of them used 1D or 2D gel electrophoresis protein separation coupled with mass spectrometry. Fernandez et al described the development of an enhanced proteomic method as an applicable tool for marker detection in chronic wounds. They combined immunoaffinity chromatography with 2D LC for isoelectric focusing and RP separation of proteins in chronic wound fluids prior to matrix-assisted laser desorption/ionisation time of flight (MALDI-TOF) MS protein characterisation [54]. A highly comprehensive approach for insights into wound healing was conducted by Edsberg et al. [51]. They investigated exudates from pressure ulcers using 2D gel electrophoresis, ELISA, and iTRAQ for a multiplexed dataset suitable for quantitation. They compared interior and periphery specific exudates samples from pressure ulcers from 32 patients over a period of 6 weeks (15 time points) and identified 21 proteins to differentiate between healing pressure ulcers and chronic pressure ulcers. A further 19 proteins showed expression level differences between the interior and the periphery of the wound. These included Profilin 1, Immunoglobulin (Ig) lamda, Ig gamma keratins, alpha-1-antitrypsin, S100 proteins A6 and A7, and the soluble isoform of RAGE. In a previous study this group applied 2D gel electrophoresis to investigate the protein content of a similar sample set from 19 patients with pressure ulcers. Their results suggested S100A9 as a potential biomarker in wound healing [52].

The protein composition of burn wounds were investigated by Pollins et al. [56]. They applied 2D difference gel electrophoresis (DIGE) to quantify temporal protein expression level changes in samples of grouped healing periods of 1-3, 4-6, and 7-10 days post-burn. Gel bands showing temporal differences (46 proteins) were analysed by MALDI-TOF. Among these were vimentin, HSP90, haptoglobin, gelsolin, keratins, and serine protease inhibitor family.

The work of Eming et al. [53] is highly relevant to this study. The protein composition in digests of 1D SDS PAGE separated exudates analysed by LC-MS/MS of non-healing



and normal healing venous leg ulcers were compared based on label-free quantitation. Their results revealed expression level differences of several protein classes such as ECM components, proteases (e.g. MMP9) protease inhibitors (serpins), and immune mediators such as S100 proteins A7, A8, and A9 or Annexin A1 (ANXA1). Although this study depicted protein expression differences essential for successful healing of a wound, the study lacks adequate sample size, with the LC-MS/MS results based on only one chronic and one acute wound fluid.

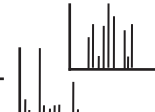
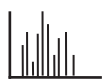
1.6. Aims and scope of this thesis

The aim of this thesis was to apply mass spectrometric proteomics to exudates from poor healing chronic wounds from T2DM patients to investigate the secretome of these wounds. Further, the protein constitution of chronic wound fluids were compared to exudates from normal healing wounds of patients with non-life threatening burn wounds to identify differences in expression levels of proteins in the fluids. Large-scale mass spectrometry with label-free-quantitation was used to identify these differences and SRM-MS was applied to validate these findings.

Further, a glycan binding material was used to develop a method to specifically enrich glycosylated proteins for mass spectrometric investigations.

A further aim of this thesis was the establishment of a robust two-dimensional targeted proteomics work flow to increase the sensitivity of peptide detection and optimise quantification of less concentrated proteins.

Finally, haemodialysis membranes were assessed in term of protein elimination by mass spectrometric investigations of spent dialysates from chronic haemodialysis patients.

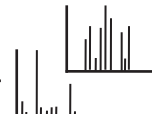


2. Motivation

The number of newly diagnosed patients with diabetes mellitus, especially T2DM, is dramatically increasing and affects millions of people worldwide. Diabetics commonly incur life threatening organ damage as a consequence to an altered metabolism. Predominantly in none or poorly treated diabetics, substantially diminished quality of life is noticeable. Diabetes mellitus patients are at high risk of cardiologic diseases, eye diseases, kidney insufficiencies, or impaired wound repair. Chronic wounds, e.g. foot ulcer, or leg ulcer, are the dominate cause for amputation in diabetics. With increasing numbers of diabetes mellitus patients, the number of chronic wounds is increasing accordingly. This will add tremendous costs to the health care system, since prolonged hospitalisation, excessive medication, wound dressing material usage, and extended home assistance has to be expected.

A clear understanding of molecular healing processes is necessary to optimise wound healing processes for improved treatment of chronic wounds and to improve the quality of life of affected patients. Therefore, the aim of this study is to investigate the protein composition of exudates from poor healing chronic foot ulcers from T2DM patients and of split thickness skin graft donor sides of burn victims showing second to third-degree burns (control group) to identify differences in protein expression level and give new insights in to molecular healing processes. MudPIT-MS/MS will be used to enable large-scale analyses of complex biological samples. In order to optimise the sample preparation and mass spectrometric peptide detection, protein enrichment strategies will be assessed. This includes high abundant protein depletion and post translational modification based enrichment of glycosylated proteins. Protein expression will be assessed using label-free spectral counting as a relative quantitation tool. If applicable, proteins showing differential expression will be selected for SRM-MS validation studies.

The progression of kidney dysfunction in diabetics to a completely non-functional kidney is a frequent development in DM patients. Thus, these patients become dependent on life-long artificial kidney replacement therapies. Chronic haemodialysis patients experience enormous reduction in quality of life. Repetitive dialysis sessions per week dominate the life. The outcome of haemodialysis depends on the performance of the employed dialysis membrane for the elimination of substances with potential toxicity. Therefore, the protein composition of spent dialysis samples derived from two different dialysis membranes will be investigated by LC-MS/MS to assess the elimination efficiency of known uremic toxins.

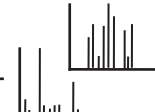


3. Material and methods

3.1. Chemicals and consumables

Table 3.1: used chemicals, proteins, and peptides in the study; all substances were obtained in the highest possible purity from the following supplier

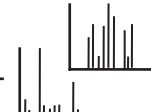
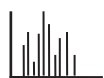
Chemical	Supplier
2-iodoacetamide	Merck
30% Acryl amide-0.8% bisacryl amide	Roth
acetic acid	J.T. Baker
acetone	J.T. Baker
acetonitrile	J.T. Baker
alpha-1-acid glycoprotein, bovine	Sigma Aldrich
alpha-2-HS-glycoprotein, bovine	Sigma Aldrich
ammonium acetate	J.T. Baker
ammonium bicarbonate	Fluka
ammonium persulfate	Merck
BCA protein assay kit	Pierce
boric acid gel	Sigma Aldrich
boronic acid	Merck
bromophenol blue	Merck
Complete protease inhibitor cocktail	Roche
Coomassie brilliant blue G250	Fluka
dithiothreitol	Sigma Aldrich
ethanol	Sigma Aldrich
formaldehyde	VWR
formic acid	J.T. Baker
gelatin	AppliChem
glycerol	J.T. Baker
glycine	Fluka
hydrochloric acid	J.T. Baker
isopropanol	J.T. Baker
isotope labelled ESDTSYVSLK peptide from CRP	Auspep
isotope labelled IQNILTEEPK peptide from PON1	Auspep
isotope labelled YVYIAELLAHK peptide from PON1	Auspep
magnesium chloride hexahydrate	Riedel de Haën
methanol	J.T. Baker
modified trypsin, sequencing grade	Promega



Chemical	Supplier
monoclonal mouse anti-human S100A8	Santa Cruz Biotechnology
monoclonal mouse anti-human S100A9	Santa Cruz Biotechnology
N,N,N,N Tetramethylethylenediamine	Sigma Aldrich
Page Ruler Plus	Fermentas
PNGase F	Sigma Aldrich
polyclonal horse anti-mouse IgG HRP conjugated	New England Biolabs
ProteoPrep [®] 20 plasma immunodepletion kti	Sigma Aldrich
reverse phase material (Luna C18)	Phenomenex
silver nitrate	Merck
sodium carbonate	Riedel de Haën
sodium chloride	J.T. Baker
sodium dodecyl sulphate	Sigma Aldrich
sodium hydroxide	J.T. Baker
sodium thiosulfate	J.T. Baker
taurine	Acros
Tris	AppliChem
Triton X-100	Calbiochem
Tween 20	Sigma Aldrich
urea	J.T. Baker

Table 3.2: consumables used in the studies

Consumable	Supplier
Amicon Ultra (MWCO 3 kDa, 50 mL)	Millipore
Costar [®] Spin-X concentrator filter	Corning Inc.
fused silica capillaries	The De Leone Corporation
microtiterplates (96 wells)	Greiner Bio One
NanoAcquity 1.7 μ m BEH130 C18 RP column	Waters
Nanosep 10K Omega (MWCO 10 kDa)	Pall
pipette tips (1 mL, 200 μ L and 10 μ L)	Starlab
PVDF-Membrane	Pall
Symmetry C18 RP trap column (5 μ m)	Waters
tubes with lid (1.5 mL and 2.0 mL)	Eppendorf
tubes with lid (15 mL and 50 mL)	DB Falcon
Whatman filter	Whatman



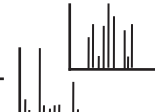
3.2. Instruments and processing software

Table 3.3: used instruments in the studies obtained from the following manufacturer

Instrument	manufacturer
4000 QTrap	ABSciex
5500 QTrap	ABSciex
Accela Pump	Thermo Fisher Scientific
Arium 611 V	Sartorius
Blot chamber Fastblot	Whatman Biometrica
ChemiDoc™ XRS+ System	BioRAD
Electrophoresis chamber Mini Protean 3	BioRAD
LTQ Orbitrap velos	Thermo Fisher Scientific
LTQ XL	Thermo Fisher Scientific
Mini centrifuge 5415 R	Eppendorf
NanoAcquity UPLC	Waters
NanoLC 2D™ System	Eksigent
pH-meter PH 270 (WTW Series)	Inolab
Photo spectrometer	Anthos
Thermomixer comfort	Eppendorf
UltiMate 1000	Dionex
Vacuum centrifuge concentrator 5301	Eppendorf

Table 3.4: software used for data acquisition and database searches

Software	Developer
ADAP Software	Anthos
Analyst 1.4 (4000 QTrap)	ABSciex
Analyst 1.5 (5500 QTrap)	ABSciex
Chromeleon 6.5	Dionex
MultiQuant 2.1	ABSciex
Proteome Discoverer 1.3	Thermo Fisher Scientific
Tune Plus 2.5 (LTQ XL)	Thermo Fisher Scientific
Tune Plus 2.6 (Orbitrap)	Thermo Fisher Scientific
XCalibur 2.0.7 (LTQ XL)	Thermo Fisher Scientific
XCulibur 2.1 (Orbitrap)	Thermo Fisher Scientific



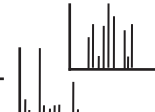
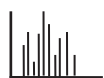
3.3. Sample cohorts

3.3.1. Human wound fluids

Human wound fluid samples were obtained from the University Hospital Bergmannsheil (Bochum, Germany). Samples were generated using polyvinyl acetate sponges applied to the wound bed to withdraw exudates. Soaked sponges were moistened with 2 mL of Complete protease inhibitor cocktail solution inhibiting serine, cysteine and metalloproteinases. To collect the wound fluid, sponges were carefully centrifuged at 125 g and repeated twice. Purified solutions were frozen in liquid nitrogen and stored at -80 °C until further analysis. Ten wound fluids from T2DM patients suffering from chronic foot ulcer for more than 30 days (mean age 66 years), and 6 wound fluids from split thickness skin graft donor sides from thigh of burn victims showing second to third-degree burns (mean age 46 years) (control group, in the following named acute wound) have been investigated in the MudPIT-MS/MS study. Nine patients showing chronic foot ulcers (mean age 58 years) and 9 patients with acute wounds (mean age 43 years) (6 thighs, 2 thoraxes, 1 abdomen) were investigated by SRM-MS. Information of patients affiliated to the studies are shown in table 3.5. Information regarding the size and depth of the acute wounds was not available. However, the acute wound fluids were known to be collected from injury to the dermal layer. Chronic wound fluids were from dermis and subcutaneous tissue layers.

Table 3.5: information on patients analysed in the comparison study of exudates from normal healing acute wounds and poor healing chronic wounds from T2DM patients

acute wound					chronic wound				
patient No.	age	gender	wound location (Split-skin donor site)	analysed by MudPIT/SRM	patient No.	age	gender	wound location and size	analysed by MudPIT/SRM
1	24	m	right thigh	Y/Y	1	68	m	midfoot (6 cm ²)	Y/Y
2	42	m	right thigh	Y/N	2	60	m	left ankle (8 cm ²)	Y/N
3	58	m	left thigh	Y/Y	3	59	m	right heel (12 cm ²)	Y/Y
4	37	m	left thigh	Y/N	4	74	m	right heel (9cm ²)	Y/N
5	67	m	left thigh	Y/Y	5	46	m	right ankle (10 cm ²)	Y/Y
6	48	m	left thigh	Y/Y	6	65	m	left footpad (6 cm ²)	Y/Y
7	32	m	abdomen	N/Y	7	64	m	left heel (9 cm ²)	Y/N



acute wound					chronic wound				
patient No.	age	gender	wound location (Split-skin donor site)	analysed by MudPIT/SRM	patient No.	age	gender	wound location and size	analysed by MudPIT/SRM
8	28	m	right thigh	N/Y	8	78	m	left heel (6 cm ²)	Y/N
9	44	m	left thorax	N/Y	9	74	m	right heel (9cm ²)	Y/N
10	52	m	left thorax	N/Y	10	68	m	left heel (8 cm ²)	Y/N
11	38	m	right thigh	N/Y	11	67	m	left phalangeal joint (4 cm ²)	N/Y
					12	69	w	left heel (12 cm ²)	N/Y
					13	56	m	left heel (8 cm ²)	N/Y
					14	70	m	right ankle (9 cm ²)	N/Y
					15	69	w	left phalangeal joint (6 cm ²)	N/Y

3.3.2. Haemodialysis samples

Dialysis sample were taken from chronic haemodialysis patients who received dialysis treatment sessions thrice a week at the Nephrology and Dialysis Unit at the Bolognini Hospital, Seriate, Italy. Samples from the first and second dialysis sessions were analyzed in the membrane permeability study to estimate elimination efficiency of the two employed high flux membrane filter devises Amembrix[®] (Xevonta Hi23 membrane) and Polyamix[™] (Gambro Polyflux 210H membrane). In total, 9 patients were treated with both membrane types. Table 3.6 shows patient relevant information. Patients in the Xevonta/Polyflux crossover (5 Patients) were treated first with Xevonta Hi23 dialysis membranes (week one) and then with Polyflux 210H membranes (week two). The four patients in the Polyflux/Xevonta crossover were treated vice versa. A representative 40 ml sample was taken from the fluid collection of each 4 h dialysis session. Roche Complete protease inhibitor cocktail tables were added to prevent uncontrolled protein degradation. Amicon ultra centrifugal filters (molecular weight cut-off 3 kDa) were used to concentrate the obtained 40 mL dialysates to 1 mL. Proteins were precipitated with cold acetone and reconstituted in 25 mM ammonium bicarbonate.

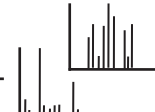
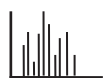


Table 3.6: information on patients analysed in the haemodialysis membrane specific protein elimination study

X/P crossover			P/X crossover		
patient No.	age	gender	patient No.	age	gender
1	78	m	1	65	w
2	75	m	2	50	m
3	70	m	3	56	m
4	55	m	4	52	m
5	41	w			

3.3.3. Ethics

Ethics approval for the study on human wound fluids was obtained from the ethics committee at the Ruhr-University Bochum, Bochum, Germany. (Appendix B)

The study on human dialysis fluids from haemodialysis dependent patients was approved by the ethics committee at the bolognini hospital, Seriate, Italy

3.4. Protein enrichment

3.4.1. Immunodepletion of highly abundant proteins

Antibody based removal of the 20 most abundant proteins (table 3.7) in the human plasma was performed with the ProteoPrep[®] 20 plasma immunodepletion kit. Minor adaptation in the workflow was made to investigate human wound fluids. Therefore, 15 mg of human wound exudates in 1 mL ammonium bicarbonate (pH 7.8) were in 100 μ L aliquots applied to the antibody resin which was previously activated and equilibrated as advised by the manufacturer. The applied wound fluid was incubated on the resin for 30 min at room temperature to ensure successful binding of targeted proteins to their specific antibodies. To elute unbound proteins (lowly concentrated proteins) 100 μ L elution buffer (provided by the supplier) was added and spun at 0.5g. This step was repeated trice. Bound proteins were eluted with 2 mL elution buffer (provided by the supplier). The resin was equilibrated with 4 mL equilibration buffer and the next aliquot was applied. Lowly concentrated proteins in the unbound fractions were precipitated with cold acetone, reconstituted in 25 mM ammonium bicarbonate (pH 7.8) and combined to one sample (~100 μ L). The sample was again applied to the antibody resin and processed as described before to achieve best possible removal of high abundant. Unbound proteins were again cold acetone precipitated and reconstituted in 25 mM ammonium bicarbonate (pH 7.8).

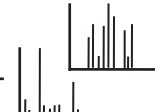


Table 3.7: list of top 20 highly concentrated proteins in the human plasma depleted by the ProteoPrep[®] 20 plasma immunodepletion kit

highly concentrated plasma proteins			
albumin	complement C3	immunoglobulin α	transferrin
apolipoprotein A1	complement C4	immunoglobulin γ	transthyretin
apolipoprotein A3	complement component C1q	immunoglobulin μ	α 1- antitrypsin
apolipoprotein B	fibrinogen	immunoglobulin δ	α 1-acid glycoprotein
ceruloplasmin	haptoglobin	plasminogen	α 2- macroglobulin

3.4.2. BAGAC affinity chromatography

For the enrichment of glycosylated proteins, 1 mL spin columns were filled with 100 mg of boric acid gel, a cross-linked copolymer of dihydroxyboryl-anilino-substituted methacrylic acid with 1,4-butanediol dimethacrylate. The material was activated with 25 mM HCl (pH 3.0), followed by equilibration with taurine buffer (50 mM taurine, 20 mM MgCl₂; pH 8.7). For optimal glycan binding, the protein mixture was denatured with 8 M urea, added to the BAGAC resin and incubated over night at 4 °C. Unbound proteins were eluted with two column volumes of taurine buffer (wash fraction). Bound proteins (elution fraction) were eluted with 10 column volumes of 20 mM HCl and 20% ACN (pH 3.0), followed by 10 column volumes of borate buffer (100 mM boronic acid and 1 M NaCl; pH 9.8), 10 column volumes of borate buffer with 20% ACN, and finally 10 column volumes of borate buffer. Proteins were precipitated with cold acetone and reconstituted in 25 mM ammonium bicarbonate (pH 7.3).

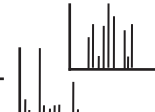
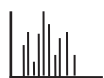
3.5. Sample specific properties and protein visualization

3.5.1. Protein concentration

Protein concentrations of investigated samples were estimated with a BCA Protein assay. Bovine serum albumin in quantities from 0 – 2 mg/mL was used to generate calibration curves optimal for low concentrated protein samples. For accurate determination of protein concentrations, samples were analysed in two replicates of two dilutions.

3.5.2. SDS-PAGE

One dimensional sodium dodecyl sulfate poly acryl amid gel electrophoresis (1D-SDS PAGE) of 20 μ g sample in 10 μ L of 25 mM ammonium bicarbonate were conducted under reducing conditions. Therefore, samples were incubated in 1x reducing buffer (table 3.8) for 10 min. at 60 °C. The gel was placed in the electrophoresis chamber, filled with



running buffer (table 3.8) and the samples were mounted onto the gel. Samples were separated by charge in a 15% SDS-PAGE gel with 4% stacking gel (table 3.8) using a constant current of approximately 50 mA. Page ruler plus (Thermo Scientific, Waltham, Massachusetts, USA) was employed as a molecular mass marker.

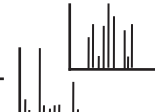
Table 3.8: gel preparation and used buffers for 1D SDS-PAGE analyses

4% stacking gel	15% separating gel	reducing buffer (5x)	running buffer
125 mM Tris-HCl (pH 6.8) 13% of 30%AA,0.8% BisAA 0.1% w/v SDS 0.1% w/v APS 1% TEMED bromophenol blue	375 mM Tris-HCl (pH 8.8) 45% of 30%AA,0.8% BisAA 0.1% w/v SDS 0.1% w/v APS 1% TEMED	500 mM Tris HCl (pH 6.8) 10% w/v glycerol 3% w/v SDS 500 mM DTT bromophenol blue	25 mM Tris-HCl (pH6.8) 192 mM glycine- NaOH (pH 8.5) 1% w/v SDS

Separated proteins were either visualised by silver staining or coomassie staining. To stain SDS-PAGE gels with silver, the gel was incubated for 30 min in 50% methanol and 10% acetic acid, followed by 15 min incubation in 5% methanol and 1% acetic acid. The gel was then washed 3 times with water, incubated in 0.02% w/v sodium thiosulfate for 90 s washed 3 times for 30 s with water and incubated in a 0.1% silver nitrate solution for 30 min. Finally the gel was developed in a solution of 3% w/v sodium carbonate, 0.05% v/v formaldehyde and 2% of the sodium thiosulfate solution.

3.5.3. Zymography

Visualisation of MMP enzyme activity requires native MMPs. Therefore separation of samples has to be conducted under non-reducing conditions. For adequate MMP intensities, 100 µg of proteins in human wound exudates were used. Prior separation, proteins were denatured at room temperature in non-reducing sample buffer (table 3.9). The samples were loaded onto a 10% SDS-PAGE separating gels with 0.1 % gelatin incorporated as a substrate for MMP2 and MMP9. The gel was run at a constant voltage of approximately 50 V until the running front reached the lower end of the gel. After separation, the gel was washed 3 times with water followed by incubation in 2.5% v/v Triton X-100 for 1 h to remove SDS and renature proteins immobilised in the gel matrix. The gel was washed 3 times with water and incubated in a digestion buffer (0.1 M Tris-NaOH pH 8.3, and 10 mM calcium chloride) overnight at 37 °C. The gel was then stained with 25 mL Coomassie blue for 1 h and and destained with acidic methanol (30%



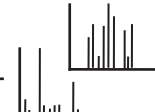
methanol, 10% acetic acid) until clear spots were seen. Clear spots (degraded gelatin) indicate enzyme activity of MMPs and correlates with the concentration of each MMP. The gel was scanned UV light for optimal contrast of the clear spots to the background.

Table 3.9: preparation of gelatin gels and zymogramm buffers

1g% gelatin separating gel (10%)	non-reducing buffer (5x)	Coomassie blue
375 mM Tris-HCl (pH 8.8)	400 mM Tris HCl (pH 6.8)	0.2% w/v Coomassie blue
45% of 30%AA, 0.8% BisAA	20% w/v glycerol	7.5% v/v acetic acid
0.1% w/v SDS	5% w/v SDS	40% methanol
0.1% w/v APS	bromophenol blue	
1% TEMED		

3.5.4. Western blot

Proteins separated on a 15% SDS-PAGE gel were transferred to a Polyvinylidene fluoride (PVDF) membrane using a semi-dry blot chamber. Therefore, two Whatman filter (1 mm) and the PVDF membrane were cut to the size of the gel. The Whatman filters were soaked with running buffer (table 3.10) and one filter was placed on the anode of the blot chamber. The PVDF membrane was activated in methanol for 2 min and place on top of the first membrane followed by the gel and the second soaked Whatman filter. The proteins were transferred at a consistent current of 2 mA/cm² for 30 min. Afterwards the gel was silver stained to check complete transfer of proteins of interest. The membrane was then blocked with 5% w/v non-fat milk over night at 4°C. Milk was removed on the membrane was washed 5 times with 10 mL Tris-base saline buffer with Tween (TBST; table 3.10). The primary antibody was added in a 1:500 dilution in 10 mL TBST to the membrane and incubated for 3 h at 4 °C. As primary antibodies monoclonal mouse anti-human S100A8 and anti-human S100A9 were used. The membrane was then washed 5 times with 10 mL TBST. Polyclonal horse anti-mouse IgG conjugated with horseradish peroxidase was added to the membrane in a 1:10000 dilution in 10 mL TBST and incubated for 1 h at 4 °C. The secondary antibody was removed and the membrane washed 5 times with 10 mL TBST. Finally, chemiluminescence was detected with the ChemiDoc™ XRS+ System using SuperSignal® West Femto Maximum Sensitivity Substrate in a 1:1 dilution of SuperSignal® West Femto Luminol/Enhancer Solution and SuperSignal® West Femto Stable Peroxide Solution.

**Table 3.10: Preparation of buffers used for western blot analyses**

TBST buffer	running buffer
50 mM Tris-HCl (pH 9.5)	25 mM Tris-HCl (pH6.8)
150 mM NaCl	192 mM glycine-NaOH (pH 8.5)
1 mM MgCl ₂	20% methanol
0.05% Tween 20	

3.6. Sample preparation

3.6.1. Trypsin digestion

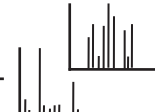
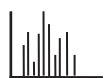
Prior digestion human wound fluids were filtrated with Costar Spin-X cellulose acetate (0.22 μ m) filter to remove tissue, or cell debris contaminations. For discovery experiments 750 μ g of proteins from each wound fluid was digested with trypsin in 1:100 ratios of trypsin to protein over night at 37 °C. For SRM analysis 1 mg of proteins in exudates or plasma was used. Cysteine residues were reduced with 10 mM dithiotreitol for 1 h at 37 °C. Reduced cysteine residues were alkylated with 25 mM iodoacetamide in the dark for 1 h at room temperature. The digestion with trypsin (1:100) was performed in 30% methanol over night at 37 °C. After methanol removal, the solution was filtered with Nanosep 10 kDa centrifugal devices and finally dried down in a vacuum concentrator and kept at -28 °C until further use.

3.6.2. In-Gel trypsin digestion

Coomassie stained SDS-PAGE bands were excised from the gel and cut into 1 mm³ cubes. The gel cubes were destained in 50% v/v ACN and 25 mM ammonium bicarbonate. The solution was renewed until the gel cubes were completely transparent. After removal of the destaining solution the cubes were dried in a vacuum concentrator. Completely dried cubes were moisturised with a trypsin solution (1:50), left for 10 min at room temperature to soak in the solution and was finally covered with a fresh trypsin solution to guarantee moisturising throughout the overnight digestion at 37 °C. The generated peptides were eluted from the gel using alternating incubation in 50% v/v ACN and 0.1% v/v formic acid and 2% v/v ACN and 0.1% formic acid. The collected fractions were combined, dried down in a vacuum concentrator and stored at -28 °C until further use.

3.6.3. PNGase F digestion

To enable the mass spectrometric characterisation of asparagine linked N-glycosylated peptides, N-glycan structures have to be removed. Therefore, peptides generated from



trypsin digestion were reconstituted in 25 mM ammonium bicarbonate and digested with PNGase F in ratios of 0.001 units PNGase F per 100 µg sample. Peptides were incubated overnight at 37 °C, dried down and stored at -28 °C.

3.7. Mass spectrometric characterisation

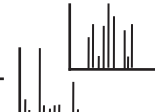
3.7.1. Column preparation

Except for the analytical columns employed in the SRM studies the column were self-packed using purchasable chromatographic batch material. Luna C18 RP material (100 Å, 3 µm) was used for hydrophobic peptide separation. polysulfoethyl was used to realise SCX-based ionic separation of a peptide solutions. MudPIT columns were prepared as exchangeable trapping columns were one end of a fused silica capillary (inner diameter: 100 µm) was closed by a highly porous silica frit or a titanium dioxide frit inside a union. This column was filled with 3 cm RP material followed by 5 cm SCX material and another phase of 3 cm RP material. This column was inline connected to an analytical column. For MudPIT analyses on the LTQ Orbitrap velos and the LTQ XL, a fused silica column (inner diameter: 100 µL) filled with 30 cm RP material was prepared. In the SRM study on the 5500 QTrap peptides were first concentrated and purified on a 5 µm Symmetry C18 RP trap column and were separated on a 15 cm nanoAcquity 1.7 µm BEH130 C18 RP column. In the SRM study on the 4000 QTrap peptides were trapped on a self-packed MudPIT or 3 cm RP traps and separated on a 15 cm RP column.

3.7.2. Liquid chromatography

Throughout the studies 3 different high performance liquid chromatography systems (HPLC) and 1 ultra-performance liquid chromatography system (UPLC) were employed. The LTQ Orbitrap velos study used an Accela HPLC, the LTQ XL study used an UltiMate 1000 HPLC and the 4000 QTrap study employed an Eksigent NanoLC 2DTM System. A nanoAcquity UPLC System was used for the SRM study on the 5500 QTrap.

Peptide elution from MudPIT columns involved an ACN gradient to transfer peptides from the first PR phase to the SCX phase, followed by consecutive salt steps of increasing ammonium acetate concentrations each followed by an ACN gradient. An ACN gradient describes the linear mixture of equilibration buffer (2% ACN, 0.1% FA, pH 3.0) and the elution buffer (80% ACN, 0.1% FA, pH 3.0) as shown in figure 3.1. On the LTQ Orbitrap velos and the LTQ XL a first ACN gradient (figure 3.1a) of 180 min (including reequilibration) was used with effective peptide separation up to 45% of the elution buffer (80% ACN, 0.1% FA, pH 3) which is common for digests of soluble proteins. The ACN gradients with ammonium acetate steps (figure 3.1b) consumed 130 min of instrument



time. In total a sample was analysed in 10 consecutive steps of 0, 25, 50, 75, 100, 125, 150, 200, 250, and 1500 mM ammonium acetate. Elution of peptides in MudPIT-SRM on the 4000 QTrap was except for autosample injection of salt steps of 15, 30, 300, and 1500 mM with ACN gradients of 30 min. In addition to the conventional flow path, a second injection loop was introduced, which was continuously filled with stable isotope labelled reference peptides by infusion using a Harvard model 22 syringe pump (Harvard Apparatus, Holliston, MA, USA). The introduction of a second injection loop is explained in detail in chapter 7. ACN gradients of 60 min in total were used for SRM analyses on the 5500 QTrap.

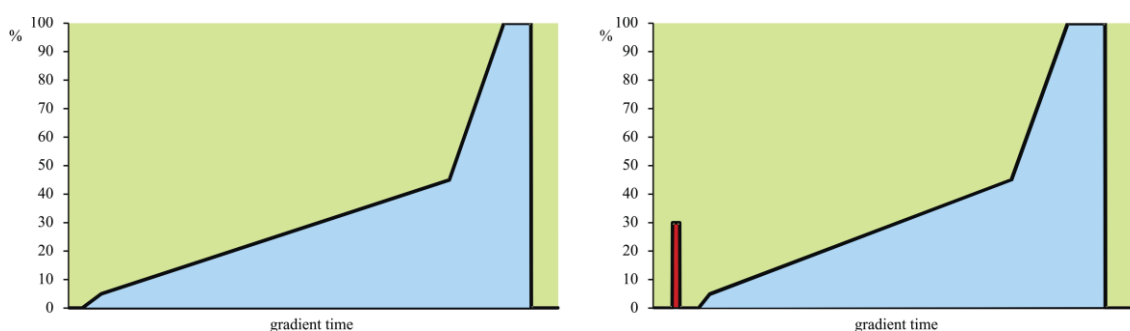


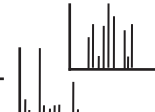
Figure 3.1: schematic of used ACN gradients without (a) or with (b) salt steps integrated; green: equilibration buffer, blue: elution buffer; red: ammonium acetate buffer

3.7.3. Tandem MS on LTQ Orbitrap velos

Peptides were transferred from the analytical column, which was placed in a heating device with an inside temperature of 45 °C, to the mass spectrometer using a spray voltage of 1.8 kDa and a desolvation capillary temperature of 200 °C. Full MS scans were performed from 400 – 2000 m/z in using FT-MS in the orbitrap followed by tandem MS/MS experiments of the 20 most intense signals in the previous full MS scan in the linear ion trap. Intensities, which have been analysed once, were rejected for 60 s (dynamic mass exclusion) to increase the accessible dynamic range. Further, charge screening was enabled and m/z values from ions higher than 3+ were rejected. Full MS spectra were acquired as profile spectra with a maximum orbitrap fill time of 500 ms in the positive ion mode. MS/MS spectra were acquired in the positive mode as centroid spectra using an ion trap fill time of maximal 100 ms and 1 μ scan per MS/MS spectrum.

3.7.4. SRM on 4000 QTrap

Eluting ions were transferred to the 4000 QTRAP mass spectrometer using a spray voltage of 2.4 kV and a heating plate temperature of 150 °C. Precursor ion were isolated in quadrupole 1 (Q1), fragmented with collision induced dissociation (CID) in Q2 by collision with nitrogen gas and their characteristic product ions were detected in Q3



allowing a dwell time for each transition of 20 ms, which is generating a cycle time of 2 – 3 s, depending on the number of transitions. In non-quantitative investigations eluting target analytes were validated using SRM triggered MS/MS scans from isolated precursor ions. Therefore, Q1 and Q2 were employed as filtering quadrupoles only. Precursor isolation, fragmentation and fragment detection was achieved using the ion trap function of Q3.

3.7.5. SRM on 5500 QTrap

Transfer of peptides into the 5500 QTrap mass analyser was achieved by applying a 2.5 kV spray voltage and a heating plate temperature of 150 °C. Q1 was used to isolate precursors, which were fragmented by CID in Q2 and their characteristic product ions were detected in Q3. A dynamic dwell time was used for each transition generates a cycle time of approximately 1 s per duty cycle.

3.7.6. Tandem MS on LTQ XL

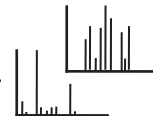
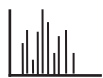
The LTQ XL settings to transfer eluting peptides into the mass spectrometer were the same as those used for the LTQ Orbitrap velos. Different to LTQ Orbitrap velos, both the precursor ions and the fragment ions were analysed in the linear ion trap. Full MS scan from 400 – 2000 m/z followed by the analysis of the 10 most intense intensities by MS/MS was conducted using an ion trap fill time of maximal 100 ms and 1 μ scan per MS/MS spectrum. The dynamic exclusion was set to 60 s. Charge state screening and charge state rejection was not possible.

3.8. Data Analysis and Statistics

3.8.1. Database searches

Proteome discoverer Software

Received MS/MS spectra from the LTQ XL and the LTQ Orbitrap velos were interpreted with the SEQUEST algorithm implemented in the Proteome Discoverer software. Spectra were searched against the human Swiss-Prot database release 15.6/57.6. All accepted human peptides had an FDR of 0.05 using reversed database searches. For LTQ Orbitrap velos derived spectra precursor mass accuracies were set to 10 ppm. Fragment ion mass tolerances were set to 1 atomic mass unit (amu). Mass accuracy for precursor and fragment ions derived from LTQ XL spectra were set to 2.5 and 1 amu, respectively. All identified peptides had peptide specific probability scores greater than 20 (software specific score). Further, the oxidation of methionine was set as a possible modification. Proteins with a minimum of 2 unique peptides identified in a MudPIT analysis were considered as presented in the sample.



Mascot Server

The MS/MS spectra derived from QTrap M/MS were searched against the human Swiss-Prot database using the Mascot algorithm. A precursor accuracy of 0.6 and a fragment tolerance of 1.2 amu were used. All identified peptide had at least a mascot specific probability score of 30.

3.8.2. SRM transition integration

5500 QTrap

The acquired SRM transitions were analyzed using the post-processing software Multi-Quant 2.1 employing the Q4 algorithm. Peak integration was performed using a 3 point peak smoothing. Within triplicate injection of sample digests retention time shifts of less than 30 s were accepted as reproducible target retention. A lower limit of detection (LLOD) of S/N below 3 times the noise and a lower limit of quantitation (LLOQ) below 10 times the noise were set as quality values. Most intense transitions of targeted peptides were normalized against the most intense transition of the spiked (15 fmol) isotope labelled CRP peptide ESDTSYVSLK (labelled amino acid underlined) peptide to estimate expression level in the wound fluids.

4000 QTrap

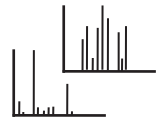
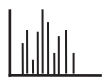
For each transition extracted ion chromatograms (XIC) were generated and the area under the curve (AUC) determined using the imbedded quantitation tool in the instrument software Analyst. This tool implements the IntelliQuant algorithm. Peak integration was performed using a 3 point peak smoothing. Within triplicate analyses retention time shifts of less than 30 s were accepted as reproducible target retention.

3.8.3. GO-Term analysis and protein localization

MS/MS identified proteins in each individual were grouped by biological functions as listed in the proteome discoverer software 1.3 (Thermo fisher scientific, San Jose; California). Protein percentage per group was estimated and mean percentages over all individuals in the chronic and the acute wound cohorts were calculated. Student's t-test was used to identify significant changes in protein numbers.

3.8.4. Statistics

One tail heteroscedastic student's t-test were used to estimate the significance of expression differences of proteins identified in the discovery study and peptides targeted in the SRM study. Protein and peptide expression level discrepancies were considered as significant with p-values < 0.05.



4. Enrichment of lower abundant proteins

In mass spectrometry, enrichment of lower concentrated proteins is in several areas necessary. With increasing complexity of a sample, limitation in detection and analysis by interfering substances or suppressing agents become dominant problems [57-59]. As a basic tool in almost any mass spectrometric analysis in the proteomic field, RP chromatography is applied to lower the amount of analytes reaching the MS detector at a given time point. Additional chromatographic approaches such as size exclusion or strong ion exchange can be applied either within the MS analysis workflow or offline prior LC separation. Besides chromatographic methods, preanalytic affinity strategies have been proven to be beneficial for mass spectrometric approaches. These include immunopurification or immunodepletion, protein interaction, or enrichment of PTM such as phosphorylation (TiO₂, IMAC), acetylation (antibody based), or glycosylation, which will be discussed in more detail in paragraph 4.1.

4.1. Enrichment of glycosylated proteins

Glycosylated proteins are proteins modified by glycan residues. Predominantly secreted proteins to the extra cellular space are post-translational glycosylated. This modification commonly serves in structural recognition pathways. Many cells extensively express glycosylated membrane bound proteins to attract specific stimulants to the cell surface. Further, receptors located in the extracellular membrane comprise high specificity for certain glycan structures and are therefore used in important outside-in signalling pathways. Additionally, glycan structure recognition is essential in pathogen defence as immunoglobulins such as IgG recognize eukaryote unusual glycan structures potentially derived from bacteria [60].

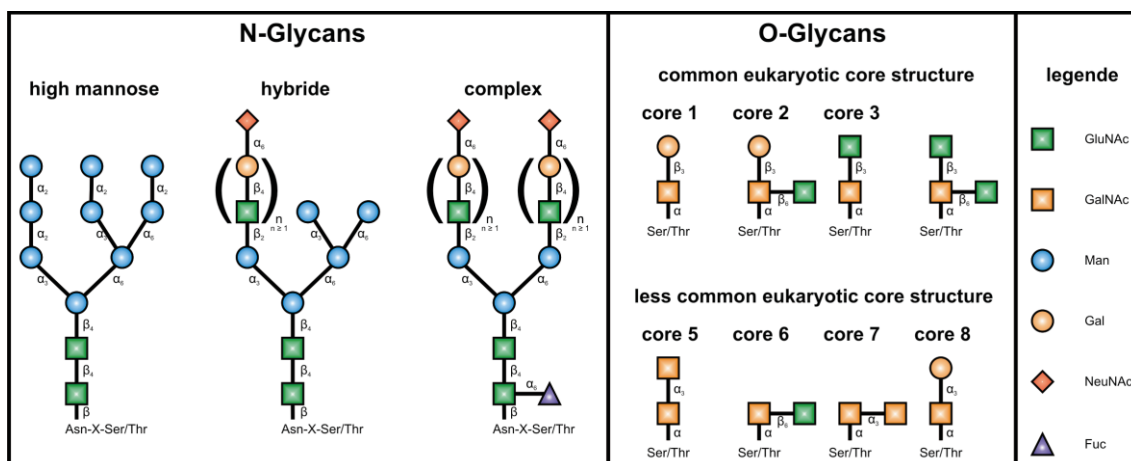
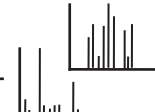
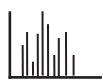


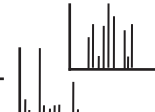
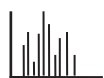
Figure 4.1: core structure of N- and O-glycosylated proteins in eukaryotic organisms



Two major forms of protein glycosylation are known (figure 4.1), the N-glycosylation of the amine group of aspartic acid residues and the O-glycosylation of the hydroxyl group of serine and threonine residues and less common of hydroxylysine and hydroxylproline residues [60]. Enzyme driven N-glycosylation occurs in the endoplasmic reticulum (ER) modifying proteins presenting Asp-X-Ser/Thr motifs where X can be any amino acid except proline. In vertebrates, N-glycans in general are attached to the protein via an N-acetyl-D-glucosamine (GlcNAc). Three types of GlcNAc N-glycosylation are described for vertebrates. All N-glycans share one core structure consisting of two GlcNAc and three mannosyl residues ($\text{Man}_3\text{GlcNAc}_2$) to form a biantennary core. High mannose N-glycans comprise additional 2 – 6 mannosyl residues. Hybrid N-glycans exhibit one mannose antennary and one antennary with lactosamine ($\text{Gal}\beta 1\text{-4GlcNAc}$) residues with possible N-acetylneuraminic acid (NeuNAc) termination. In complex N-glycans both antennaries have lactosamine residues with possible NeuNAc termination and a potential L-fucose modified Asp-linked GlcNAc. The final N-glycan structure arrangement on a protein depends on the accessibility of the glycan and the time the protein spent in the Golgi apparatus. Each N-glycan is first attached as a high mannose glycan then processed to its final occurrence by mannose cleaving enzymes and GlcNAc, galactose and NeuNAc transferring enzymes in the Golgi [61].

The enzyme regulated O-glycosylation of serine or threonine residues occur in the Golgi apparatus. Investigations have not succeeded to identify a common O-glycosylation motif. However, certain necessities were described which includes a proline residue and uncharged amino acids in the vicinity of glycosylation as well as alanine, and additional serine or threonine residues next to the glycosylation site. Different to N-glycans, in O-glycosylation N-acetyl-D-galactosamine serves as the linkage between oligosaccharides and the protein. Further, O-glycans comprise a larger variety of core structures (figure 4.1), varying from short single antennary structures to highly complex biantennary glycans with multiple lactosamine repeats. Therefore, O-glycosylation is a more complex and less generalized PTM compared to N-glycosylation [62].

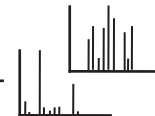
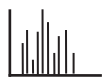
In general, investigations into glycoproteins utilize enrichment of glycosylated proteins by affinity chromatography. Several different strategies for glycoprotein enrichment have been developed [63-74]. All of them have in common that the used resin bind to specific structure or the entire glycan attached to glycoprotein. For enrichment purposes lectins are frequently used [63-69, 75-78]. Lectins are proteins with high specificity for carbohydrates. They were found throughout all organisms. However, mainly



used in enrichment strategies are plant derived lectins, predominantly concavalin A (ConA) and wheat germ agglutinin (WGA). ConA is a representative of mannose binding lectins, WGA binds GlcNAc. Therefore, lectin enrichment strategies are specific for a certain protein or a subset of glycoproteins exhibiting a particular glycan species. Especially in targeted proteomics, a defined enrichment of the target protein can overcome detection limitation as presented by Ahn et al. [64]. They described enrichment of glycosylated TIMP 1 from plasma of colorectal cancer patients using the lectin Phytohaemagglutinin followed by SRM quantification. This strategy allowed the identification of TIMP 1 at atomolar concentrations.

Lectin based investigations have been reported and rigorously applied by the group of W. Hancock [65-69, 75-78]. Combination of multiple lectins within a single affinity chromatography enabled the co-enrichment of different glycan species. However, acquired data by multi lectin affinity chromatography (MLAC) still represent only a subset of the glycoproteome. Therefore, other materials to enrich glycosylated proteins were investigated. Hydrazine for instance enables the enrichment of glycoproteins or glycopeptides by covalent binding of the attached glycan structures [70]. The hydrazine resin condensates with free hydroxyl-groups of a cyclic sugar from polysaccharide chains in 2-3 position. In order to regain bound glycoproteins either protein digestion on the enrichment resin or enzyme based cleavage of the hydrazine – glycan complex has to be performed. Immobilized hydrazine glycopeptide capture was described by Zhang et al. [71]. PNGase F digestion was performed to release the glycopeptides from the resin by cleaving the Asp-GlcNAc bond. Investigation of glycosylated peptides is therefore limited to N-linked glycoproteins as only N-glycans can be cleaved under mild conditions without protein damage. O-glycan cleavage involves aggressive chemical reactions causing extensive peptide modifications.

It has been shown [74] that boric acid derivatives demonstrated high potential in binding glycoprotein via 1, 3- or 1, 4-diole. Hence, boric acid derivatives are capable to enrich a broad variety of glycosylated proteins Xu et al. [79] used immobilised boronic on gold surfaces and demonstrated applicability to complex samples. Further, hybrid affinity chromatography of p-aminophenyl boronic acid and lectins (BLAC) were applied to achieve high specificity for a certain subset of glycoproteins but without losing the context of differently glycosylated proteins [73].



4.1.1. Boric acid gel affinity chromatography of glycoproteins

Although numerous different enrichment strategies have been established for glycoproteins the optimal strategy for competitive glycoproteomics is still missing. Therefore, boric acid gel (Sigma Aldrich) was investigated for enrichment efficiency of glycoproteins.

The enrichment efficiency and the applicability of the boric acid gel affinity chromatography (BAGAC) to complex samples was assessed by the enrichment of purified glycosylated bovine proteins, purified bovine glycoproteins spiked in to a complex matrix (wound fluid with glycoproteins) and by the efficiency of enrichment of glycoproteins present in human wound fluids. BAGAC was performed using the workflow depicted in figure 4.2.

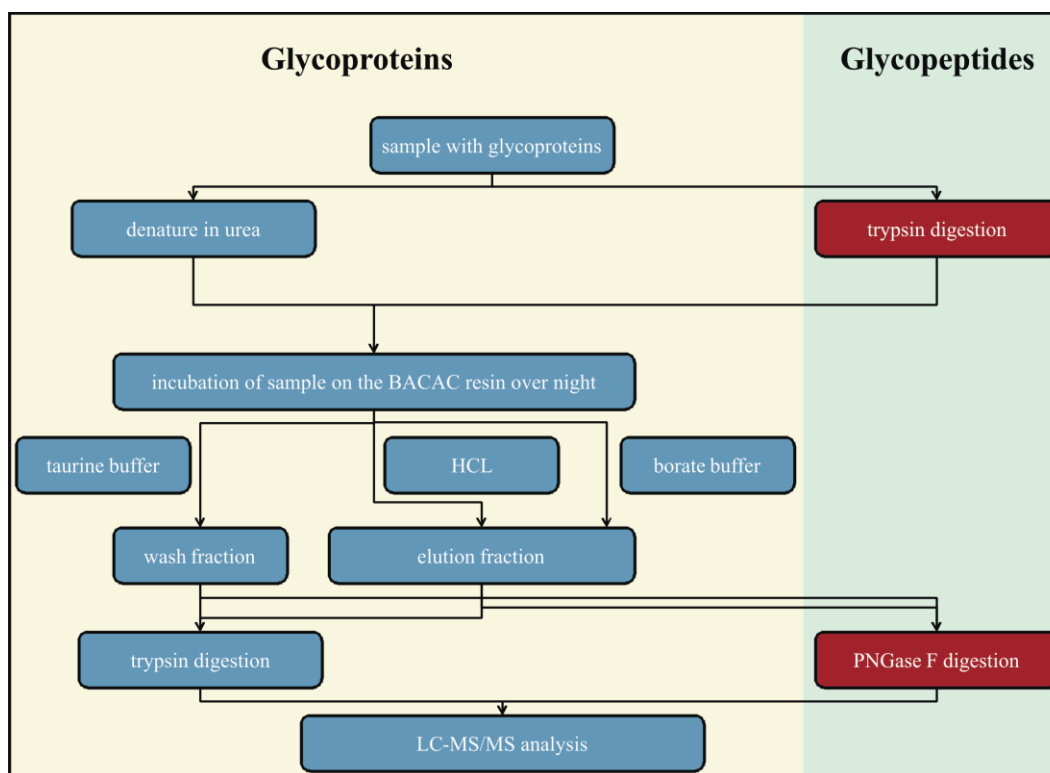
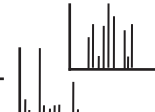
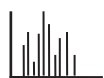


Figure 4.2: BAGAC workflow used for glycoprotein (yellow) and glycopeptide (green) enrichment

As depicted in figure 4.3, SDS-PAGE analysis demonstrated the ability of BAGAC to enrich the purified bovine glycoproteins alpha-2-HS-glycoprotein (fetuin A) and alpha-1-acid glycoprotein (A1AG). However, fetuin A showed more efficient enrichment by BAGAC than A1AG. The gel showed beside the A1AG bands in the elution fractions of bound glycoproteins with hydrochloric acid and the borate buffer (lane 2-3 and lane 2-4), a weak band in the wash fraction (lane 2-2). Although A1AG is present in the wash fraction, the larger portion of applied A1AG was bound by the boric acid gel. Fetuin A was



identified in the combined elution fraction (lane 1-3) but not in the wash fraction (lane 2-2). Therefore, both proteins demonstrate successful enrichment by the BAGAC resin.

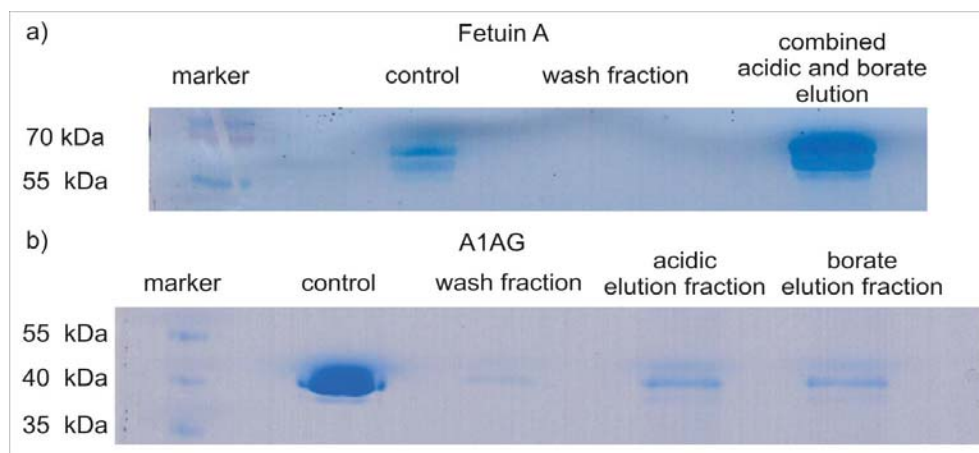


Figure 4.3: coomassie stained SDS-PAGE of recovered BAGAC enriched purified bovine glycoproteins fetuin A and A1AG using taurine wash (wash fraction), 1 M HCl (acidic elution fraction) and borate buffer washes including ACN borate buffer (borate elution fraction)

Since BAGAC is capable of enriching purified glycoproteins, these proteins were spiked in a 1:10 ratio in to a complex human matrix. To enhance the binding ability of glycoproteins to the BAGAC resin, the used samples were denatured with 8 M urea prior enrichment. Collected wash and elution fractions were analysed in triplicates by mass spectrometry to evaluate the enrichment efficiency under competing conditions. In agreement to the SDS-PAGE of purified glycoproteins, mass spectrometric analysis showed enrichment of fetuin A and A1AG within a complex matrix (table 4.1) based on spectrum count and sequence count comparison of the wash and elution fraction. Fetuin A was identified in two of three replicates with one spectrum in the wash fraction but with 2 – 6 unique peptides and 4 – 12 spectra in the elution fraction replicates. Thus, presence of fetuin A in the wash fraction is insignificant. In two of three replicates of spiked A1AG, this glycoprotein was exclusively identified in the elution fraction with 80 spectra from 7 peptides and 39 spectra from 9 peptides. In one analysis A1AG was detected in the wash fraction and the elution fraction. It was found with 14 spectra from 7 peptides in the wash fraction but with 32 spectra from 9 peptides in the elution fraction, presenting comparable results to the SDS-PAGE in which A1AG was detected in the elution but also less intense in the wash fraction when enriching purified glycoproteins. Assumedly, the BAGAC resin is less specific for A1AG.

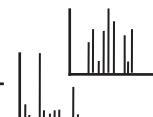


Table 4.1: BAGAC wash and elution fraction specific spectrum and peptide counts of identified bovine fetuin A and A1AG peptides spiked in to human wound fluids

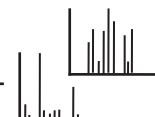
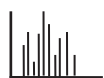
Fetuin

wash fraction		elution fraction	
spectrum count	peptide count	spectrum count	peptide count
-	-	4	2
1	1	12	6
1	1	8	5

A1AG

wash fraction		elution fraction	
spectrum count	peptide count	spectrum count	peptide count
-	-	80	7
-	-	39	9
14	7	32	9

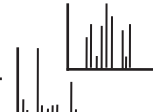
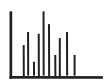
Nonetheless, the SDS-PAGE and the spike-in experiment revealed the applicability of BAGAC to enrich glycosylated proteins using purified or complex samples. As a final validation experiment BAGAC was used to enrich glycosylated proteins in a human wound fluid sample. Triplicate analysis (40 µg each) revealed 104 glycoproteins to be identified in total of which 58 proteins were present in at least two of three analyses (table 4.2). These proteins were assessed by spectral counting to estimate the enrichment efficiencies. Spectral counting demonstrated satisfying enrichment of almost 85% of the 58 glycoproteins with only 3 proteins (5 %) depicting higher spectrum counts in the wash fraction. Human fetuin A was among nine other proteins (17%) exclusively identified in the elution fraction. Twenty seven glycoproteins (46%), one of them human A1AG1, were more often identified in the elution fraction but were also present in the wash fraction. Ten proteins (17%) were in two of three replicates more often identified in the elution fraction but showed in one replicate equal or higher spectrum counts in the wash fraction. Therefore, in correlation to the bovine glycoprotein experiments, BAGAC demonstrate different specificity for a given glycosylated protein. A reasonable explanation for influences in the enrichment efficiency could be secondary, tertiary and quaternary protein structures. The proteins applied to the BAGAC resin were denatured under non-reducing conditions, thus disulphide bonds still stabilising specific protein structures which might decrease the binding strength of certain glycoproteins. Further, the binding strength is influenced by the number of glycosylated residue. The higher the number of polysaccharides attached to a protein the higher the binding strength to the BAGAC resin. Therefore, a protein with one glycosylation site is bound weaker to the resin and thereby



more likely to be identified in the wash fraction, whereas multiple glycosylated proteins such as fetuin A, clusterin, heparin cofactor II, some complement system proteins, leucine-rich alpha-2-glycoprotein, and alpha-2- macroglobulin-like protein 1 are bound tighter to the resin and were more efficiently enriched.

Table 4.2: triplicate analysis of BAGAC enriched human wound fluids contrasting identified proteins with known glycosylation sites according to the SwissProt database in the wash and elution fractions; colour indication: green: glycoproteins were exclusively or more abundantly identified in the elution fraction, red: glycoproteins were exclusively or more abundantly identified in the wash fraction, black: glycoproteins were equally often or not identified in the replicate; synonyms used sq: sequence, pep: peptide

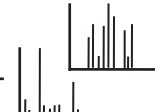
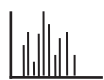
accession number	protein	wash 1		elution 1		wash 2		elution 2		wash 3		elution 3	
		sq	pep	sq	pep	sq	pep	sq	pep	sq	pep	sq	pep
P02763	A1AG1	4	4	10	6	7	2	8	4	-	-	6	5
P01011	AACT	9	6	39	16	16	7	20	10	-	-	16	7
P01009	A1AT	17	14	58	20	17	9	24	10	9	5	28	16
P04217	A1BG	8	5	12	9	-	-	3	3	-	-	-	-
P02765	Fetuin A	-	-	5	2	-	-	4	2	-	-	-	-
P01023	A2MG	24	18	32	24	6	6	14	13	-	-	7	6
A8K2U0	A2ML1	-	-	5	5	-	-	-	-	-	-	8	8
P01019	ANGT	4	3	8	6	9	6	6	4	-	-	-	-
P01008	ANT3	-	-	18	10	7	4	10	7	-	-	6	5
P02647	ApoA1	5	5	7	5	5	3	9	6	-	-	-	-
P04114	ApoB	6	6	4	4	2	2	6	6	-	-	-	-
Q9UI42	CBPA4	2	2	-	-	-	-	-	-	4	3	-	-
P07339	CATD	4	4	6	4	2	2	-	-	-	-	7	4
P00450	CERU	9	8	2	2	-	-	3	3	-	-	2	2
P10909	CLUS	-	-	4	3	-	-	3	3	-	-	-	-
P01024	CO3	44	28	38	27	11	9	26	20	3	3	18	15
P0C0L4	CO4A	10	8	-	-	3	2	7	5	-	-	-	-
P01031	CO5	-	-	4	4	-	-	-	-	-	-	2	2
P02748	CO9	2	2	3	3	-	-	3	3	-	-	-	-
P00751	CFAB	2	2	8	8	3	3	6	5	-	-	-	-
P08603	CFAH	6	5	15	10	2	2	6	4	-	-	2	2
P05156	CFAI	-	-	2	2	-	-	2	2	-	-	-	-
Q15517	CDSN	-	-	3	2	-	-	3	2	-	-	4	3
P08185	CBG	-	-	-	-	-	-	2	2	-	-	3	2
Q08554	DSC1	3	2	10	7	-	-	5	3	-	-	-	-
Q14574	DSC3	7	6	5	4	-	-	-	-	-	-	9	8
Q02413	DSG1	11	8	13	10	6	4	7	5	-	-	17	11
P02671	FIBA	-	-	-	-	-	-	4	4	-	-	4	4
P02675	FIBB	24	11	6	5	4	3	9	5	-	-	4	4
P02679	FIBC	8	5	4	4	-	-	3	3	-	-	3	3
P02751	FINC	11	10	34	25	8	7	13	11	-	-	2	2



accession number	protein	wash 1		elution 1		wash 2		elution 2		wash 3		elution 3	
		sq	pep	sq	pep	sq	pep	sq	pep	sq	pep	sq	pep
P00738	HPT	6	6	26	13	-	-	7	7	-	-	-	-
P69905	HBA	10	2	9	4	3	2	4	3	5	2	7	4
P68871	HBB	10	7	14	7	7	4	4	3	3	2	10	7
P02790	HEMO	24	2	9	5	7	2	6	3	-	-	-	-
P05546	HEP2	-	-	6	4	-	-	2	2	-	-	-	-
P04196	HRG	6	5	8	6	4	2	4	3	-	-	-	-
P01876	IGHA1	4	3	5	3	-	-	5	2	-	-	2	2
P01857	IGHG1	15	6	20	7	10	4	15	5	-	-	11	5
P01859	IGHG2	10	5	16	4	-	-	13	3	-	-	8	2
P01871	IGHM	-	-	-	-	-	-	2	2	-	-	2	2
P19827	ITIH1	6	5	12	9	2	2	4	3	-	-	-	-
P19823	ITIH2	2	2	8	6	-	-	6	4	-	-	-	-
Q14624	ITIH4	5	4	19	14	8	7	9	7	-	-	-	-
P01042	KNG1	2	2	4	4	-	-	3	3	-	-	-	-
P02788	TRFL	15	13	11	10	3	2	7	6	-	-	9	8
P05164	MPO	2	2	3	3	-	-	-	-	4	3	-	-
P80188	NGAL	5	5	3	3	-	-	-	-	2	2	-	-
Q15063	POSTN	2	2	-	-	2	2	4	4	-	-	-	-
P36955	PEDF	-	-	5	4	4	3	5	5	-	-	-	-
P05155	IC1	-	-	15	10	10	5	6	4	-	-	3	3
P12273	PIP	-	-	3	2	-	-	-	-	16	3	6	2
Q02383	SEMG2	-	-	-	-	10	8	-	-	-	-	2	2
P02787	TRFE	16	5	25	13	12	7	21	9	-	-	9	9
P36952	SERP5	9	7	8	8	-	-	-	-	-	-	3	3
P02768	ALBU	136	16	37	15	22	8	46	14	12	7	30	13
P02766	TTHY	8	7	4	4	-	-	8	7	-	-	-	-
P25311	ZA2G	8	7	8	7	3	3	3	3	-	-	10	7

Another important aspect is the efficiency of glycosylation. The degree of modified potential glycosylation sites depends on the amino acid following the asparagine in the NXS/T motif and the distance to the C-terminus [80]. With increasing abundance of a protein with few or only one glycosylation sites, a non-glycosylated species of a particular glycoprotein might be present in detectable quantities. This effect and also a possible deglycosylation could be an explanation for the presence of high abundant proteins such as alpha-2-macroglobulin (A2MG), ceruloplasmin, complement C3 (CO3), fibrinogen beta (FIBB), fibrinogen gamma (FIBG), and serotransferrin in the wash fraction.

The identified plasma proteins haemoglobin A and B and serum albumin are not post-translational glycosylated but are susceptible for glycation as previously described by non-enzyme controlled reactions with free glucose or glucose metabolites. Depending on the



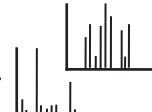
free glucose level in the blood the degree of glycosylated proteins vary greatly, which is influencing the outcome of BAGAC enrichment of these proteins.

Despite the protein based drawback, the BAGAC method proved to be an applicable strategy to enrich proteins from complex human specimens showing 49 proteins (85%) more often or exclusively identified in the elution fraction. Comparing these findings to the conventionally used MLAC enrichment of glycosylated proteins, the BAGAC strategy demonstrate advantages in terms of sample handling using less complex elution steps, which reduces the risk of protein losses and the cost for the enrichment since carbohydrates for the elution and lectins for the enrichment are not necessary. Further, the BAGAC method revealed 85% enrichment of glycoproteins, while for the MLAC strategy an enrichment of 75% was reported [81]. Therefore, BAGAC demonstrates a more efficient enrichment of glycoproteins.

4.1.2. Boric acid gel affinity chromatography of N-glycosylated peptides

Based on the applicability of BAGAC to enrich glycosylated proteins, this method was used to enrich glycosylated peptides for comparative analysis of glycosylation sites in normal versus poor healing wounds. The workflow showed in figure 4.2 was adjusted to handle glycopeptides. Briefly, cysteine residues of proteins in the wound fluids were reduced and alkylated to increase accessibility and detectability of proteins with disulphide bonds. Proteins were digested with trypsin as described in paragraph 3.6. After filtration peptides were applied to the enrichment resin. The resin was washed and the peptides eluted under the conditions previously used to enrich glycoproteins. Peptides in the collected fractions were digested with PNGase F to remove N-glycans and allow mass spectrometric characterisation of N-glycosylated peptides. O-glycosylated peptides were not investigated due to the difficulties in O-glycan removal discussed previously.

Analysis of N-glycosylated peptides from bovine A1AG and fetuin A as well as N-glycosylated peptides from human wound fluids demonstrated insufficient enrichment by the BAGAC material (table 4.1 and figure 4.4). A1AG possesses 5 potential glycosylation sites. Two of those are located on detectable tryptic peptides. The other three are located on peptides comprising difficulties for mass spectrometric characterisation due to the peptide length. Both detectable glycopeptides were more often identified in the wash fraction. EYQTIEDKC*VYN[#]C*SF⁺IK (C* indicating carbamidomethylation [+57.02146 Da] of cysteine residues and N[#] indication deamidation [-0.98401 Da] of asparagine residues) was identified with one corresponding MS/MS spectrum in the wash



fraction, TFMLAASWN[#]GTK was identified with 3 MS/MS spectra in the wash fraction and two spectra in the elution fraction.

Table 4.3: N-glycosylated peptides derived from tryptic digest of the bovine proteins A1AG and fetuin A; used synonyms: n/d not detectable by mass spectrometry due to the peptide length; n/i: not identified by MS/MS

protein	peptide	wash fraction	elution fraction
A1AG	EYQTIEDKC [*] VYN [#] C [*] SFIK	1	-
	MALLWALAVLSHLPLDDAQSPEC [*] ANLMTVAPI		n/d
	TN [#] ATMDLLSGK		n/i
	NPEYN [#] K		n/i
	QN [#] GTLSK		n/i
	TFMLAASWN [#] GTK	3	2
Fetuin A	LC [*] PDC [*] PLLAPLN [#] DSR	4	3
	RPTGEVYDIEIDTLETTTC [*] HVLDPTPLAN [#] C [*] SVR	7	1
	VVHAVEVALATFNAESN [#] GSYLQLVEISR	30	2

N-glycosylated peptides of fetuin A demonstrated similar to A1AG more frequent identification in the wash fraction. VVHAVEVALATFNAESN[#]GSYLQLVEISR, LC^{*}PDC^{*}PLLAPLN[#]DSR, and RPTGEVYDIEIDTLETTTC^{*}HVLDPTPLAN[#]C^{*}SVR were identified with 30, 4, and 7 corresponding MS/MS spectra in the wash fraction and 2, 3, and 1 spectra in the elution fraction. Investigation of N-glycosylated peptides in human wound fluids revealed comparably results. In total 61 glycopeptides were identified, 56 in the wash fraction and 13 in the elution fraction of which only 5 were exclusively identified in the elution fraction.

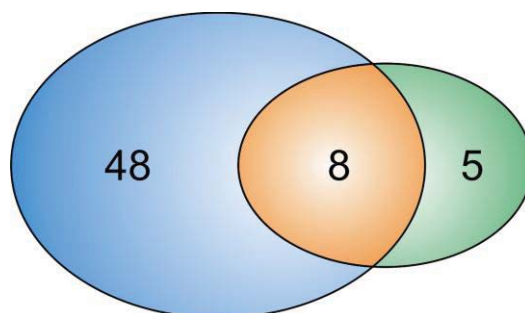
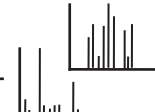


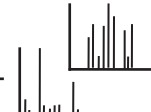
Figure 4.4: number of identified N-glycosylated peptides from human wound fluids in the wash fraction (blue) and the elution fraction (green) and peptides the were identified in both (orange)

For glycoproteins that contain multiple carbohydrate moieties, successful enrichment by BAGAC was demonstrated, therefore, it can be assumed that the binding strength of a singly glycosylated substance is not strong enough to resist the taurine wash step. These finding correlate with the assumption made in the glycoprotein enrichment where proteins with multiple glycosylation sites were more efficiently enriched than singly glycosylated proteins. In conclusion, BAGAC demonstrated successful enrichment of glycosylated proteins but failed in the enrichment of glycopeptides most likely due to the limited glycosylation sites per molecule.

4.2. Immunodepletion of high abundant proteins

Especially in the time of mass spectrometry with low resolving power, antibody based depletion of highly abundant proteins was rigorously applied to complex samples, predominantly plasma [82-93]. Purchasable products vary from albumin removal only up to depletion of the top 20 high abundant plasma proteins. Several kits are available from numerous suppliers either binding high abundant proteins or enriching low concentrated proteins by restricted antibody binding per protein.

In the early phase of work flow development for human wound fluid analysis we approved the ProteoPrep[®] 20 Plasma Immunodepletion kit as an applicable strategy to increase the accessible concentration range in human wound fluids [91]. Anderson and Anderson showed [94] that human plasma possesses a dynamic range over 10 orders of magnitude, whereas mass spectrometer around that time were able to accessed dynamic range of 3 – 4 orders of magnitude. With developing high resolution mass spectrometer, the accessible dynamic range increased dramatically. Therefore, analyses have been carried out to assess the necessity of immunodepletion of human wound fluids by comparing MudPIT analyses of two wound fluids depleted and non-depleted. Surprisingly, both wound fluids demonstrated better results for the non-depleted variant. Protein identification increased 1.5 – 2 fold compared to the depleted samples (figure 4.5). Further,



depleted wound fluids still contained plasma proteins which supposed to be removed by the antibodies. Their relative concentration, estimated by spectral counting, was still higher than any other protein of interest. The expression levels of identified spectra derived from proteins supposedly depleted was more than 30%, whereas these proteins made up less than 20% in non-depleted sample. This indicates that, besides depletion of highly abundant plasma proteins, a significant elimination of other proteins occur which might have a relevant influence in wound healing and might distort the conclusions drawn from the results. Therefore, proteins known to be involved in wound healing processes, such as the S100 protein family, MMP family, Interleukins and their enhancer, and growth factors and their stimulants were compared by spectral counting (table 4.4). For almost all selected proteins the number of identified unique peptide sequences and the assignment of peptide sequences to MS/MS spectra increased significantly. Moreover, proteins unable to be identified in the depleted sample were able to be detected in the non-depleted sample. Interleukins and their enhancer for instance were almost exclusively identified in the non-depleted wound fluid sample, some in quantities suitable for quantification. These findings demonstrate an enormous advantage of non-depleted wound fluids analysis with high resolution and fast scanning mass spectrometer.

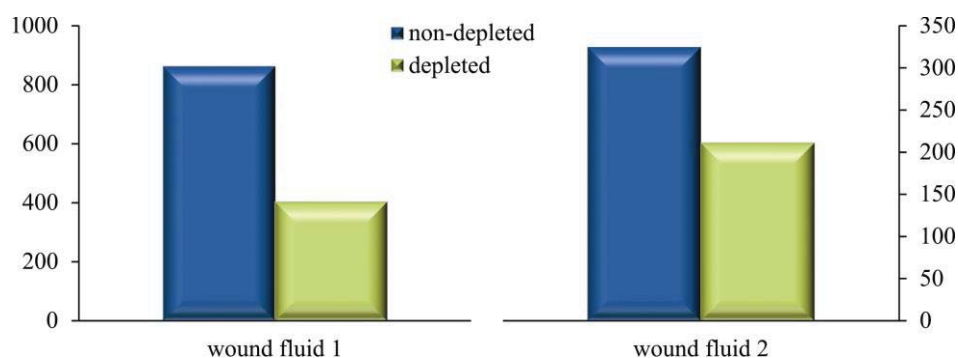
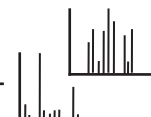
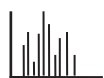


Figure 4.5: number of identified proteins in top 20 immunodepleted and non-immunodepleted variants of human wound fluids

Table 4.4: crucial proteins associated to healing processes identified in a non-immunodepleted human wound fluid compared to a top 20 high abundant plasma protein immunodepleted variant of the same wound fluid

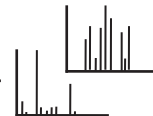
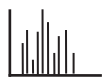
accession number (SwissProt)	protein	immunodepleted variant		non-immunodepleted variant	
		spectrum count	unique peptides	spectrum count	unique peptides
P35858	ALS	43	7	42	13
P04083	ANXA1	67	15	101	20
P50995	ANXA2	1	1	11	4
P07355	ANXA5	5	3	23	5
P51858	HDGF	3	2	9	3



accession number (SwissProt)	protein	immunodepleted variant		non-immunodepleted variant	
		spectrum count	unique peptides	spectrum count	unique peptides
Q04756	HGFA	3	1	-	-
P26927	HGFL	1	1	5	2
P24592	IBP6	1	1	3	1
Q16270	IBP7	-	-	1	1
P01583	IL1A	1	1	-	-
Q9UBH0	IL1F5	2	1	1	1
Q9NZH8	IL1F9	-	-	1	1
P18510	IL1RA	-	-	5	2
P05231	IL6	-	-	4	3
P40189	IL6RB	-	-	1	1
P13232	IL7	-	-	1	1
Q99665	IL12R2	-	-	1	1
Q14005	IL16	1	1	1	1
Q12905	ILF2	-	-	2	2
Q12906	ILF3	-	-	13	4
P03956	MMP 1	3	3	23	10
P08253	MMP 2	16	4	26	12
P08254	MMP 3	-	-	7	4
P22894	MMP 8	8	4	56	13
P14780	MMP 9	48	9	38	14
P09238	MMP 10	-	-	4	3
P26447	S100A4	2	1	16	7
P06703	S100A6	-	-	6	4
P31151	S100A7	5	2	35	8
P05109	S100A8	68	6	184	21
P06702	S100A9	281	10	379	20
P31949	S100A11	35	1	36	6
P80511	A100A12	11	3	72	15

4.3. Concluding aspects of protein enrichment

Enrichment or depletion strategies as demonstrated here show in some areas advantages but also bear the risk of substantial analyte losses. Many lowly concentrated proteins are to some extent binding partners or interacting partners of high abundant plasma proteins. These interactions could cause co-depletion of those proteins while depleting highly abundant plasma proteins. Enrichment of glycosylated proteins encounters similar difficulties. Further, it is a method highly specialized for glycoproteome analysis. Investigating protein regulation for potential biomarker discovery in complex specimens highly specialized methods and methods susceptible to extensive protein losses are unfavourable. Therefore, analysis of human wound fluid was performed without fractionation or depletion prior to chromatographic separation and mass spectrometric characterisation to ensure homogeneity in sample preparation and analysis.

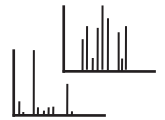
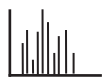


5. Molecular healing processes

T2DM derived poor healing ulcers, predominantly at the lower leg and foot, are common complications with significant decreases in the quality of life. Wounds are classified as poor healing wounds based on the time needed to heal. If a wound exceeds the time to heal extensively, this wound is termed “problematic wound”. Poor healing wounds or chronic wounds show abnormalities in regulating processes with prolonged inflammation [95, 96], reduced response to growth stimulation, and diminished tissue strength to close the wounding area [7, 17].

The prolonged inflammation in chronic wounds of diabetics is mainly derived by excessive neutrophil invasion into the wounded area due to higher vascular permeability. Neutrophils release elastase and cathepsin G normally degrading foreign material, and damaged tissue. However, persistent presence of neutrophils leads to extensive degradation of healthy tissue as well as immunoglobulins, clotting factors, complement system proteins, and cytokins [97-101]. It has been shown in a diabetic mouse model that mice with reduced neutrophils demonstrated faster wound closure [102]. In general, wounds with reduced inflammation demonstrated accelerated healing. To reduce protease activity, exogenous protease antagonists can provide promising improvements in wound repair. The first substance used to inhibit proteases in the wounded area was the tetracycline family antibiotic doxycycline. It is an inhibitor of metalloproteases and the tumour necrosis factor alpha (TNF α) converting enzyme [103]. The impact of tetracyclines were further demonstrated in animal studies either using doxycycline or chemically tetracycline analogues [104-107]. It was demonstrated that the application reduced MMP8 and MMP13 mRNA level [107]. MMPs are common targets for therapeutics as these proteases were identified in several studies to be elevated in the fluids of chronic wounds [108-112]. In turn, TIMPs were identified in lower expression levels [113, 114].

Increasing the amount of substrates for specific proteases is another approach to regulate the protease activity. MMPs for instance are gelatin degrading proteins. Introduction of a gelatin matrix into the wounded area is showing decreased MMP activity. Further, application of films, hydrogels, hydrofibers, and foams are used as dressing materials to reduce necrotic debridement and the excess of MMPs, and hydrates the wound bed [115]. A strategy additionally used to dressing materials applied to a chronic wound is the negative pressure therapy. The vacuum assisted closure (V.A.C.) therapy demonstrated accelerated wound closure. Assessment of wound fluid revealed increases of IL 8 and



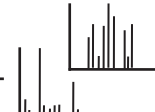
VEGF expression levels as a result of therapy [116], which are important mediators of wound repair progression.

However, not every protease inhibitor positively contributes to the healing process. In a plasminogen activator inhibitor 1 (PAI1) deficient mouse model for instance demonstrated accelerated wound closure compared to the wild type (wt) mice [117].

Analyses of exudates from acute wounds and chronic wound applied to different cell types demonstrated diverse results in terms of cell response. Acute wounds stimulated cell proliferation of fibroblasts, endothelial cells and keratinocytes [118], whereas chronic wounds demonstrated anti-proliferation and anti-angiogenic properties [119, 120]. Therefore, wound bed preparation additionally includes the application of growth factors. Growth factors are important initiators of angiogenic processes. It was identified that chronic wounds frequently demonstrate reduced angiogenesis, mainly derived from missing growth factors stimulation [121-126]. External application of growth factors is therefore a strategy to stimulate vascularisation of the dermis [127-131].

The application of PDGF, FGF, EGF, and TGF β 1 provided beneficial wound healing outcome demonstrated in several clinical trials [132-137]. They are commonly integrated into wound bed dressing matrices. A promising strategy for *in-situ* production of growth factors is the introduction of recombinant growth factor DNA plasmids into the wounds avoiding growth factor adsorption and inhibition at structural proteins of the ECM and more directly stimulation of angiogenesis [138]. Gene and stem cell therapy to treat chronic wounds is a more advanced technology, proceeding from wound bed preparation to wound bed regeneration. Introduction of DNA plasmids of positive wound repair stimulation proteins can more effectively trigger inflammation reduction and cell growth mechanism. Stem cells possess the ability to differentiate into various cell types, which can substitute cell types crucial to wound healing which are somehow inactivated or absent. Stem cell therapy has been shown to be beneficial in a clinical trial on 3 patients [139]. Further, the implantation of skin either from a different part of the body or bioengineered skin are possible application to treat poor healing wounds.

Nonetheless, all these methods imply thoroughly maintenance of the debridement. This includes the removal of necrotic material from the wound edge, phenotypically altered cells within the wound, and bacteria possibly imbedded in the wound. Without debridement management initially healing chronic wound bear the risk to regress to a non-healing wound [22, 115, 140].



5.1. General assessment of wound fluids

To assess the protein composition of exudates from T2DM patients showing chronic foot ulcers and exudates derived from thick skin donor sites of patients showing non-life-threatening burns, these samples were submitted to the proteomics work flow. BCA assay analysis of the wound fluids (table 11.1) demonstrated an equal distribution in protein concentrations in the chronic and the acute wound fluid with mean concentrations of 38.3 and 31.2, respectively. Initial analysis of proteins present in the two wound fluid types was accomplished by 1D-SDS PAGE separation of 20 μ g aliquots of representatives of the acute and chronic wound cohort. Figure 5.1 demonstrated similar distribution of housekeeping proteins throughout the compared fluids with minor differences, especially in the lower molecular weight range. For detailed information of the protein constitution, exudates of chronic wounds and acute wounds were analysed in triplicates by MudPIT-FT-MS/MS.

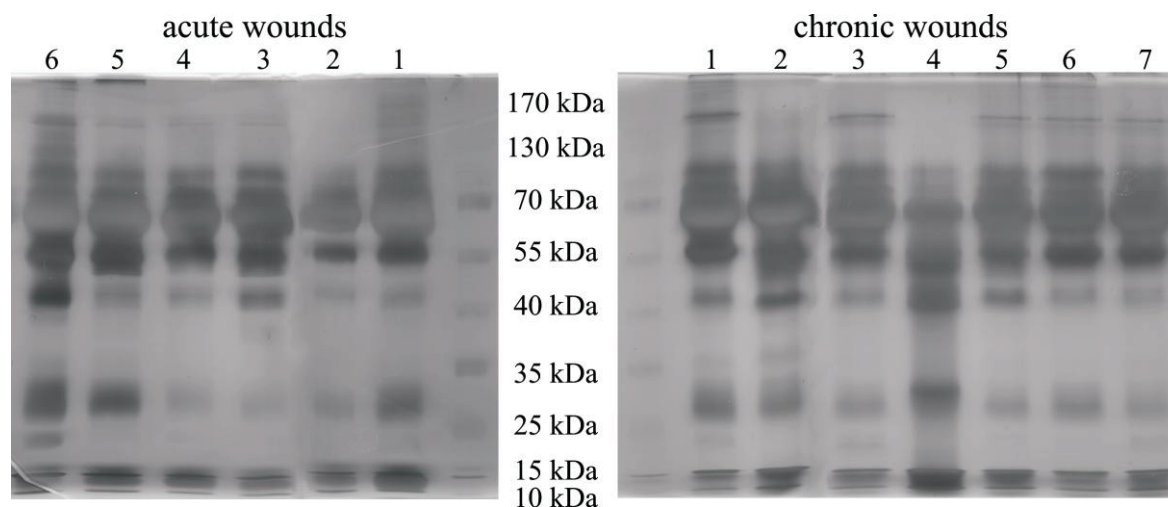
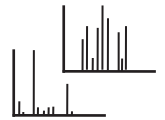
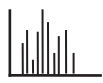


Figure 5.1: 1D-SDS PAGE separation of 20 μ g each of 6 acute and 7 chronic wound fluids

Label-free normalised spectral counting was employed as a relative quantitation tool to identify regulation differences in the wound fluids. In total 6 acute and 10 chronic wound fluids were investigated by MudPIT-MS/MS. Data analysis revealed 714 proteins to be present in the exudates. Housekeeping proteins such as alpha-2-macroglobulin, albumin, and immunoglobulins (IgA, IgG, IgM) or the lower abundant protein vitronectin showed no variation in normalised spectral counting (1 ± 0.2 -fold) (figure 5.2). This is demonstrating reproducible detection of these proteins throughout the data set of patients analysed in this study. However, some lower abundant proteins showed higher normalised spectral counting differences in expression (figure 5.2) as a consequence of biological variation in the compared fluids. Biological variation is always an issue in inter-individual



comparison studies. Therefore, proteins demonstrating spectral counting differences ≥ 2 -fold and p-values ≤ 0.05 were considered as significantly differentially expressed. Additionally, proteins that were more frequently (≥ 6 PHW and < 3 NHW or ≥ 4 NHW and < 5 PHW) identified in one wound type were also consider as differentially expressed. According to these criteria, 151 proteins (table 11.2) were identified in significantly higher expression levels in PHW, while 37 proteins (table 11.3) were at significantly lower expression levels in PHW. Interestingly, the inter-individual variations of protein expression level, especially for S100 proteins, are in the exudates of acute wounds less dominant than the variations in the exudates from chronic wounds. This might indicate less specific control of secretion processes in the chronic wounds.

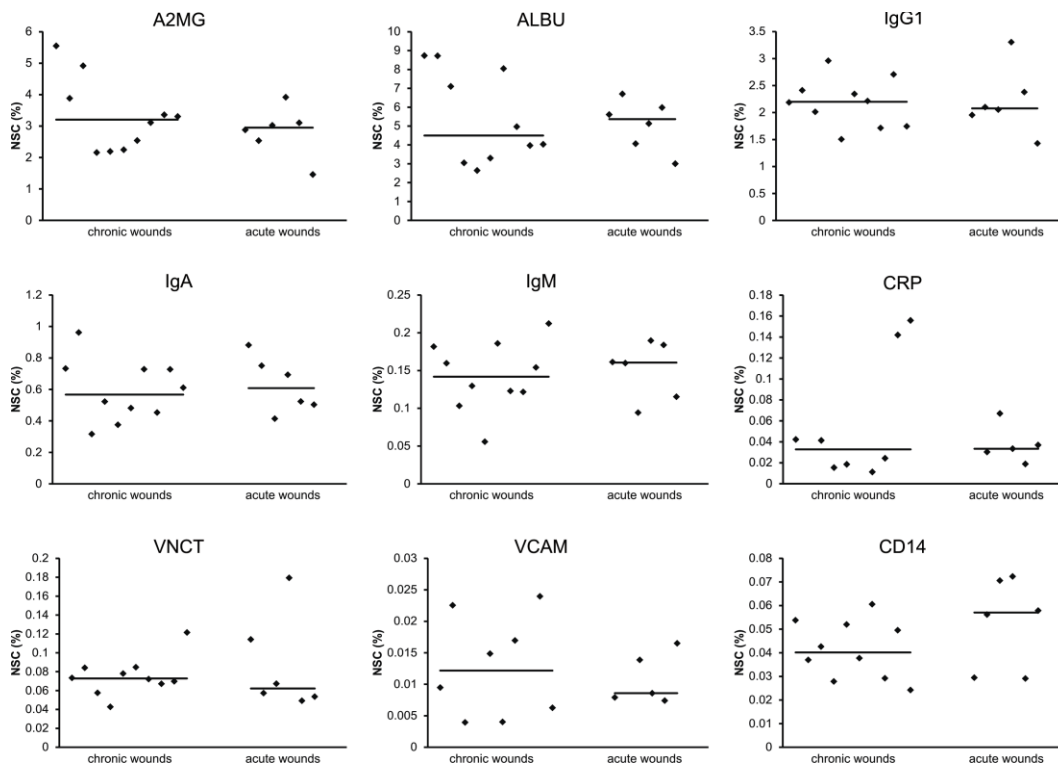


Figure 5.2: differential plot of housekeeping protein distribution in the compared wound fluids

Proteins identified in the wound fluids comprised several biological functions. The distribution of these functions is depicted in figure 5.3. The shown percentages are based on the number of proteins, not on spectral counting. In many categories, both wound fluids demonstrated similar percentages of identified proteins. However, PHW differed from the NHW in essential wound healing processes. Proteins involved in cell organization and biogenesis ($p < 0.01$), and biological development ($p < 0.01$) were more frequently identified in fluids from chronic wounds, whereas the number of proteins involved in the response to stimulation ($p = 0.01$), the defence response ($p < 0.02$), and coagulation ($p = 0.03$), were higher in fluids from acute wounds.

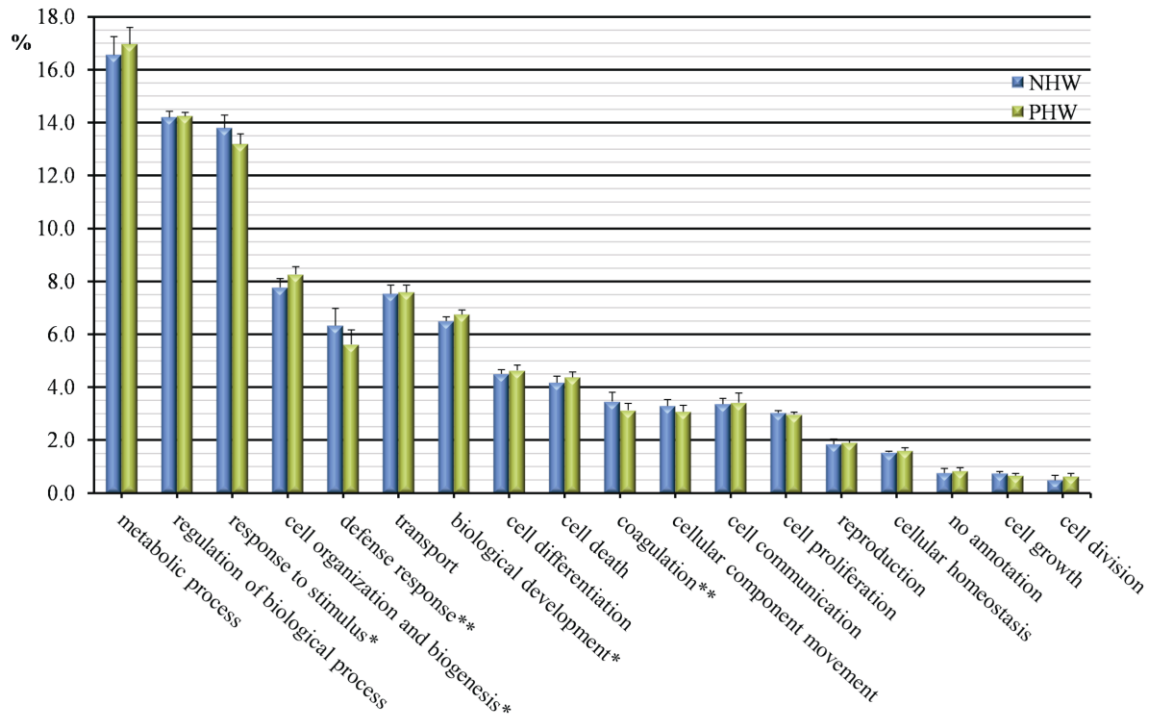
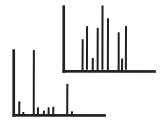
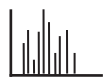
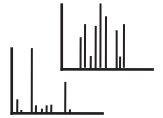
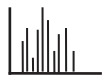


Figure 5.3: GO term protein function histogram of proteins identified in chronic and acute wounds, * $p \leq 0.01$, ** $p \leq 0.05$

Inferring from the protein function distribution, chronic wounds demonstrated regulation processes to keep the status of the wound, rather than regulating tissue redevelopment. Additionally, the chronic wounds might be more susceptible to invading pathogens. Besides the differences observed in protein numbers in the protein functions, spectral counting based comparison of PHW to NHW demonstrated protein expression differences in several areas, e.g. inflammatory response, coagulation, vasculogenic and angiogenic stimulation, and extracellular cell death stimulation with pivotal impact on healing regulation.

5.2. Coagulation

Coagulation to prevent extensive blood loss and pathogen invasion is the initial step in the response to an occurred wound and stimulates inflammation and cell growth. As demonstrated in the GO-term analysis, chronic wound fluids showed lower numbers of proteins involved in coagulation. This is further demonstrated by differing protein expression levels of coagulants and anti-coagulants in the assessed wound fluids. Coagulation factors (FA) play a pronounced role in the generation of the fibrin clot and platelet activation. Different pathways are known. The intrinsic pathway involves FA XII conversion to active FA XII (FA XIIa) after contact with damaged surfaces. The extrinsic pathway involves FA VII activation due to tissue trauma. Both pathways lead to the



activation of FA X, which converts prothrombin (FA I) to thrombin (FA Ia). Thrombin in turn converts fibrinogen (FIB; FA II) to fibrin (FA IIa) which is then transformed by FA XIIIa to fibrin clots. However, the activation of FA X is also stimulated by platelet membrane phospholipids [141].

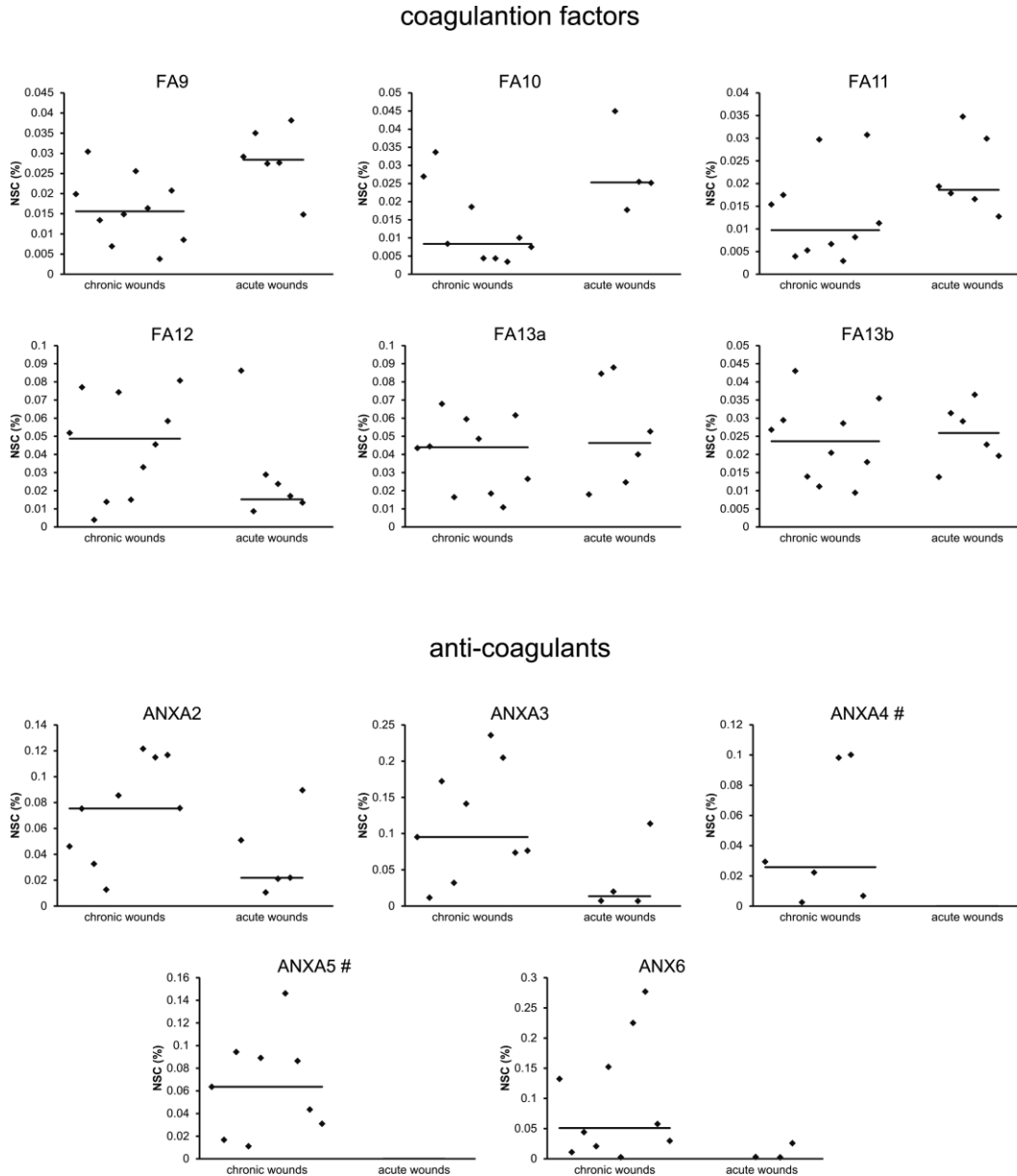
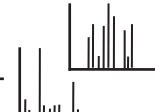
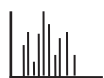


Figure 5.4: plot of individual expression level of coagulation involved proteins identified in the compared wounds fluids

The identified FAs (figure 5.4) in the compared wound fluids suggest the intrinsic pathway as the common coagulation motif. FA XII was 3.2-fold elevated in the chronic wounds. However, FAs in the downstream cascade of the intrinsic pathway showed lower expression levels (FA XI 1.8-fold, FA IX 1.9-fold, FA X 3.0-fold). As FA X is significantly lower expressed in the fluids from chronic wounds, it is reasonable to assume that thrombin generation is limited. Further, equal expression of the anti-coagulant

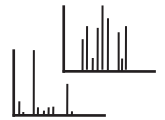
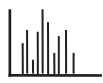


antithrombin 3 (ANT3) should then dramatically decrease the activity of thrombin. Thus, the conversion of fibrinogen to fibrin is limited. The fibrinogen chains alpha, beta, and gamma were identified in both wound fluid cohorts. FIBA was similar expressed in the compared wound fluids, while FIBB and FIBG were 2-fold elevated in the chronic wounds. This could infer accumulation of FIBB and FIBG in the fluids due to impaired conversion of fibrinogen to fibrin.

ANT3 and the thrombin-activable fibrinolysis inhibitor (TAPI; carboxypeptidase B2) are important anti-coagulants. Both were found at similar expression level in the wound fluids. Other endogenous anti-coagulants are members of the ANX family. ANXs are Ca^{2+} binding proteins enabling a unique membrane binding motif via phospholipids integrated in the membrane. ANXA2, A3, A4, A5 and A6 are known proteins to function as anti-coagulants [142]. All five were identified as higher (ANXA2, ANXA3 and ANXA6) or exclusively expressed (ANXA4 and ANX5) in fluids from chronic wounds (figure 5.4). Phospholipid binding of ANXs inhibits the phospholipid derived FA X activation. Therefore, chronic wounds exhibit reduced coagulation and elevated inhibition of phospholipid mediated coagulation. These conditions might indicate reduced numbers of platelets and the platelet secreted growth factors.

5.3. Inflammation signalling

The inflammation signalling S100 proteins were identified in differing expression levels in the compared wound fluids. S100A8 and S100A9 were detected as highly elevated in PHW at levels of 8-fold and 10-fold, respectively (figure 5.5). These proteins are secreted by myeloid cells, mainly neutrophils and monocytes, and are important stimulators of the local inflammatory response. Binding of the S100A8/S100A9 heterodimer to RAGE or TLR leads to the release of pro-inflammatory cytokines to increase the inflammatory response. Although less excessive, other S100 proteins also demonstrated elevated expression levels in PHW (figure 5.5). Expression levels of S100A4, S100A11, and S100P varied from 3.5 to 4.4-fold. S100A6 was unable to be quantified as it was exclusively but infrequently identified in patients with PHW (4 of 10 cases). Therefore, S100A6 was not considered as differently expressed in fluids from chronic wounds. S100A12 showed 1.9-fold higher expression in PHW. It is another binding partner for RAGE. Additionally, S100A12 chelates Zn^{2+} ions to build complexes with different proteins. As some proteins bind Zn^{2+} in inactive forms, higher expression of S100A12 could negatively influence the activation of those proteins [143].



Stimulation of RAGE and TLR pathways induce pro-inflammatory cytokine secretion that further mediates S100 protein release. The anti-inflammatory protein ANXA1 inhibits NF-kappaB DNA binding and thereby the translation of pro-inflammatory cytokines [144]. ANXA1 was 5.2-fold higher expressed in PHW, suggesting an environment of reduced inflammatory potential. The 2.6-fold higher expressed lacto-transferrin, a protein with anti-microbial and anti-inflammatory properties, and the presents of interleukin 1 receptor antagonist (IL-1RA) with higher frequency in PHW (5/10 cases) compared to 1 of 6 cases in NHW are supporting this observation.

Nonetheless, the acute phase serine protease inhibitor (serpin) A3 (alpha 1 antichymotrypsin; AACT), a protein induced in the wounded area to reduce leukocyte activity [145] and thus, reduce inflammatory signalling, was identified as 3.5-fold lower expressed in PHW, suggesting endocrine derived pro-inflammatory conditions in PHW. AACT is an inhibitor of cathepsin G and mast cell chymase which are potent proteases degrading connective tissue, leading to further release of pro-inflammatory molecules. Therefore, although anti-inflammation signalling is induced by the wound proximity, endocrine derived pro-inflammatory conditions are accelerating inflammatory signalling. Eming et al. [53] showed comparable results for the calcium binding proteins S100A8, A9, ANXA1 and lactotransferrin in patients suffering from crural ulcer (ulcis cruris) if compared to NHW. Immunohistology and LC-MS/MS analyses presented higher expression for these proteins in the ulcer. However, the described higher expression of anti-microbial proteins in the ulcers was not observed in the foot ulcer.

Especially diabetics with hyperglycaemic episodes comprise elevated levels of non-enzyme controlled glucose or glucose metabolite modified proteins in the plasma [146, 147]. Plasma proteins are able to migrate into wounded areas. It is reasonable to assume the presence of AGE modified plasma proteins in the wounded area, leading to increased RAGE stimulation and might be an explanation of elevated S100 protein concentrations in chronic wound fluids. The pro-inflammatory cytokine IL6 might indicate increased RAGE stimulation. It was identified in 8 of 10 cases in PHW but in only 1 of 6 cases in NHW. Thus, chronic wounds display a continuing competition between inflammation increasing processes and anti-inflammatory signalling influencing the overall performance of the wounded area.

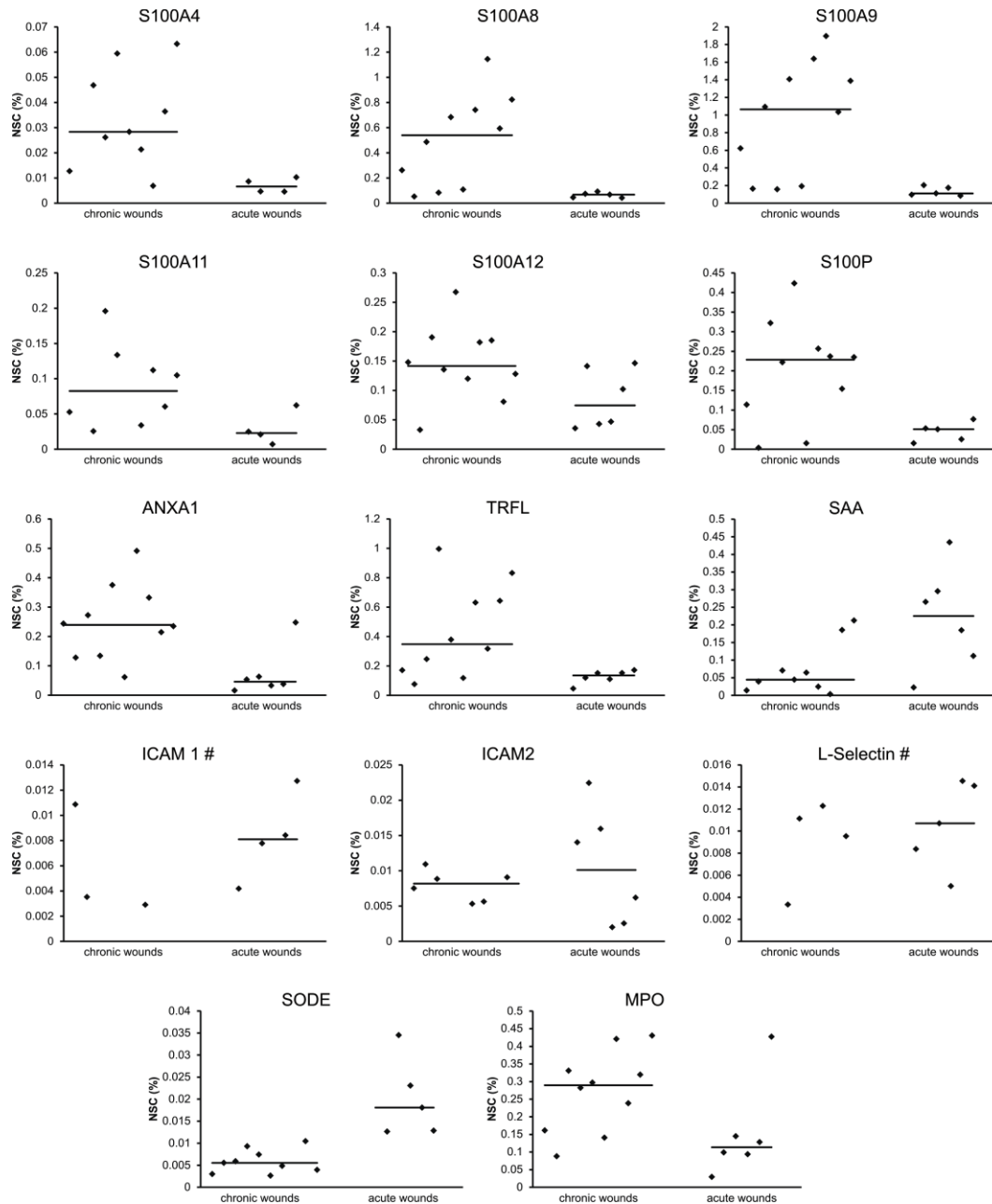
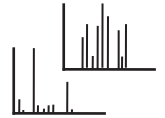
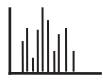
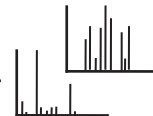
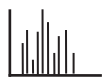


Figure 5.5: individual expression level plots of S100 proteins, anti-inflammation signalling proteins, cell adhesion proteins and endocrine derived proteins in the wound fluids; # means expression level unable to be calculated due to infrequent detection within sample cohort and statistics not applicable

Leukocytes are highly required for inflammation. Transendothelial migration of leukocytes involve adhesion molecules such as the intercellular adhesion molecules (ICAM), and the vascular cell adhesion molecules (VCAM) expressed by endothelial cells into the blood stream [148]. ICAMs and VCAMs are membrane proteins. Mass spectrometric identification in the exudates is therefore only possible of truncated soluble isoforms generated by cell surface shedding by a disintegrin and metalloprotease (ADAM) or MMPs. In the blood stream soluble isoforms of ICAMs and VCAMs are involved in the time management of leukocyte transendothelial migration. Soluble forms reduce the



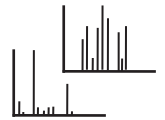
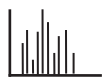
attachment of leukocytes to endothelial cells and thereby the transendothelial migration rate. Similar to the blood stream, soluble ICAM (sICAM) and sVCAM in the exudate of wounds could regulate the attachment of leukocytes and reduce the endocrine derived inflammatory signalling. Elevated inflammation should stimulate endothelial cells to express ICAMs and VCAMs, which in turn should lead to elevated sICAM and sVCAM. However, ICAM1 and ICAM2 were more frequently identified in fluids from acute wounds (ICAM1: 3/10 PHW, 4/6 NHW; ICAM2: 6/10 PHW; 6/6 NHW), VCAM1 was equally expressed. Similar results were found for L-selectin, which is involved in the transendothelial migration of lymphocytes. It was identified in 5 of 6 cases in the acute wound fluids, but only in 4 of 10 cases in chronic wound fluids. In conclusion acute wound fluids demonstrate early inflammatory response reducing properties, while chronic wounds further accelerate the inflammatory response.

Neutrophils, as early invading leukocytes in wound repair processes, generate reactive oxygen or nitric oxide species to defeat invading pathogens. In order to prevent excessive tissue damage oxidoreductases need to be present in the extracellular space. The extracellular superoxide dismutase (SODE), which converts O_2^- radicals to O_2 and H_2O_2 , was 3.3-fold lower expressed in PHW, inferring increased free O_2^- radicals in the extracellular matrix, possibly damaging health tissue leading to extracellular oxidative stress. However, myeloperoxidase (MPO), which reduces H_2O_2 in a halogenide oxidizing manner, was 2.5-fold elevated in the fluids of PHW, demonstrating an impairment of the H_2O_2 circle. H_2O_2 has been demonstrated to facilitate VEGF signalling, an important angiogenesis stimulator. Elevated H_2O_2 reduction might diminish this function, especially with lowered SODE new production of H_2O_2 . In this manner, the retinol binding protein (RBP) 4, a protein delivering the anti-oxidant retinol, was also identified as 3.8-fold lower expressed in the chronic wound fluids. Therefore, the fluids of chronic wounds show extensive reduction in anti-oxidative processes.

5.4. Vascularisation

5.4.1. MMP mediated angiogenesis

Oxygen and nutrition supply are essential for healthy cells and tissue. As developing tissue needs to be attached to the blood vessel and lymph network, signalling pathways for capillary growth have to be activated. Vessel growth from already existing vessels is termed angiogenesis, whereas vasculogenesis describes the process of new vessel development. Both are initiated differently but follow similar regulation pattern after initiation. ECM degrading proteins such as MMPs are positive regulator of angiogenic



processes. Cleavage of collagens by MMPs release important growth factors and cytokines stored in the ECM. Degradation of the ECM further increases cell mobility. However, elevated MMP concentrations, as common in chronic wounds, would generate extensive degradation of collagen, including the destruction of newly produced granulation tissue architectures, which mainly contains collagens, and would reduce vascularisation abilities.

MMP1, MMP2, MMP8, and MMP9 (figure 5.6) were consistently identified in this study, whereas MMP 3 and 19 were infrequently detected in the compared wound fluids, thus the latter ones were not feasible for relatively quantitation. Significantly higher expressed in PHW were MMP1 (2.2-fold), MMP2 (2.3-fold), and MMP8 (3.7-fold). Increased concentration of these proteases should dramatically decrease of collagen architectures, as these structural proteins are the major targets of these 3 MMPs. Collagen (CO) type 1, 2 and 3 are commonly degraded by MMP1 and MMP8. MMP 1 additionally degrades CO7, and CO10. MMP2 targets CO4, CO5, CO7, and CO10. Collagens comprise several interprotein interactions, creating a tight collagen network. Mass spectrometric characterisation of these proteins in wound exudates is therefore only accomplishable after predigestion of collagens by their endogenous proteases to generate soluble fragments of the network. Collagens were predominantly identified in PHW (figure 5.6). Collagen type 1 alpha 1 (CO1A1) and CO5A2 were, except for 1 NHW sample, exclusively identified in PHW, CO1A2, CO3A1, CO5A1 and CO6A3 were at higher levels in PHW. It is reasonable to assume that higher expression of collagens emerge from highly active MMPs in the chronic wounds, which extensively degrade their target collagens. The basement membrane perlecan is another substrate for MMPs and other ECM degrading proteases [149]. Analogue to collagens, perlecan was identified in higher expression level in the exudates of chronic wounds and supports the presumption of excessive metalloproteinase activity in the chronic wounds.

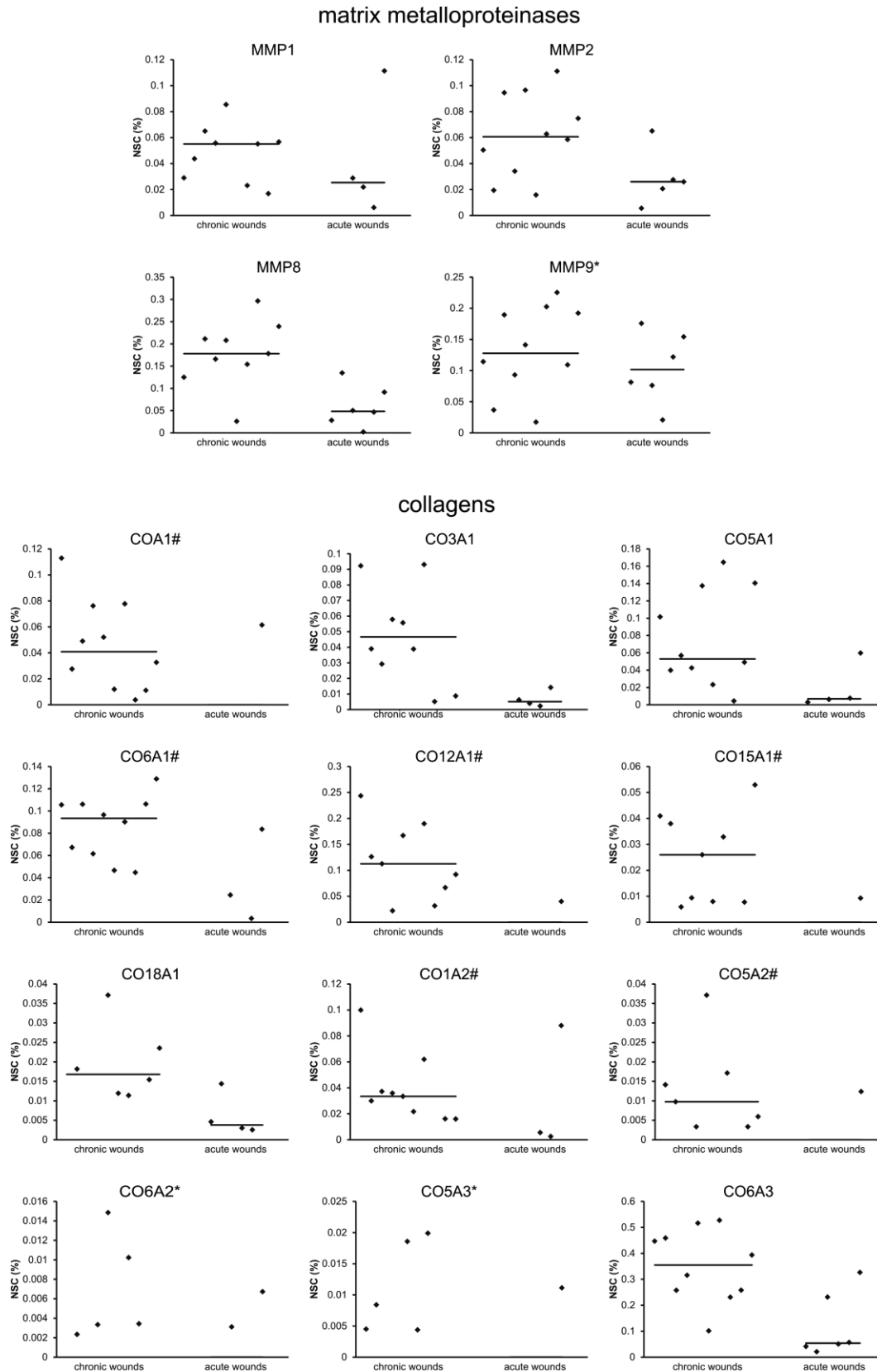
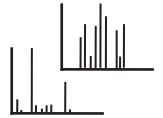
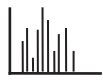


Figure 5.6: plot of individual expression level of MMPs and collagens in the acute and chronic wounds fluids; symbols indicates: # expression level unable to be calculated due to infrequent detection within the sample cohorts and statistics not applicable, * infrequently identified in both fluids but more often in chronic wounds fluids

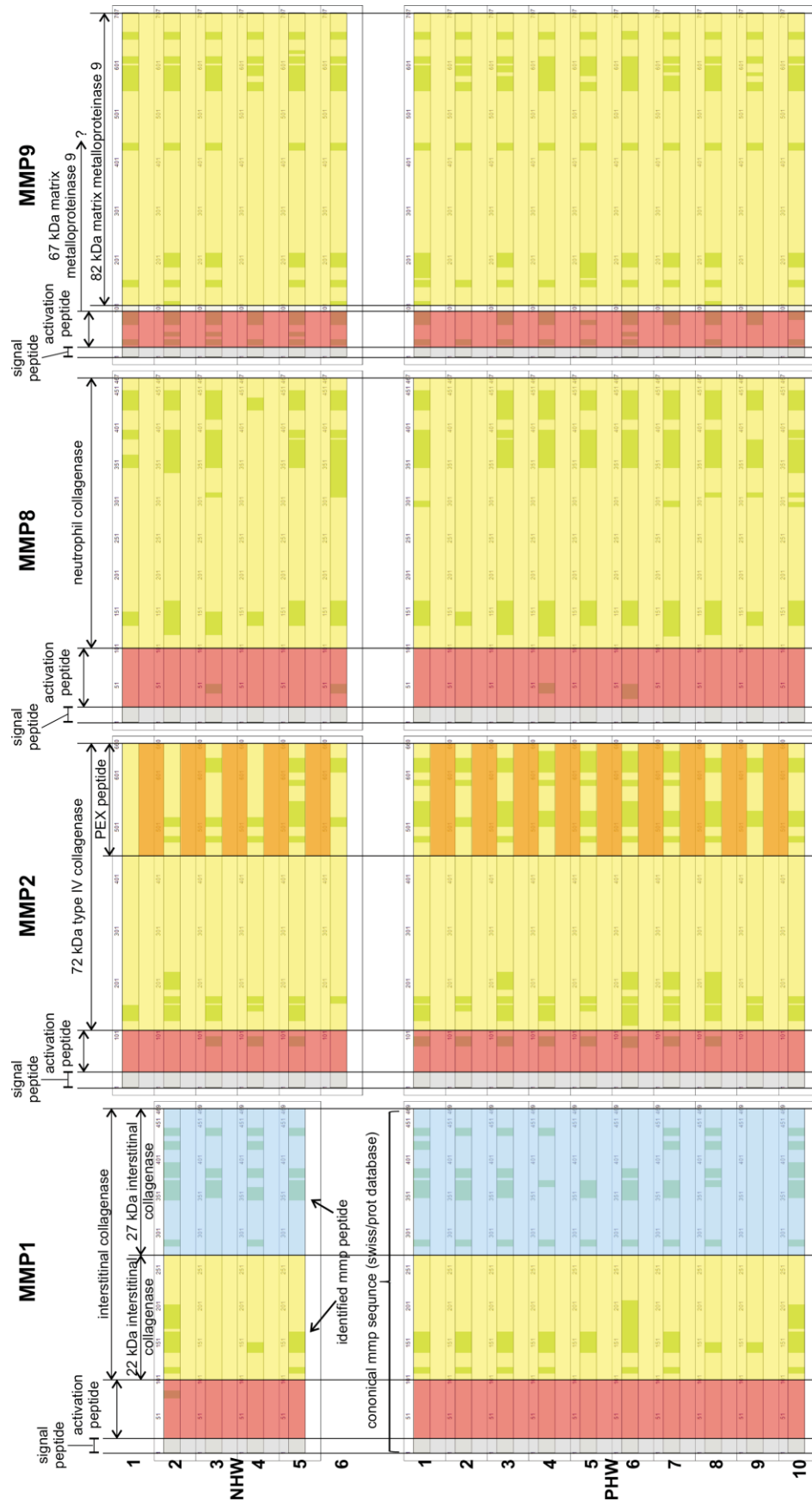
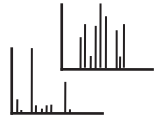
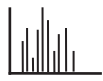
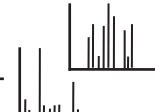
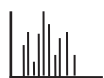


Figure 5.7: MudPIT-MS/MS identified peptides derived from different regions of MMP1, MMP2, MMP8, and MMP9



MMPs are secreted by keratinocytes, macrophages and fibroblasts in an inactive form. In general, activation occurs after cleavage of an N-terminal activation peptide in an autoproteolytic manner, or by other MMPs or proteases. Several MMPs such as MMP2 and MMP9 exhibit bound Zn^{2+} in the latent form. Zn^{2+} removal in a cysteine switch motif expresses the cleavage site for MMP activation. Figure 5.7 depict the identified peptides derived from different regions and cleavage products of MMP1, 2, 8, and 9. Interesting, MMP 2 and MMP 9 showed more frequent identification of peptides derived from the activation region in the chronic wound fluids, inferring excessive secretion of these two proteases. Further, more peptides representing the PEX region of MMP2 were detected in fluids from chronic wounds. Autocatalytic cleavage of this region generates an anti-angiogenic peptide [150, 151] that inhibits cell migration and cell adhesion of FGF2 and vitronectin. Assumedly, elevated expression levels of MMP2 should in turn generate high concentration of free PEX in PHW and thus, decrease angiogenic stimulation. The activation region of MMP1 and MMP8 were not identified.

The activities of MMP2 and MMP9 were further investigated by gelatin-SDS-PAGE zymography (figure 5.8). Except for one acute wound fluid with very minor levels (lane 2.5), the active isoform of MMP2 (64 kDa) was only visible in the chronic wounds (except 1.5). The latent isoform (72 kDa) was present in 4 of 10 chronic wounds (lane 1.2, 1.6, 1.9, 1.10), indicating ongoing secretion of MMP2. Latent MMP9 (92 kDa) and active MMP9 (82 kDa) isoforms were identified in the acute and the chronic wounds. The acute wound fluids showed roughly similar distribution of active and latent MMP9 within each individual whereas chronic wounds demonstrated higher expression in some chronic wounds (lane 1.3, 1.4, 1.9 and 1.10) and lower or similar expression in other chronic wounds (lane 1.1, 1.2, 1.5, 1.6).

These finding were supported by the calculated normalised spectral count percentage of MMP2 and MMP9 from the MudPIT-MS/MS study (table 5.1). These values are consistent with the intensities measured from the zymogram. Therefore, although spectral counting revealed similar expression of MMP9 in the chronic and acute wound fluids, zymographic results add crucial information about MMP9 secretion and activation. From these results it can be assumed that the fluids from chronic wounds demonstrate dramatic impairment in the secretion of MMP9 in the investigated patients.

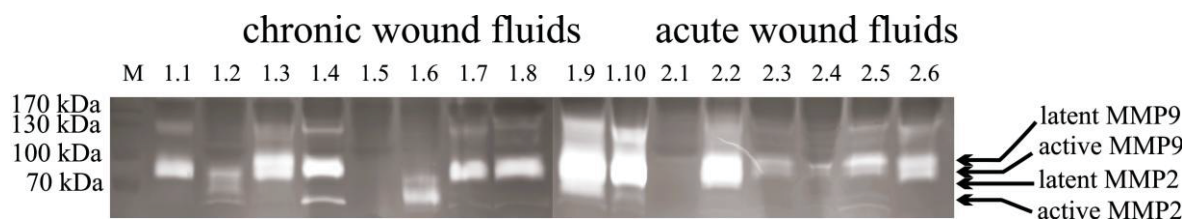


Figure 5.8: gelatin zymogram of active (64 kDa) and latent (72 kDa) MMP2 and active (82 kDa) and latent (92 kDa) MMP9 in the exudates of chronic (1.1 – 1.10) and acute wound (2.1 – 2.6) previously analysed in the MudPIT-MS/MS study

Although TIMPs are the main inhibitor of MMPs, other inhibiting proteins might have an impact on MMP activation and angiogenic stimulation. The inflammatory signalling protein S100A12 was described to have a significant influence on MMP activation inhibition [143]. In addition to Ca^{2+} binding S100A12 comprise several binding sides for doubly charged zinc or copper ions. Goyette et al. demonstrated S100A12 chelating of zinc ions in the cysteine switch region of MMP2, MMP3 and MMP9. Activation of these three MMPs occurs after zinc removal and exposure of the cleavage side of the activation peptide. The chelating effect of S100A12 prevents zinc removal and thereby inhibits the activation of these enzymes. S100A12 was found to be almost 2-fold elevated in the chronic wound fluids and might function as a response to elevated MMPs in the chronic wounds. An MMP activation inhibiting effect of TIMPs was not possible to investigate as TIMPs were unable to be detection in the MudPIT-MS/MS study.

Table 5.1: normalised spectral count percentages of MMP2 and MMP9 identified in the MudPIT-MS/MS study which were analysed by zymography

zymogram lane	chronic wound fluids									
	1.1	1.2	1.3	1.4	1.5	1.6	1.7	1.8	1.9	1.10
MMP 9 (%)	0.09	0.14	0.19	0.19	0.04	0.02	0.11	0.11	0.23	0.20
MMP 2 (%)	0.03	0.10	0.07	0.09	0.02	0.02	0.06	0.05	0.11	0.06

zymogram lane	acute wound fluids					
	2.1	2.2	2.3	2.4	2.5	2.6
MMP 9 (%)	0.08	0.15	0.12	0.02	0.08	0.18
MMP 2 (%)	-	0.03	0.03	0.02	0.07	0.01

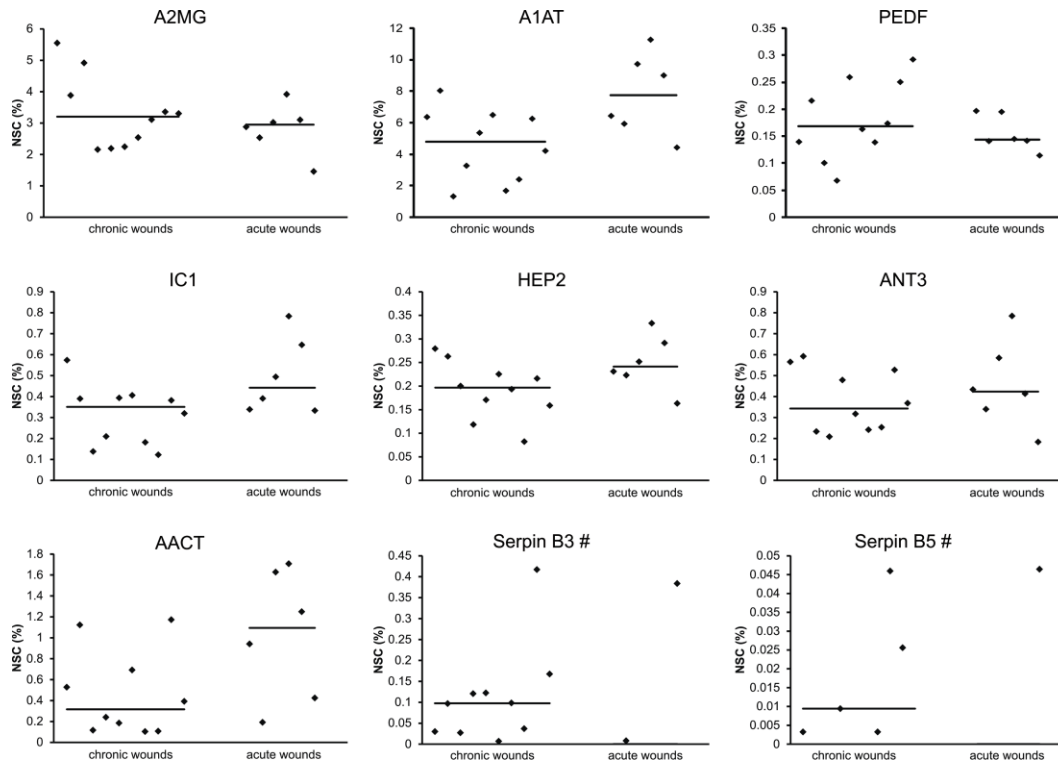
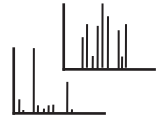
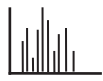
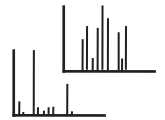
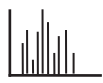


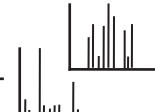
Figure 5.9: plot of individual expression level of identified serpins in the compared wound fluids; # infrequently identified in the fluids of acute wound, estimation of expression level differences was not applicable

Other protease inhibitors identified in this study are the serine proteases inhibitors (serpins). Serpins are involved in several enzyme inhibition pathways. Most serpins identified in the compared wound fluids, such as alpha-1-antitrypsin (A1AT), alpha-2-antiplasmin (A2AP), ANT3, proteinase C 1 inhibitor (IC1), heparin cofactor (HEP2), or pigment epithelium derived factor (PEDF), were not differently expressed in the fluids from chronic wounds when compared to those from acute wounds. Serpins that were identified in this study showing differential expression levels dramatically influence angiogenic processes. The previously discussed AACT is suggested to support smooth muscle cell spreading through the extracellular matrix [152], an important mechanism for new vessel development and vessel growth. AACT was 3.5-fold lower expressed in PHW, demonstrating less smooth muscle cell mobility in chronic wounds as in acute wounds. Therefore, vessel growth might be negatively influenced by the lowered expression of AACT. The non-functional serpin B5 (maspin) was predominantly identified in fluids of PHW. Serpin B5 was identified in 5 patients of the PHW cohort but only in one NHW patient. Although Serpin B5 is a non-functional serine protease inhibitor, it comprises growth blocking properties and functions as a negative angiogenic stimulator [153].



5.4.2. Angiogenesis regulation

Growth factors are highly important for vasculogenic and angiogenic stimulation. Due to their short amino acid sequence and their low abundance, identification of growth factors by mass spectrometry is challenging. Therefore, only the hematoma derived growth factor and the hepatocyte growth factor-like protein were identified. TGF β receptor type III (TGF β R3) was exclusively identified in NHW, assumedly the soluble isoform. The soluble isoform of TGF β R3 prevents TGF β binding to the two membrane bound receptors TGF β R1 and TGF β R2 and thereby controls TGF β signalling. Surface bound TGF β R3 enhance the TGF β signalling by presenting TGF β to the other two receptors [154]. Exclusive identification in the acute wound fluids suggests sTGF β R3 function as a guardian to prevent excessive TGF β signalling in the acute wounds. TGF β has a crucial role in wound healing as it stimulates macrophages to secrete MMPs [155]. Therefore, sTGF β R3 might be important to reduce MMP expression. In general, overstimulation of TGF β has been shown to be contra productive and leads to cell cycle arrest or apoptosis [156, 157]. Cell growth in wound healing depends on capillary growth, which in turn depends on proteins involved in cell-cell adhesion. Nonetheless, cell adhering proteins can positively or negatively influence vessel growth. A positive regulator of angiogenesis is the vascular endothelial cadherin (cadherin 5; CHD5). Membrane bound, CHD5 links epithelial cells and mediates their proliferation and is therefore indispensable in neovascularisation [158]. CHD5 is a single pass membrane with a large extracellular region and a short transmembrane and cytosolic domain. Identification of CDH5 in the wound fluids indicate shedding of CDH5 from the cell surface which is derived by ADAM 10 [159] and regulates epithelial cell-cell interaction and migration. sCHD5 was 2.1-fold higher expressed in the acute wound fluids indicating higher cell mobility of endothelial cells in acute wounds, which in turn facilitates vessel growth. Further, CDH5 has been shown to link epithelial cells. The common epithelial cells in the skin are the keratinocytes. Migrating keratinocytes as a consequence of CDH5 shedding are necessary for epithelial repair mechanism. Assumedly, acute wounds show accelerated reepithelisation. Similar to CHD5, the neuroblast differentiation-associated protein AHNK (desmoyokin) functions as an intercellular connecting protein, if present in the extracellular space. As a member of the desmosomal, desmoyokin belongs to the cadherin family. Desmoyokin was identified in fluids from acute wounds in 5 of 6 cases while it was identified in only 3 of 10 individuals with chronic wounds, inferring higher expression levels in the acute wound fluids. The neuronal cell adhesion molecule L1 like protein (CHL1) was also more



frequently identified in fluids from acute wounds (4/10 PHW, 5/6 NHW). CHL1 is involved in the nervous system development. It is known that diabetics have impaired nerve development. Thus, CHL1 might be involved in this impairment.

Negative influence on vessel growth is derived by collagens. Although collagens are involved in platelet activation, collagens establish unspecific immobilisation of cells reducing cell motility [160]. Anyhow, in wound repair mechanism collagen structures are essential for cell sprouting. As previously observed (figure 5.4), chronic wounds demonstrate extensive degradation of these structure, diminishing cell mobility. Additionally, CO15A1, and CO18A1 comprise an angiogenesis inhibiting peptide at the C-terminus side (endostatin) which is released after proteolytic process. Both collagens were higher expressed in PHW, inferring a higher concentration of endostatin in the chronic wounds to be present. High concentration in the extracellular space is common in a late state of healing. However, elevated inflammation paired with increased MMP levels identified in chronic wound fluids demonstrates an early wounding stage where angiogenesis has yet to be initiated. Furthermore, ANXA6 was identified as highly elevated in chronic wound fluids (16-fold). ANXA6 is another protein known to establish cell-cell and cell-ECM connections in a heteromeric complex of two ANXA6 and S100 proteins. Similar to the collagens, this cell-cell or cell-ECM connection serves tissue structure stabilizing motifs rather than being growth supportive.

One of the major angiogenic mediating proteins is angiostatin. It is generated by proteolytic cleavage of its precursor plasminogen. Angiostatin inhibits angiogenesis in an endothelial cell adhesion-dependent manner [161]. Although neither plasminogen nor angiostatin region derived peptides were identified as differently expressed, the kingle-4-domain binding protein tetranectin was identified as 2.7-fold lower expressed in the chronic wound exudates. Tetranectin regulates angiostatin derived angiogenesis inhibition by preventing cell surface binding of angiostatin [162]. Assumedly, equal abundance levels of plasminogen in the acute and chronic wound fluids along with reduced tetranectin expression in PHW lead to increased angiostatin mediated angiogenesis inhibition. An effect derived by ANXA2 might further enhance angiogenic inhibition. In presence of Ca^{2+} ANXA2 is extracellular bound to the phospholipid membrane. This attracts plasminogen to the cell surface [142]. ANXA2 was 3.5-fold elevated in fluids from chronic wounds (figure 5.5), inferring increased presence of plasminogen close to the cell surface.

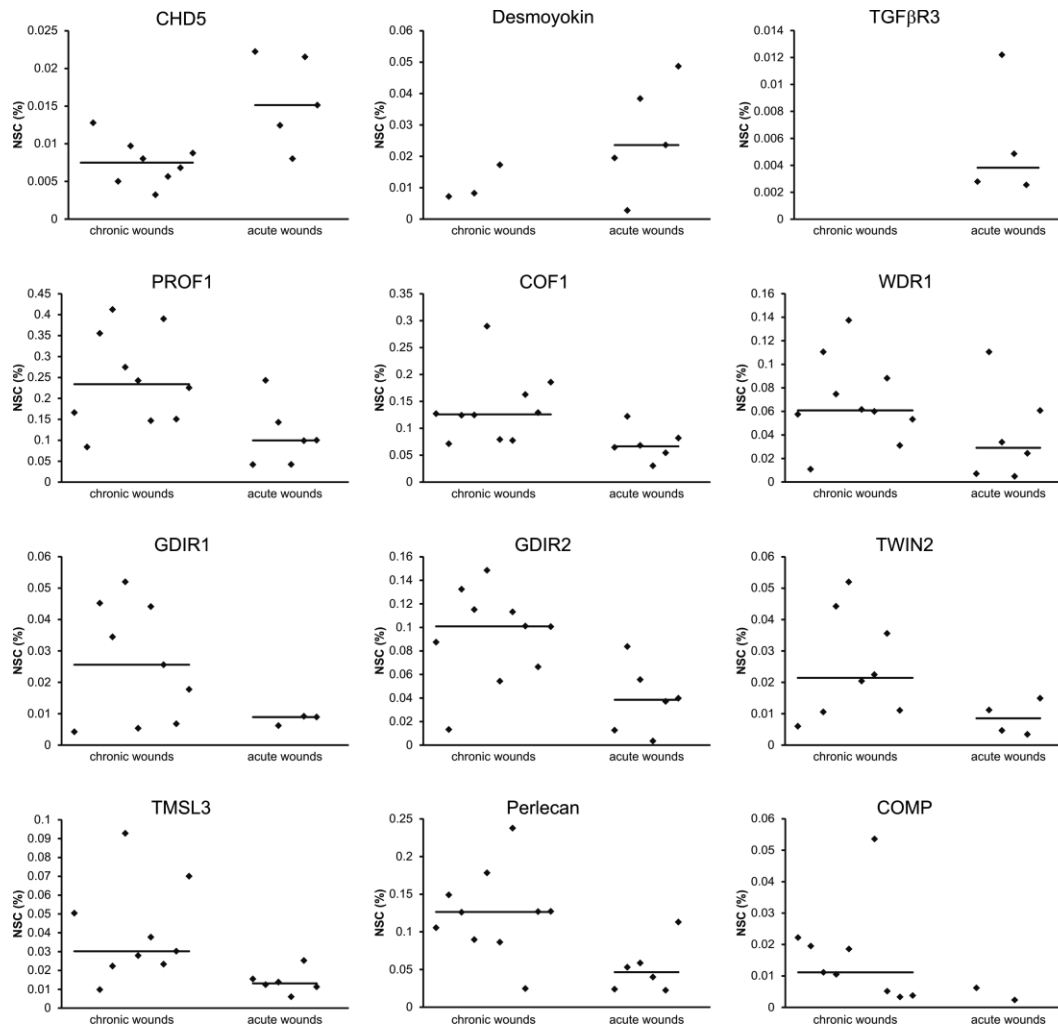
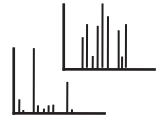
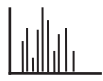
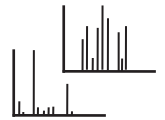
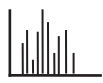


Figure 5.10: individual expression level plot of proteins involved in angiogenic regulation processes, which were identified as differentially expressed in the chronic wounds

One of the most important proteins in cell migration support required for blood vessel growth is the structural protein actin. Actin filaments are involved in cell motility, cell division and the establishment of cell junction. A relation of anti-angiogenic environments and anti-actin properties were demonstrated by Sreenivasan et al. [163]. They showed disruption of actin filaments (F-actin) derived by HSP beta-1. It is mediated by endorepellin, a cleavage product of perlecan. The perlecan precursor was identified as 2.7-fold elevated in PHW. The perlecan precursor was described to have angiogenic promoting properties, whereas its proteolysis product endorepellin is a negative stimulator of angiogenesis by F-actin disruption. Elevated perlecan concentration found in fluids from chronic wounds suggests elevated free endorepellin to be present in the wound fluids. In agreement with endorepellin caused F-actin disruption, the WD-repeat containing protein 1 (WDR1) and Cofilin 1 are involved in filament actin disassembly. Cofilin 1 further prevents polymerisation of globular actin (G-actin) in a pH-dependent manner. Cofilin 1



was 1.9-fold ($p < 0.02$) and WDR 1 was 2.1-fold elevated in chronic wound fluids. Profilin 1, thymosin beta-4 like protein 3, and twinfilin 2 are G-actin polymerisation inhibiting proteins. All three were found in higher expression levels in fluids from chronic wounds with excess rates varying from 2.3 to 2.7-fold. Further, the Rho GDP-dissociation inhibitor (GDIR) 1 & 2 were identified as higher expressed in chronic wound exudates, where GDIR1 was 2.9-fold and GDIR2 was 2.6-fold elevated. Both proteins showed involvement in the disruption of the actin cytoskeleton [164].

In conclusion, the expression of proteins in the fluids of chronic wounds depicted fundamental differences in vasculogenesis and angiogenesis stimulation (figure 5.12). The chronic wounds demonstrated down-regulation of positive stimulator of vessel growth and up-regulation of growth inhibiting proteins and molecules. These proteins are depicted in figure 5.11 to visualize the processes in which these stimulators and inhibitors are involved. The control of angiogenesis and its inhibition towards the scar remodelling phase is essential to prevent uncontrolled cell growth. However, as previously discussed the elevated inflammation in chronic wounds suggests a large area of damaged tissue where the intact cells in the vicinity still secrete pro-inflammatory proteins to accelerate inflammation and proliferation. Therefore, the establishment of a highly vascularised granulation tissue is required. It has been described that chronic ulcers, especially those derived from diabetes mellitus, show diminished angiogenic activities and suggested to be one of the major source for healing difficulties [165]. An important factor contributing to decreased angiogenesis in the chronic wounds might be the identification of the basement membrane component tenascin in high quantities. All analysed fluids from chronic wounds demonstrated high excess rates of tenascin. It was 14-fold elevated in the chronic wound fluids. High concentration of tenascin is normal for the hyper proliferating epidermis which normally is several layers of cells away from the wounded area [166]. Identification of tenascin in the wound bed suggests incomplete repair of the basement membrane. Tenascin accelerates cell proliferation, a known complication in psoriasis and venous ulcers [166, 167].

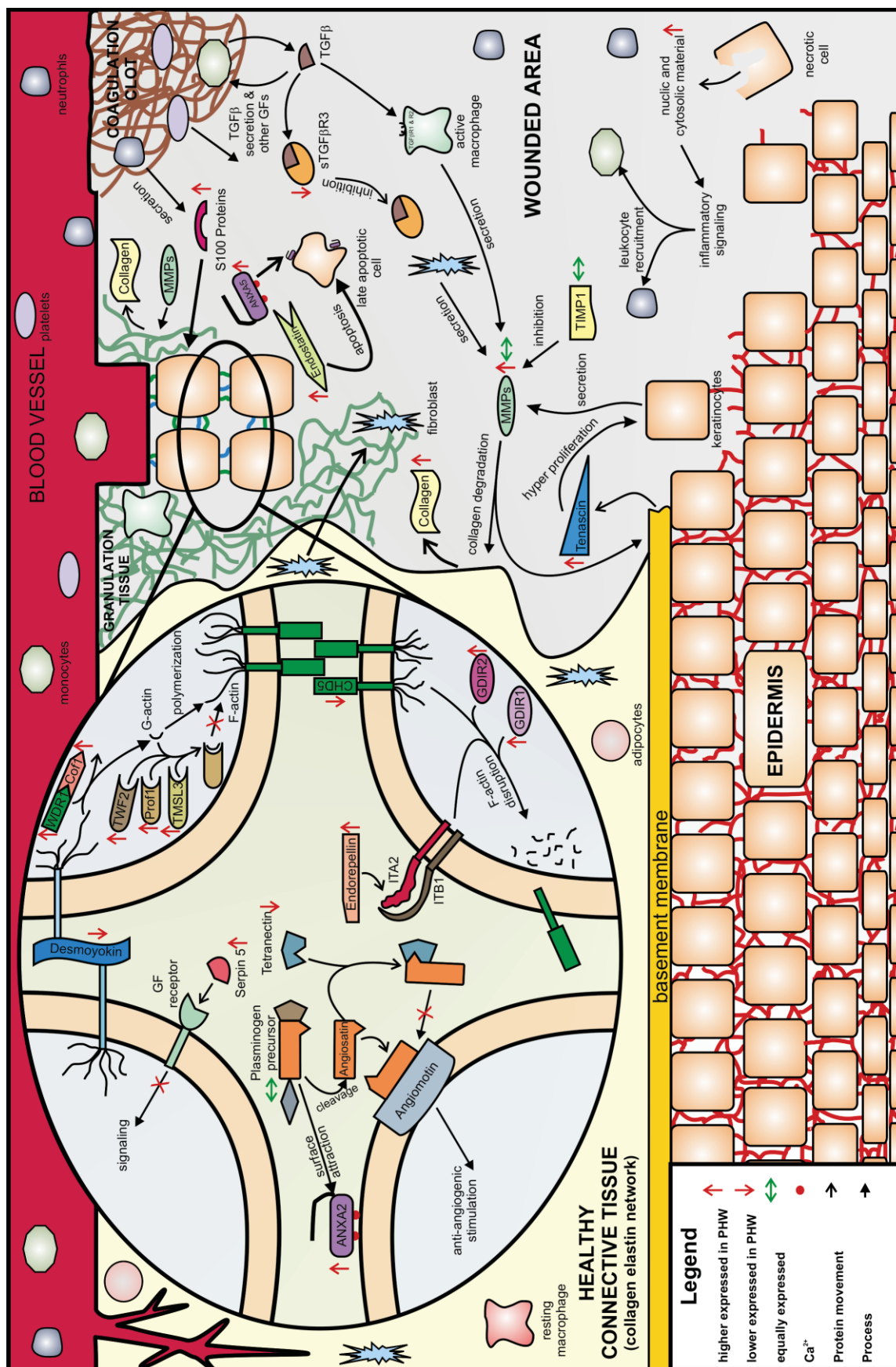
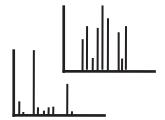
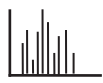


Figure 5.11: schematic of angiogenic processes showing differences in the exudates of chronic wounds



Another protein involved in psoriasis is the squamous cell carcinoma antigen serpin B3 [168]. It was predominantly identified in patients suffer from chronic wounds (10 of 10 cases) but only in 2 of 6 patients showing acute wounds. The function of serpin B3 is still poorly understood. So far autocrine and paracrine expression in a cell culture study demonstrated serpin B3 derived deregulation of cell adhesion by reducing CHD5 and increasing beta catenin concentration similar to the endothelial mensenchymal transition mechanism [169]. Differences in cell adhesion were identified in exudates from chronic wounds showing lower expression levels of CHD5 and desmoyokin in the chronic wounds, which is in agreement to this study.

5.5. Cell death promoting environment

Hyperproliferating conditions paired with anti-angiogenic environment should dramatically increase the number of cells undergoing cell death due to a lack of oxygen and nutrition supply. ANXA5 present in the extracellular space infers increased cells exposing phosphatidylserine, an indicator of apoptotic cells. Apoptosis undergoing neutrophils secrete ANXA1 in order to reduce inflammatory signalling. Continuous inflammation signalling activates cell cycle control mechanisms leading to cell growth arrest or apoptosis to prevent uncontrolled growth. Therefore, apoptosis contribute to anti-inflammatory signalling. As the number of apoptosis undergoing cells is elevated in chronic wounds, assumed from ANXA5 to be detectable exclusively in the fluids of PHW, the higher expression level of ANXA1 can be explained.

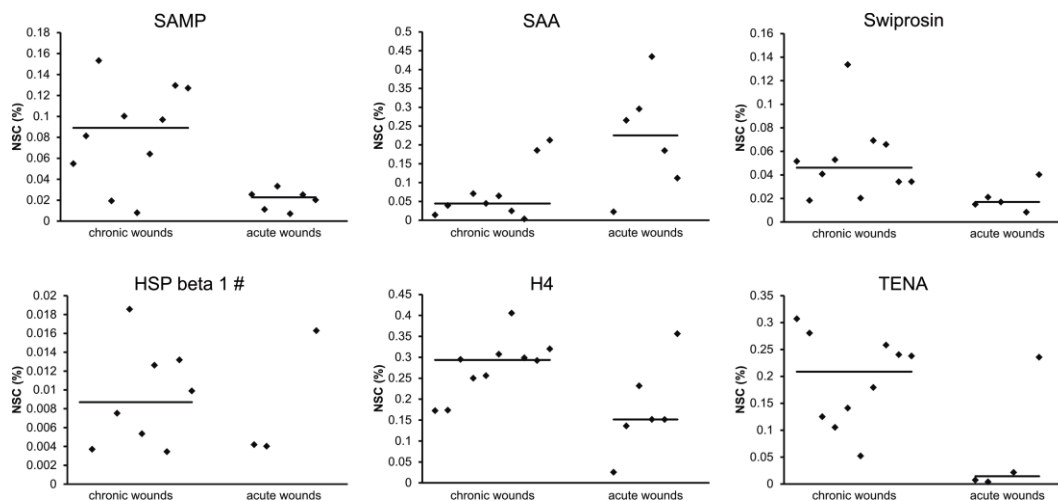
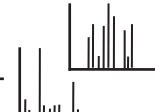
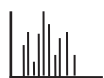


Figure 5.12: individual expression level plot of proteins identified as differentially expressed in cell death stimulation



Further, Swiprosin-1 (EF-hand domain-containing protein D2) an initiator of spontaneous apoptosis after cell – B-cell interaction was 2.7-fold elevated in PHW. Both, ANXA5 and swiprosin 1 demonstrate apoptotic conditions in chronic wounds. The distribution of locations of identified proteins in the fluids from chronic wounds (figure 5.13), was not significantly different from acute wound fluids based on a student's T-test ($p > 0.05$), despite a higher number of proteins derived from inner cellular locations.

Extracellular identified histones, especially histone H4 (1.9-fold higher expression level in PHW), were described as cell death mediators via TLR2 and TLR4 pathway [170]. In the acute phase of inflammation presence of intracellular material derived from damaged cells are early stimulators of the inflammatory response cascade. Consequently, necrosis comprises pro-inflammatory properties and act against apoptosis derived anti-inflammation. The acute wounds reside in an acute phase demonstrate by highly elevated (5.1-fold) serum amyloid A (SAA) expression levels. The chronic wounds should have passed this phase considering the lapse of time since the wounds have been occurred. However, the ability to detect proteins from the cell interior, e.g. histones, HSP, and other cytosolic and nucleic material demonstrates uncontrolled leakage of inner cell material into the extracellular space. This is further confirmed by elevated (3.9-fold) serum amyloid P-component (SAMP) in the chronic wound fluids. SAMP is known to bind DNA fragments and histones in the extracellular space. Increased oxidative stress in the extracellular space discussed in the paragraph 5.3 might be one explanation for cell rupture.

In conclusion, mass spectrometric characterisation of exudates from chronic wounds revealed dramatic differences in the protein composition to acute wounds with excessive inflammation, increased cell death, and diminished vascularisation.

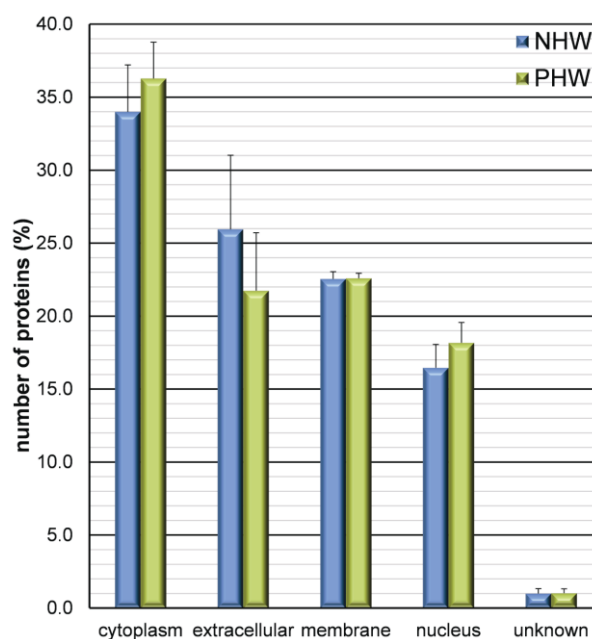
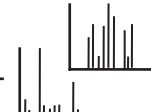
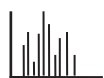


Figure 5.13: subcellular localisation of proteins identified in the acute and chronic wound exudates



6. SRM Investigation of proteins found at differing expression level

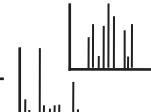
Initial results and conclusions drawn from large biological sample sets, as presented in chapter 5, require validation. For label free quantitation of mass spectrometric data it is important to avoid misinterpretation of quantitative data due to protein/peptide specific and mass spectrometry specific interferences. Peptide specific interferences involve chromatographic performance, ionisation ability, natural variants in amino acid sequences in a subgroup, or unknown modifications occurred to the protein/peptide during handling or due to the origin of the sample, e.g. exposed to oxidative stress. On the mass spectrometry side, the complexity of the sample is a limiting factor, as the mass analysers are restricted in terms of simultaneous identification of ions.

The gold standard for absolute quantitation in biological systems is usually immunoassay. This approach enables for highly accurate and reproducible analyte concentration determinations. However, immunoassays also encounter limitations in terms of lowly concentrated target quantitation, as well as the need for antibody availability and specificity. Further, immunoassays for a large number of targets can be extremely costly. Fortunately, targeted quantitation using SRM-MS has proven to be a powerful strategy for reliable, accurate and simultaneous quantitation of numerous analytes in biological matrices [37-39, 171, 172]. Versatile enrichment and quantitation options have been described, including isotope labelled reference peptides [71, 173, 174], anti-peptide antibodies [175], or PTM-specific enrichment of proteins/peptides [64, 176, 177]. Appropriate selection of monitored transitions [178] paired with increasing sensitivity, accuracy and analysis speed of mass spectrometry, it is likely that SRM-MS will become a comprehensive alternative to conventional immunoassay quantitation in clinical routines [36-40].

This chapter reports on the validation of 17 proteins identified in differing concentration in chapter 5 using SRM-MS with isotope labelled peptides for quantitation.

6.1. SRM validation of differentially expressed proteins in human wound fluids

Proteins chosen for SRM validation were selected by significant expression level differences identified in the MudPIT-MS/MS study (chapter 5). Transition lists were either generated from known transitions published and integrated into the SRM Atlas database [179], from empirical data derived from the discovery study or by optimizing manually selected transition. Peptide selection followed the guidelines for reliable SRM transition selection [34].



All selected peptides were tested in preliminary studies for detectability, specificity, and reproducibility. Overall 29 peptides from 17 proteins were targeted by SRM with mainly 3 transitions per peptide in tryptic digests of 9 chronic and 9 acute wound fluids. As loading controls 50 fmol of a stable isotope labelled peptide solution was spiked into the wound fluids. The C-reactive protein (CRP) peptide ESDTSYVSLK and serum paraoxonase/arylesterase 1 (PON1) peptides YVYIAELLAHK (peptide 1) and IQNILTEEPK (peptide 2) were used as reference peptides and targeted with 3 transitions each as shown in table 7.1. In total 99 different transitions (87 targets + 12 references peptides) were monitored in the SRM study (table 6.1). For most proteins more than one peptide per protein was used for quantitation, however, under the applied SRM-MS conditions for some proteins only one peptide was applicable for quantitation. Mass spectrometric peptide detectability depends on numerous conditions, including peptide length, amino acid composition, peptide behaviour on chromatographic materials and ionisation ability of the peptide. Each peptide comprises different properties which makes SRM-MS quantitation compared to conventionally used immune-based quantitation, more challenging, but also enables quantitation of targets which are otherwise not accessible, see Chapter 1.4.3. To guarantee an optimal correlation between time spend on each transition and the overall duty cycle, the list of transitions was split into two SRM methods only differing in the list of targeted transitions. In the first method 56 (44 + 12) transitions were monitored, the second method monitored 55 (43 + 12) transitions. Randomised analyses of injection triplicates of each wound fluid were conducted. Peak-AUC were determined for each transition and used to estimate expression level differences in the fluids of chronic and acute wounds. Intra individual estimated AUC demonstrated mean coefficients of variation (CV) of 0.920% varying between 0.007 – 15.234%. A mean CV of less than 1% is inferring good reproducibility of the conducted experiments. Individual AUC values of the most intense transitions of all investigated samples are shown in table 11.4.

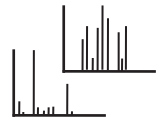
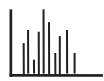
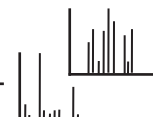
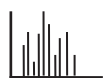


Table 6.1: list of targeted peptide transitions derived from tryptic digests of human wound fluids of proteins identified as differentially expressed in chronic wounds; synonyms used: n/d: not detectable, n/q: not quantifiable

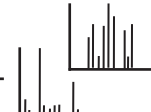
protein	peptide sequence	precursor (m/z)	fragments (m/z)	peak area acute	peak area chronic	mean expression change	p-value
ANXA1	GLGTDEDTLIEILA SR	851.9	1015.6	n/q ^{c)}	3.32e ⁺⁵	-	-
			688.4				
			801.5				
ANXA3	GAGTNEDALIEIL TTR	837.4	732.4	n/d ^{d)}	9.08e ⁺⁵	-	-
			845.5				
			958.6				
	GIGTDEFTLNR	611.8	1052.5	n/d ^{d)}	4.69e ⁺⁵	-	-
			894.4				
			995.5				
GDIR1	AEEYEFLTPVEEA PK	876.4	769.4	1.55e ⁺⁵	1.27e ⁺⁶	8.21	0.01
			870.5				
			1130.6				
GDIR2	TLLGDGPVVTDPK	656.4	812.4	5.86e ⁺³	3.31e ⁺⁵	5.66	0.01
			755.4				
			927.5				
MMP2	AFQVWSDVTPLR	709.8	973.5	9.58e ⁺⁴	5.79e ⁺⁵	6.05	0.02
			787.4				
			1200.6				
MMP8	YYAFDLIAQR	630.3	933.5	1.62e ⁺⁶	1.26e ⁺⁶	0.78	0.23
			1096.6				
			862.5				
	DAFELWSVASPLI FTR	926.5	1090.6	1.73e ⁺⁵	2.53e ⁺⁵	1.46	0.21
			833.4				
			904.5				
MMP9	AFALWSAVTPLTF TR	851.4	1034.5	7.44e ⁺⁵	1.15e ⁺⁶	1.54	0.05
			933.5				
			734.4				
	LGLGADVAQVTG ALR	841.0	1092.6	3.45e ⁺⁵	2.51e ⁺⁵	0.73	0.23
			934.5				
			744.4				
	QLSLPETGELDSA TLK	720.9	815.5	7.62e ⁺⁴	3.54e ⁺⁵	4.78	0.07
			1029.6				
			818.400				
MMP19	AFQEASELPVSGQ LDDATR	1017.490	1158.580	3.85e ⁺⁵	2.51e ⁺⁵	0.97	0.23
			579.791				
			871.5				
PROF1	TFVNITPAEVGVL VGK	822.5	968.6	1.66e ⁺⁶	5.32e ⁺⁶	3.20	0.04
			1069.6				
			887.5				
	SSFYVNGLTGQ K	735.9	986.6	2.15e ⁺⁵	1.11e ⁺⁶	5.05	0.02
			773.4				
			708.4				
SAMP	AYSLFSYNTQGR	578.8	1057.5	n/q ^{c)}	8.32e ⁺⁵	-	-
			871.5				
			1000.5				



protein	peptide sequence	precursor (m/z)	fragments (m/z)	peak area acute	peak area chronic	mean expression change	p-value
S100A4	VGEYSLYIGR	703.8	825.4	n/q ^{c)}	6.43e ⁺⁵	-	-
			972.5				
			738.4				
			551.3				
S100A4	ALDVMVSTFHK	445.7	464.3	n/d ^{d)}	383e ⁺⁵	-	-
			648.3				
			849.4				
			948.5				
S100A8	ELPSFLGK	624.3	718.4	8.36e ⁺⁵	3.12e ⁺⁶	3.73	0.02
			965.4				
			1066.5				
			1196.5				
S100A8	ALNSIIDVYHK	711.4	705.4	1.33e ⁺⁵	3.58e ⁺⁶	26.86	0.04
			1196.5				
			661.3				
			974.5				
S100A9	LLET*PQYIR	636.8	1151.5	7.75e ⁺⁵	2.47e ⁺⁷	31.78	0.002
			776.4				
			967.5				
			643.3				
S100A9	LGHPDTLNQGEFK	871.9	1148.6	1.34e ⁺⁵	8.45e ⁺⁵	6.29	0.04
			634.3				
			1123.5				
			554.3				
S100A11	VIEHIMEDLDTNA DK	904.0	1236.6	2.22e ⁺⁵	8.66e ⁺⁵	3.90	0.02
			1034.6				
			818.5				
			905.5				
S100A11	C*IESLIAVFQK	654.4	710.4	2.03e ⁺⁵	4.33e ⁺⁵	2.14	0.08
			563.3				
			448.3				
			835.4				
S100A12	GHFDTLSK	452.7	1108.5	5.49e ⁺⁵	2.19e ⁺⁶	3.99	0.07
			964.5				
			417.2				
			833.4				
S100P	ELPGFLQSGK	679.8	736.4	1.15e ⁺⁵	1.15e ⁺⁶	10.09	0.03
			790.4				
			538.3				
			833.4				
TIMP 1	EPGLCTWQSLR	673.8	790.4	1.41e ⁺⁵	2.17e ⁺⁵	1.54	0.42
			689.4				
			1217.6				
			1217.6				

6.2. Chronic inflammation

The discovery study demonstrated significantly higher inflammation signalling in the chronic wounds, where S100 proteins were identified as many fold higher expressed (figure 5.5). To validate these findings S100 isoforms A4, A8, A9, A11, A12 and P were analysed by SRM. Monitoring of S100 proteins confirmed the expression level differences (table 6.1) found in the discovery study. Estimation of mean fold changes for the targeted S100A4 peptide ALDVMVSTFHK (figure 6.1) was not applicable since the intensity of



the extracted ion chromatogram (XIC) was in most fluids from acute wounds (≥ 6) below the lower limit of detection (LLOD) defined as $S/N \leq 3$ or the lower limit of quantitation (LLOQ) defined as $S/N \leq 10$. Chronic wound fluids revealed quantifiable transitions for the ALDVMVSTFHK peptide.

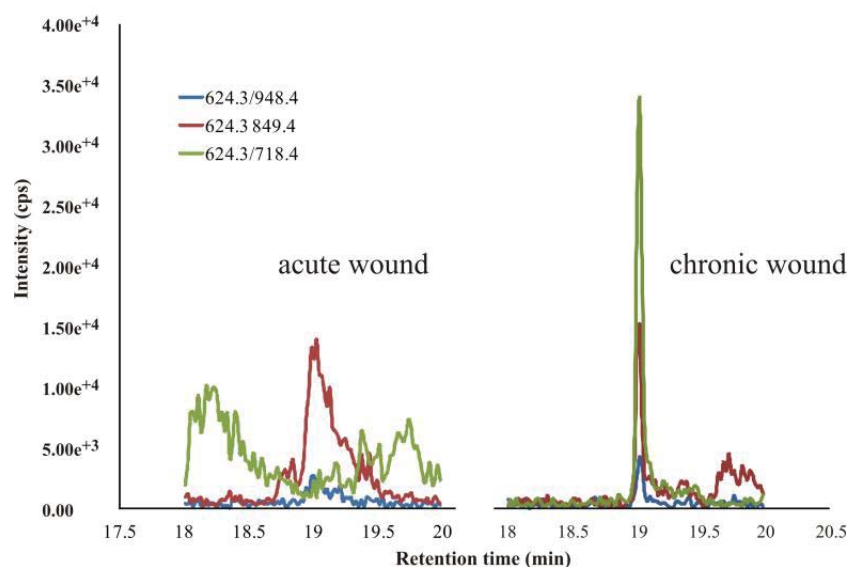
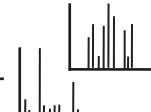


Figure 6.1: example XIC of targeted transitions from the protein S100A4 peptide ALDVMVSTFHK with a corresponding precursor m/z of 445.7

Similar to the discovery study, the targeted peptides of S100A8 and S100A9 demonstrated the highest change in expression level. However, as shown in table 6.1 the excess rates of S100A9 varied from 3.2 to 17.6-fold depending on the targeted peptide. S100 proteins are low molecular weight proteins with masses of 10 – 15 kDa and therefore short in length. Thus, optimal target selection is restricted. Due to these limitations selected peptides might differ in the ability to ionise, which influence the XIC intensity and thereby the quantitation. The S100A9 peptide NIETIINTFHQYSVK comprises a natural variation in the protein sequence where the histidine residue can be replaced by arginine. This natural variation than would change the peptide properties and might influence quantitation. However, the SRM results still clearly demonstrate elevation of S100A8 and A9 in the chronic wound fluids. Although spectral counting based MudPIT-MS/MS and SRM-MS revealed elevation of S100A8 and S100A9 in fluids from chronic wounds, the expression of S100A8 and S100A9 was further investigated by western blot analysis. Figure 6.2 shows S100A8 and S100A9 expression in the wound fluids analysed in the MudPIT-MS/MS analysis. Band intensities of both proteins were more intense in the chronic wounds, which is consisted with the found higher expression of S100A8 and S100A9 in the fluids of chronic wounds. Western blot of S100A9 still showed the presence



of the homodimer (S100A9)₂ at 28 kDa and the heterodimer with S100A8 at 25 kDa although analysed samples were reduced and denatured in Laemmli buffer at 95 °C.

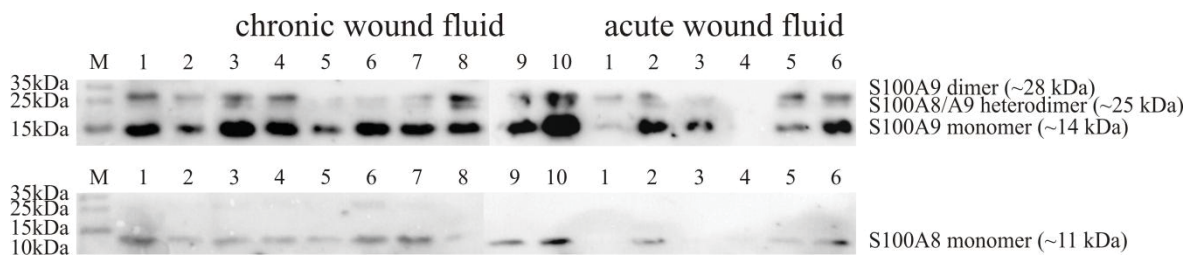


Figure 6.2: western blot analysis of human S100A8 and S100A9 in the fluids from chronic and acute wounds previously analysed by MudPIT-MS/MS and gelatin zymogram

SRM targeted GLGTDEDTLIEILASR peptide of the anti-inflammation signalling protein ANXA1 was identified in quantifiable abundances in the chronic fluids but remained below the LLOQ in fluids from acute wounds (figure 6.3). Therefore, SRM confirms the higher abundance of ANXA1 in the chronic wound exudates and the discrepancies between ongoing inflammatory signalling and inflammation inhibition.

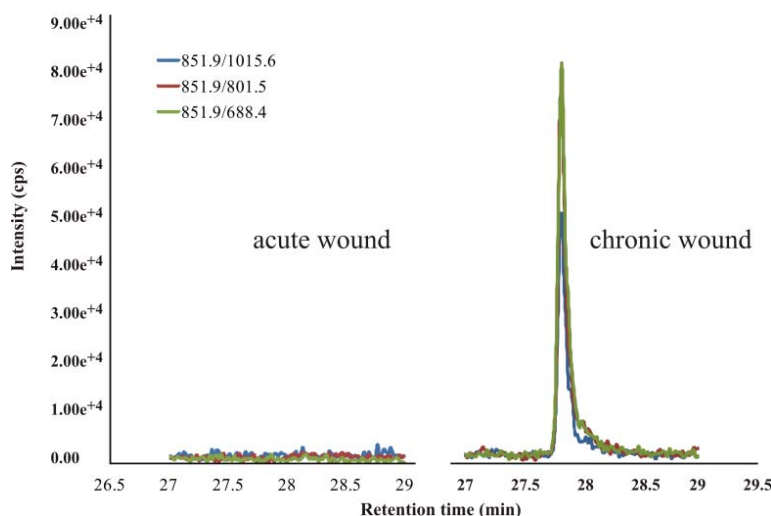
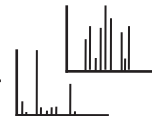
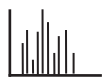


Figure 6.3: example XIC of targeted transitions from the ANXA1 peptide GLGTDEDTLIEILASR with corresponding precursor m/z of 851.9

6.3. Angiogenic regulation

6.3.1. SRM investigation of MMPs

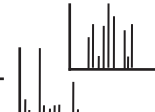
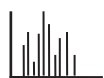
MMP degradation of the ECM initiates growth acceleration signalling and thereby stimulates tissue remodelling processes including capillary new or redevelopment if thoroughly regulated. However, the MudPIT study and the zymography demonstrated impairment of MMP expression. To further validate these impairments, MMP2, MMP8,



MMP9, and MMP19 were targeted by SRM using the transitions shown in table 6.1. MMP2 demonstrated 6-fold mean peak area increases in the fluids of chronic wounds and is thereby confirmed by SRM-MS to be higher expressed in the chronic wounds. AUC determination of the targeted MMP9 peptides AFALWSAVTPLTFTR and LGLGADVAQVTGALR showed similar expression level in the compared wound fluids, consistent with the discovery study. However, the QLSPETGELDSATLK peptide showed 4.7-fold higher mean expression levels in the chronic wound fluids. According to the applied statistics, this higher expression had a significance level of $p = 0.07$. This is explained by infrequent detection of quantifiable abundances of this peptide in the acute wound fluids (4 of 9 cases) whereas peak integration was applicable in 9 of 9 patients with chronic wounds. This specific peptide is located in the activation peptide region of MMP9. Since this region is removed in the active isoform, increased concentration of this peptide in fluids from chronic wounds demonstrates high level of latent MMP9, thus a high rate of newly secreted MMP9.

In addition to MMP2 and MMP9 peptides of MMP8 and MMP19 were investigated by SRM. Although the discovery study showed increased expression levels of MMP8 in the chronic wound exudates, both targeted MMP8 peptides were determined as equally expressed throughout the compared wound fluids. In contrast to all other targeted peptides, MMP8 peptides exhibited broad peak width. Especially the late eluting DAFELWSVASPLIFTR peptide revealed peak width broader than 60 seconds. Therefore, these peptides are considerably more susceptible to interference with co-eluting peptides with similar m/z causing quantitation error.

MMP19 was only identified in 2 fluids from acute wounds in the discovery study. Thus, estimation of expression levels in the compared wound fluids was not applicable. Therefore, the MMP19 peptide AFQEASELPVSGQLDDATR was targeted by SRM. Although MMP19 was infrequently identified in both types of analysed wound fluids, estimated AUC in fluids from chronic and acute wounds demonstrated similar expression. The cartilage oligomeric matrix protein (COMP; Thrombospondin 5) is a collagen structure binding protein and is a substrate for MMP19. In the MudPIT-MS/MS study COMP was detected in 9 of 10 patients representing chronic wounds but in only 2 of 6 patients showing acute wounds. This suggests higher expression levels of COMP in the chronic wound fluids. The mass spectrometric detection of COMP requires endogenous predigestion analogue to the collagens, therefore higher expression in the chronic wound fluids suggests higher activity of MMP19 similar to the other MMPs. It could be assumed



that TIMPs were lower expressed in fluids from chronic wounds. However, the SRM approach enabled the detection of the TIMP1 peptide EPGLC*TWQSLR in similar expression level in the compared wound fluids (table 6.1). Further targeted TIMP1 peptides were unable to be quantitated as their abundance was below the limit of detection. TIMP1 is known to inhibit several MMPs including MMP1 and MMP9. MMP2 activation involves TIMP2 binding. Since TIMP2 was unable to be detected by SRM, its influence on MMP2 activation was not feasible. Identification of MMP1 by SRM and validation of the observed differences in expression level found in the MudPIT-MS/MS study was not possible, as selected MMP1 peptides were below the LLOD.

6.3.2. SRM-MS of selected proteins involved in angiogenic processes and cell death

The actin involved cell adhesion and cell motility was assumed to be disturbed in the chronic wounds according to differing expression levels of actin binding proteins. The G-actin binding protein profilin 1 and the F-actin disrupting proteins GDIR1, and GDIR2 were investigated by SRM (table 6.1). Peak area estimation demonstrated 8.2-fold higher expression of GDIR1 and 5.7-fold higher expression of GDIR2 in PHW. The Profilin 1 peptides SSFYVNGTLGGQK, and TFDVITPAEVLGVGK were identified in PHW to be 5.1-fold and 3.2-fold elevated.

In addition to elevated inflammation and down regulation of angiogenesis, the chronic wounds demonstrated higher rates of cell death. Proapoptotic processes mainly occur within the cell. In this study only the protein content of the extracellular space was investigated. Therefore, SRM validation of apoptotic conditions is challenging due to limited extrinsic apoptotic signalling. ANXA5 in the extracellular space is a late apoptotic state marker protein. ANXA5 was identified in the discovery study as exclusively expressed in exudates from chronic wounds. However, targeting ANXA5 peptide in the compared wound fluids was not feasible as the selected peptides remained in both wound fluid types below the LLOD. Although apoptosis seems to be elevated in chronic wounds, the extensive presence of intra cellular material in the fluids of chronic wounds suggests additional cell death by necrosis. SAMP, a protein binding to material from the nucleus present in the extracellular space, was found as elevated in fluids from chronic wounds. SRM investigated SAMP peptides AYSLFSYNTQGR and VGEYSLYIGR showed comparably to S100A4 and ANXA1 peptides peak intensities applicable for quantitation purposes in fluids from chronic wounds but remained below the LLOD or LLOQ in the acute wound fluids (figure 6.4). As this was consistent for both peptides SAMP was confirmed to be at higher expression levels in chronic wound fluids.

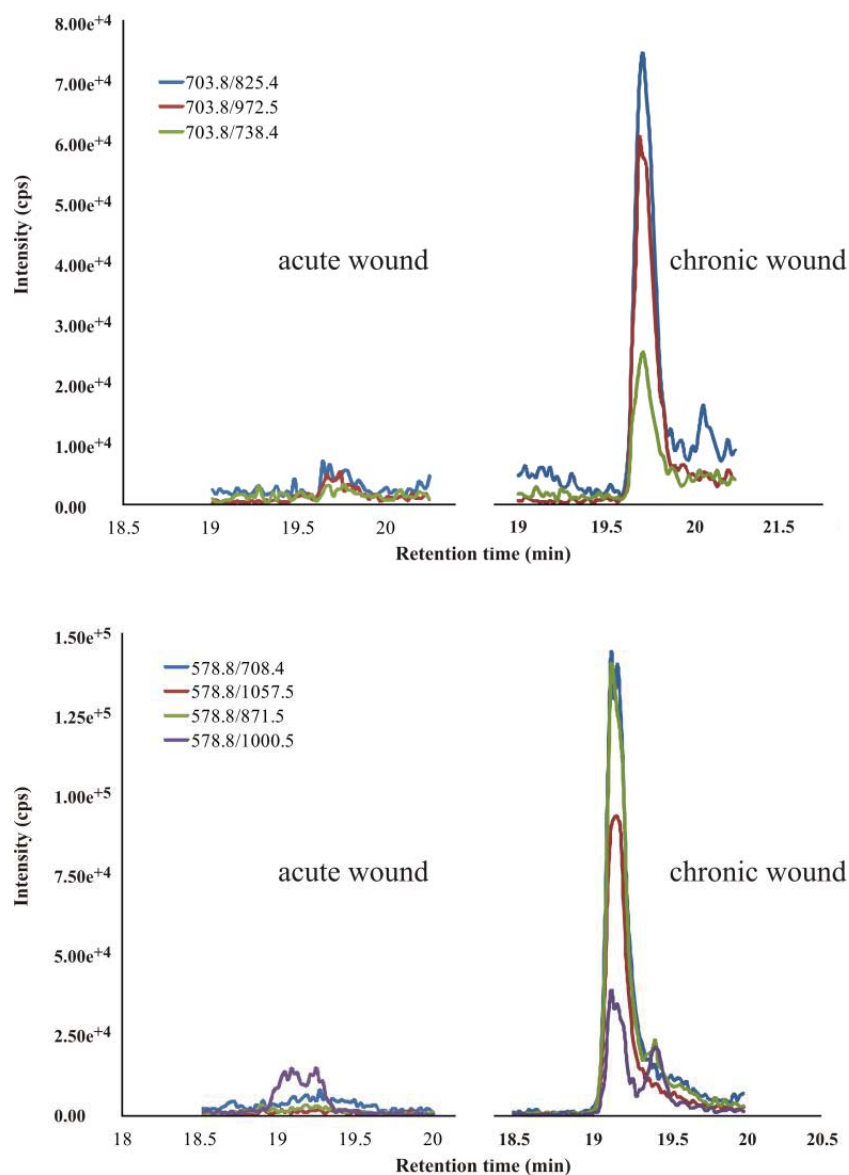
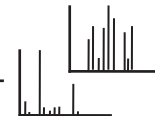
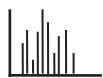
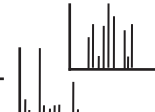
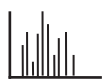


Figure 6.4: example XIC of targeted transitions from the SAMP peptide AYSLFSYNTQGR (top) and VGEYSLYIGR (bottom) with corresponding m/z of 578.8 and 703.8, respectively

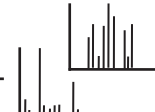
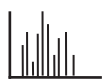
In conclusion, SRM-MS results correlate very well with the MudPIT-MS/MS derived expression level differences. Therefore, the assumed consequences of proteins involved in several regulating and stimulating processes as reported in Chapter 5 has been validated.



7. Targeted mass spectrometry with advanced multiplexing potential

In biomedical and pharmaceutical research the highly selective and sensitive SRM method is commonly applied. During the last years, efforts have been made to integrate SRM into clinical applications [36-40, 172, 174, 180-187] as a substitution of or an extension to established laboratory quantitation strategies. Enabled by highly sensitive target molecule detection and fast analysis time of defined ions, SRM is extensively applicable to complex protein mixtures, which is common to biological specimens.

Nonetheless, detection of less abundant proteins in complex solution is even with a highly sensitive SRM approach challenging. Fractionation strategies are still necessary to reduce sample complexity and to overcome ion suppression and interferences from co-eluting molecules. Strategies discussed in Chapter 4 can be implemented here among others. Lately, immunoenrichment of analytes by monoclonal anti-peptide antibodies are a common way to access lowly concentrated proteins realized in the stable isotope standard capture with anti-peptide antibodies (SISCAPA) strategy. SISCAPA combines anti-peptide immunoenrichment with stable isotope labelled peptide dilution commonly used in relative and absolute quantitative SRM approaches [175]. However, antibody based peptide enrichment is so far still a cost intensive strategy and consumes time if antibodies have to be generated. Therefore, the cost effective strong cation/anion exchange chromatography (SCX/SAX) is predominantly used. This robust, charge-based fractionation method can either be applied prior mass spectrometric analysis on proteins or peptides or as demonstrated before in an online work flow [31, 188, 189] used in discovery-based proteomics. Interestingly, so far SRM analysis work flows only made use of offline SCX/SAX fractionation [174, 176, 177], although the MudPIT strategy combines sample purification (desalting), prefractionation and concentrating within a simple chromatographic gradient. The reduction in sample complexity facilitates sensitivity enhancement and allows for better usage of the dynamic range of the employed mass spectrometer. Further, online based fractionation overcomes crucial peptide losses, especially of lower abundant proteins. Losses of analytes are usually associated with numerous sample manipulation steps in offline methods which include sample concentration, purification, resuspension, or buffer exchanges. Therefore, the MudPIT-SRM method will be assessed in terms of sensitivity and quantitation improvements of target proteins in complex specimens for biomarker applications.



7.1. Automated MudPIT-SRM

Integrating SCX into an automated SRM work flow is the basic step to develop a robust and precise method with minimal sample handling. In conventional automated SRM work flows an auto sampler injects the mixture of analytes onto a trap column. For peptide analysis C18 RP traps are normally used. In the MudPIT-SRM work flow the trapping system was modified replacing the RP trap with a MudPIT trap. The trap was positioned in a 10-port valve enabling the integration of the trap column either in line with the analytical column (elution) which is connected to the mass spectrometer, or directly to the waste (sample loading). Peptide elution from SCX material is usually achieved by increasing salt gradients. In MudPIT analyses peptide elution is realised by sequential salt injection with increasing salt concentration prior each RP gradient. Besides the SCX phase the MudPIT column consist of two C18 RP phases, one before the SCX and one after. The first RP phase functions as a purification step. Injected peptides are retained on that phase and contaminants will be washed through. This step is necessary as it desalts the sample before reaching the SCX phase. An initial RP gradient transfers retained peptides from the first RP phase to the SCX phase to allow charge based fractionation. In a two buffer HPLC system as used in this study, the SCX salt elution has to be performed via auto sampler injections of defined NH_4Ac concentrations. Salt injection transfers retained peptides from the SCX phase to the second RP phase and will be eluted into the mass spectrometer by the following RP gradient. The two flow paths available on the used HPLC, where flow channel 1 allowed a high flow rate (5 – 10 mL/min) and flow channel 2 allowed a low flow rate (≤ 1 mL/min), facilitates analysis time per sample as samples and salt injections can be performed while the analytical column is equilibrating. The described trapping configuration is shown in figure 7.1 to visualise loading and elution conditions used in the study.

In addition to the MudPIT trapping system a secondary injection loop was introduced in to the system. This loop had a defined capacity and was continuously filled with the isotope labelled standard peptides used in the SRM-MS validation study. These peptides were transferred to the analytical column while the sample or ammonium acetate was injected onto the trap column. Thus the standard peptides were present in each analysis and function as a quality control and as a normalising tool for MudPIT-SRM investigated samples. Reproducibility of retention time and peak area of standard peptides introduced into the MudPIT-SRM work flow was assessed by repeating injection and mass spectrometric characterisation (figure 7.1 and table 7.1).

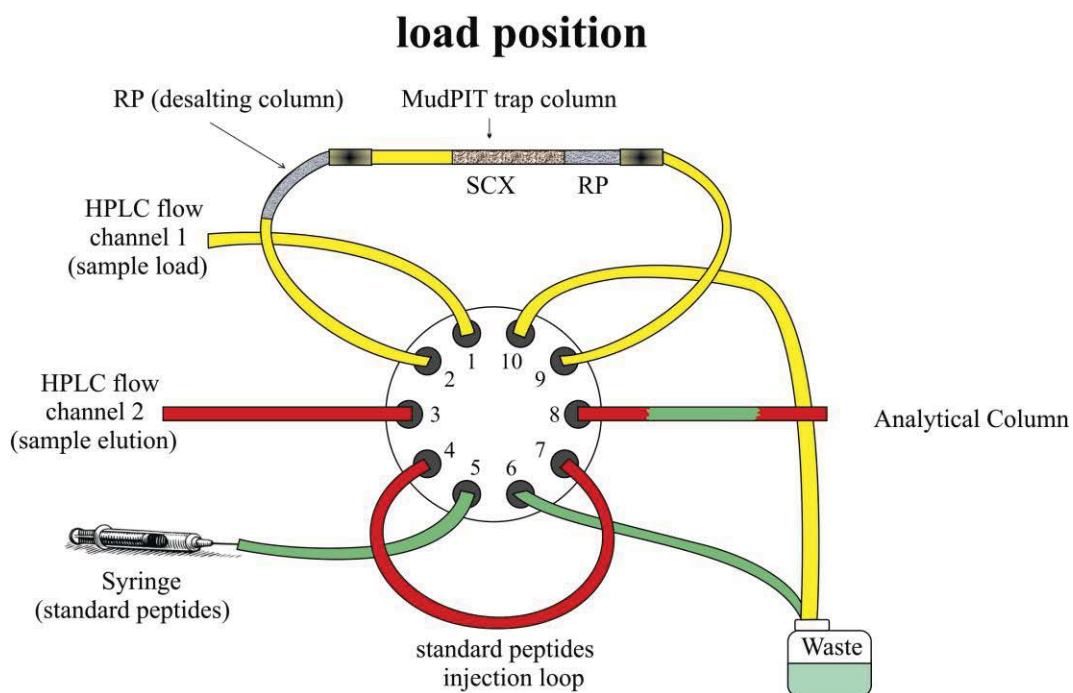
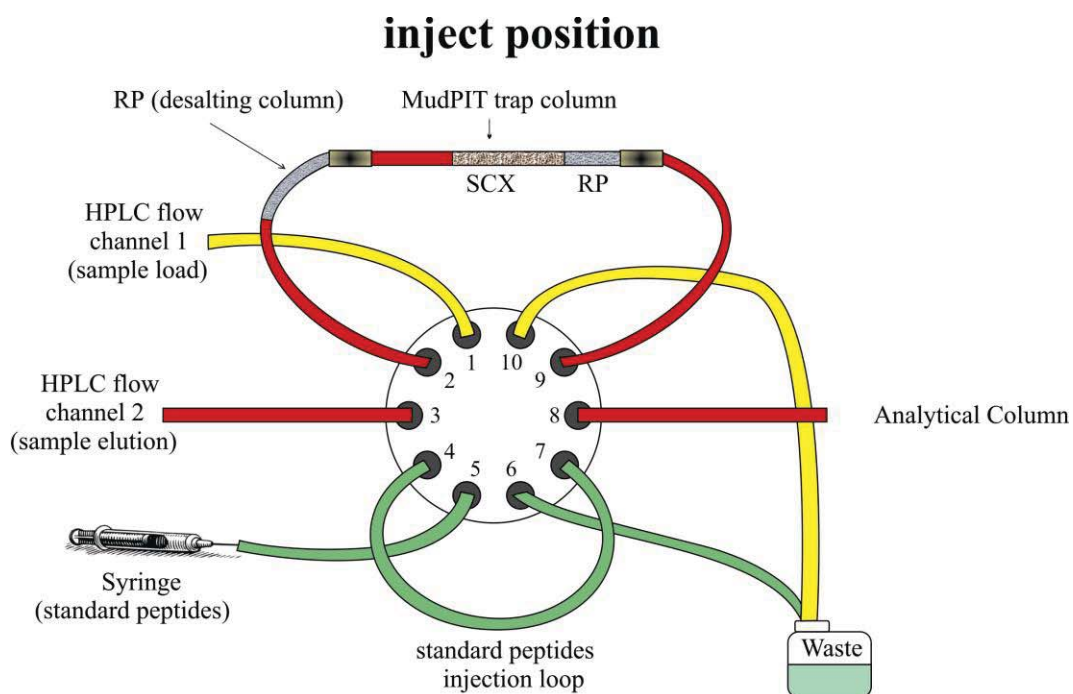
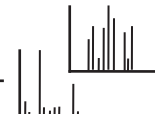
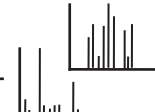


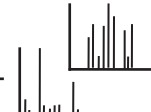
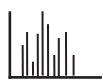
Figure 7.1: scheme of flow paths on a 10-port valve to realise analyte peptide trapping and reproducible reference peptide introduction in each analysis in MudPIT-SRM applications

**Table 7.1: peak area estimation of targeted reference peptides in triplicates including CV**

peptide	transitions (m/z)	replicate 1 (cps)	replicate 2 (cps)	replicate 3 (cps)	CV (%)
CRP	568.4/919.5	2.78E+05	2.72E+05	2.65E+05	2.39
	568.4/703.5	7.75E+05	7.63E+05	7.43E+05	2.13
	568.4/616.5	5.83E+05	5.72E+05	5.59E+05	2.10
PON1 Pep 1	443.3/789.5	4.04E+05	4.10E+05	4.37E+05	4.22
	443.3/902.5	7.44E+04	7.58E+04	7.90E+04	3.09
	443.3/476.3	1.43E+05	1.49E+05	1.46E+05	2.05
PON1 Pep 2	596.4/950.6	1.08E+06	1.03E+06	1.04E+06	2.52
	596.4/603.3	2.15E+05	2.06E+05	2.13E+05	2.24
	596.4/723.4	3.59E+05	3.45E+05	3.55E+05	2.04

7.1.1. MudPIT-SRM of high abundant plasma proteins

MudPIT-SRM efficiency and reproducibility applied to albumin and IgG depleted human plasma was investigated by comparing MudPIT-SRM to conventional RP-SRM. Five successive fractionation steps were used to analyse human plasma with MudPIT-SRM. In the initial step injected samples were desalted and transferred to the SCX resin using an ACN gradient. Step 2 – 5 included consecutive salt injection of increasing concentration of 15 mM, 30 mM, 300 mM, and 1.5 M ammonium acetate, peptide transfer to the second RP phase and ACN gradient elution (effective 30 min elution) into the mass spectrometer. In total each sample analysis by MudPIT-SRM consumed 7 h of instrument time including sample loading, and analytical column reequilibration. To maintain similar retention times and loading capacities in RP-SRM, the MudPIT trapping system was kept consistent throughout the entire comparison. Desalting followed by high salt injection was used to simulate RP-SRM. In both strategies 32 peptides from 24 high concentrated plasma proteins were targeted with one transition each (table 7.2) which were previously assessed by analytical performance and showed high quantitative reproducibility using nanoflow LCMS on a 4000 QTrap in a cancer patient study [190]. Known from offline SCX experiments some peptides tend to spread through several collected fractions, therefore, the set of monitored peptides were used in each successive SRM analysis. In order to analyse the selected transitions in an optimal correlation between analysis time spent on each transition and overall duty cycle, the dwell time was optimized. Therefore, reference peptides from CRP and PON1 were continuously injected into the mass spectrometer and the intensities dependence on the dwell time detected (Figure 7.2). Selected transitions for



the reference peptides were integrated into the transition list of targeted peptides from human plasma to simulate a multiplexed analysis with 42 transitions in total. A dwell time of 20 ms was selected. This dwell time demonstrated good correlation between dwell time and cycle time with acceptable transition intensities. For some reference peptide transitions longer dwell times showed greater intensities but would dramatically increase the cycle time causing reduced data point acquisition across an eluting target peptide.

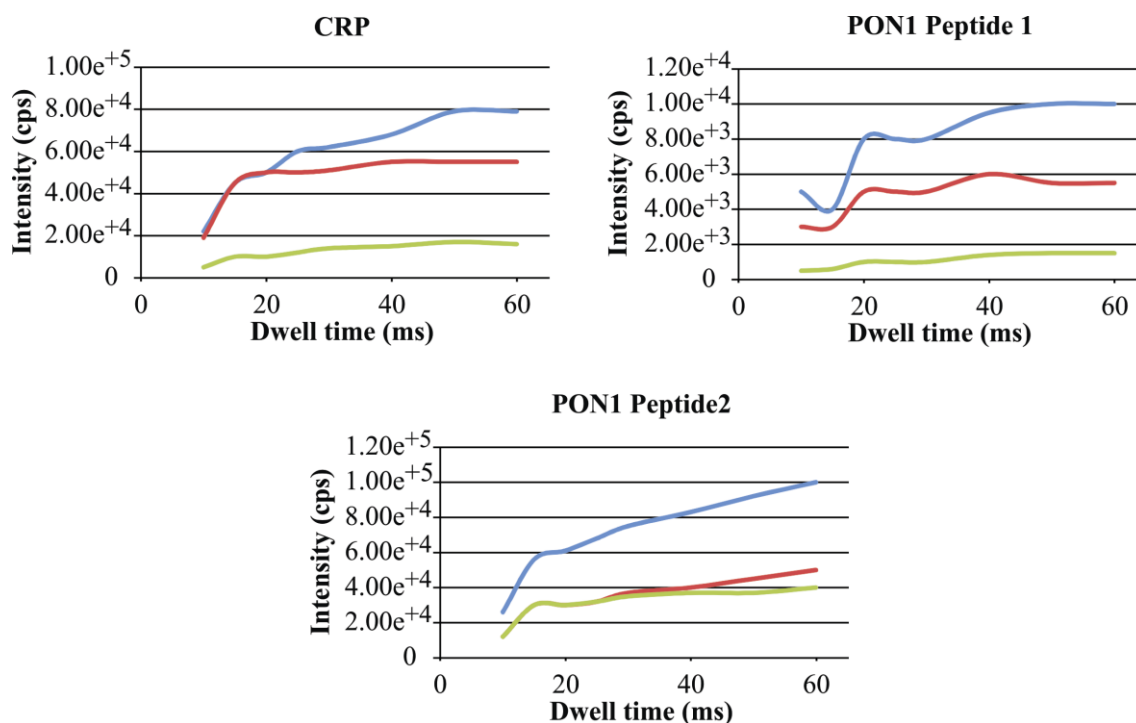


Figure 7.2: SRM dwell time optimization by continuous injection of the reference peptides PON1 peptide 1 and peptide 2 and CRP into the 4000 QTrap mass spectrometer; blue represents most intense transition, red middle intense transition, green lowest intense transition of the specific peptide

MudPIT-SRM analysed plasma demonstrated (figure 7.3) distinct elution profiles for each salt step fraction. As expected some peptides from highly expressed proteins were identified in multiple fractions within the MudPIT-SRM analysis with a high intensity in one fraction and a low intensity in the following. However, the peak intensities of those peptides were above the LLOQ in each fraction in which they were identified. Thus, quantitation of these peptides was applicable and allowed for multi-fraction AUC data to be totalled.

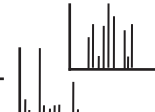
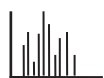
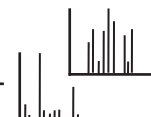


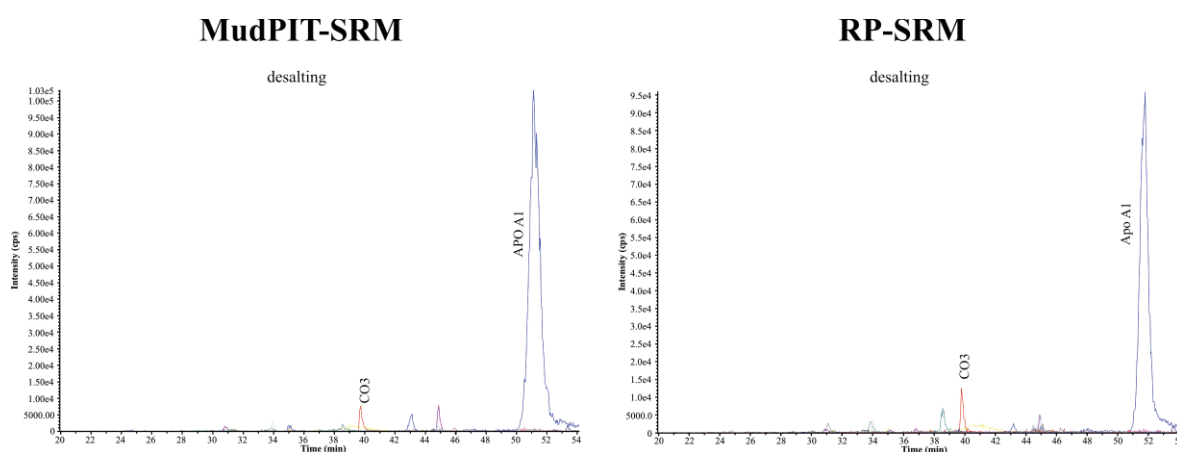
Table 7.2: list of MudPIT-SRM and RP-SRM targeted peptides transition of highly abundant proteins in human plasma including mean peak areas, peak area increases, and CVs of MudPIT analysed peptides

protein code	peptide sequence	precursor mass (m/z)	product ion mass (m/z)	mean peak area MudPIT-SRM	mean peak area RP-SRM	peak area increase MudPIT vs. RP-SRM (%)	CV MudPIT-SRM (%)
A1AG2	TEDTIFLR	497.8	764.4	1.60E+06	1.10E+05	93.09	11.81
A1AT	LSITGYDLK	556.0	797.4	3.43E+06	1.55E+05	95.48	5.34
A2MG	QTVSWAVTPK	558.8	788.4	2.70E+05	7.25E+04	73.18	4.62
AACT	ADLSGITGAR	480.8	574.3	1.35E+06	2.49E+05	81.47	6.85
AMBP	ETLLQDFR	511.3	565.3	2.85E+05	1.86E+04	93.47	2.76
ANGT	SLDFTELDVAEE K	719.3	975.5	2.82E+05	2.28E+04	88.63	5.78
	VLSALQAVQGL LVAQGR	862.0	1111.7	2.54E+05	1.41E+04	95.02	2.09
	ALQDQLVLVAA K	634.9	956.6	2.01E+05	4.51E+04	82.24	0.63
APOA1	QGLLPVLESEFK	615.8	819.5	3.22E+07	2.37E+04	72.45	6.96
	DYVSQFEQSAL GK	700.8	1023.5	1.32E+07	3.90E+06	87.90	4.86
	VSFLSALEEYTK	694.3	940.5	1.04E+07	1.01E+06	90.32	8.14
APOB	GFEPTLEALFGK	655.0	975.6	4.57E+05	1.04E+06	92.13	3.46
APOC3	DALSSVQESQV AQQAR	859.0	1144.6	9.54E+05	3.04E+04	93.35	7.95
CO3	IHWESASLLR	602.3	695.3	2.08E+05	1.80E+05	81.10	5.62
	TELRPGETLNVN FLLR	624.8	875.5	1.15E+06	3.75E+04	82.01	9.23
	SSLSVPYVIVPLK	701.6	928.6	2.17E+06	1.10E+05	90.44	6.14
CO4A	LELSVDGAK	466.3	689.4	2.51E+05	1.46E+05	93.26	3.11
	VGDTLNLNLR	557.8	629.4	1.93E+06	8.10E+03	96.77	8.21
FIBA	GLIDEVNQDFT NR	761.3	894.4	1.25E+07	1.15E+05	94.06	1.34
FIBB	DNENVVNEYSS ELEK	885.1	1197.6	4.78E+06	1.31E+06	89.53	3.73
FIBG	LDGSVDFK	440.7	652.3	8.48E+05	5.08E+04	98.94	10.79
HEMO	GGYTLVSGYPK	571.5	650.4	1.26E+06	8.20E+04	90.34	2.26
HPT α	TEGDGVYTLND K	656.3	1081.5	1.90E+05	1.66E+05	86.86	1.93
HPT β	VTSIQDWVQK	602.3	1003.5	2.47E+06	2.59E+04	86.34	6.54
KNG1	YFIDFVAR	515.8	720.4	5.61E+05	2.58E+05	89.57	2.33
	DIPTNSPELEETL THTITK	714.1	813.5	1.15E+05	4.11E+04	92.67	7.04

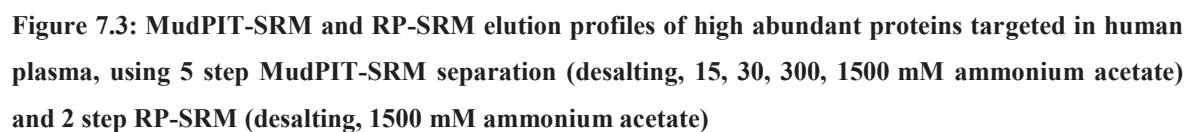


protein code	peptide sequence	precursor mass (m/z)	product ion mass (m/z)	mean peak area MudPIT-SRM	mean peak area RP-SRM	peak area increase MudPIT vs. RP-SRM (%)	CV MudPIT-SRM (%)
SAA	SFFSFLGEAFDGAR	776.0	822.4	4.51E+04	5.66E+03	95.06	4.19
THRB	ELLESYIDGR	597.8	710.3	1.48E+05	9.08E+02	97.99	9.89
TRFE	EGYYGYTGAFR	642.8	771.4	4.78E+06	7.10E+03	95.22	2.77
TTHY	GSPAINVAVHVFR	683.9	941.5	5.12E+05	5.04E+05	89.45	4.46
VTDB	VPTADLEDVLPLAEDITNILSK	1183.7	1313.7	7.92E+05	1.27E+05	75.11	9.23
VTNC	FEDGVLDPDYPR	711.8	875.4	2.37E+05	6.42E+04	91.89	2.89
Mean						89.22 ± 5.26	5.40 ± 2.44

The desalting fraction of MudPIT-SRM and RP-SRM contained except for one APOA1 peptide and one CO3 peptide no other target peptides indicating sufficient binding capacity of the MudPIT trapping system. Comparison of the MudPIT-SRM elution profiles to the high salt elution fraction of RP-SRM (figure 7.3) demonstrated significant peak intensity increases by up to 50% using MudPIT-SRM. Examples of the increases are shown in figure 7.4 for the CO3 peptide TELRPGETLNVNFLLR (intensity > 10⁶) and for the SFFSFLGEAFDGAR peptide of serum amyloid A protein (intensity < 10⁵). Furthermore, a median peak AUC increase of 89.2 ± 5.3%, varying from 73 – 98%, was observed, demonstrating markedly improved sensitivity. Estimated CVs for target peptides analysed by MudPIT-SRM (table 7.2) demonstrated good reproducibility with a median CV of 5.40 ± 2.44% (0.6 – 11%) comparable to conventional RP-SRM CVs conducted on 4000 QTraps [180, 190, 191].



RP-SRM



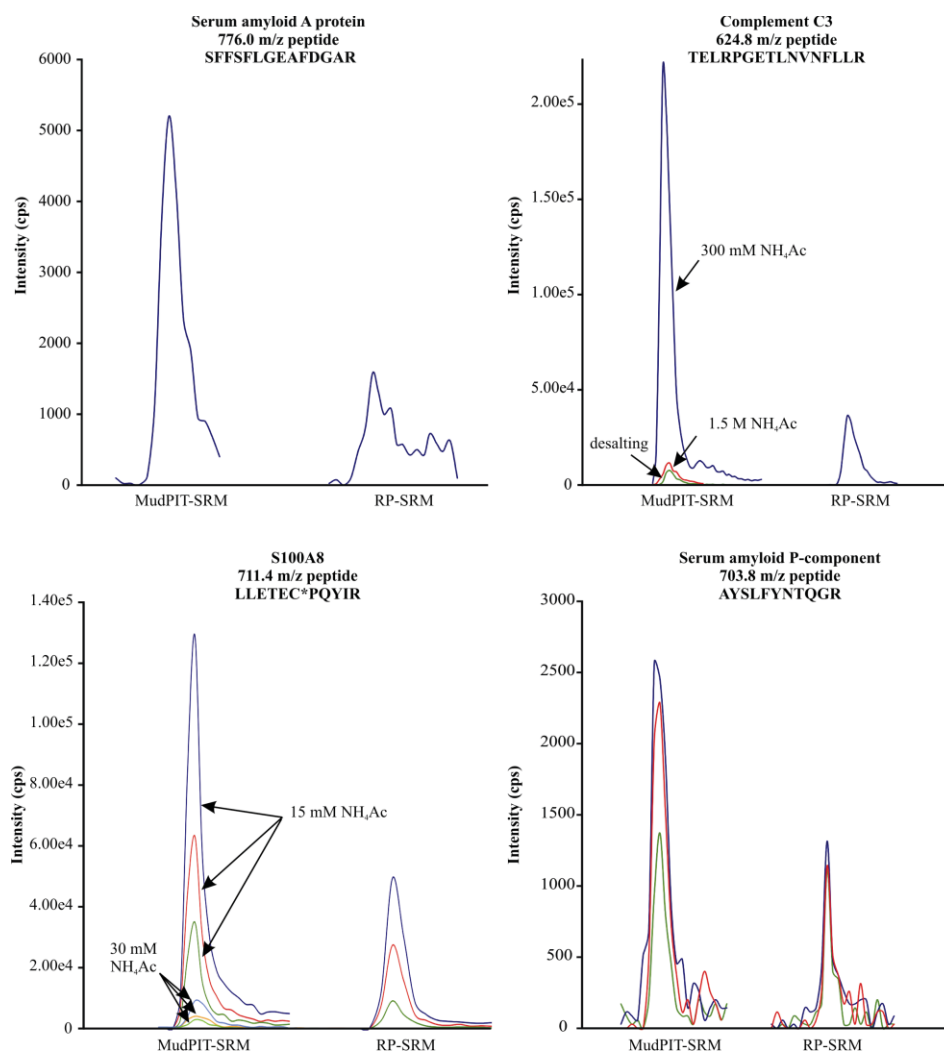
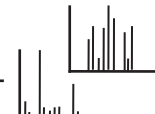
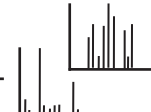
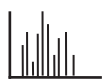


Figure 7.4: comparison of targeted peptide XICs from serum amyloid A and complement C3 in human plasma and from S100A8 and serum amyloid P-component in human wound using MudPIT-SRM or RP-SRM

Increased peptide purity achieved by multiple salt step elutions reduces the complexity of each elution step and further minimises known electrospray ionization (ESI) complications. Mass spectrometry analyses commonly suffer from ion suppression caused by co-eluting molecules reducing the peak intensity by a certain degree [57-59]. To assess changes in ion suppression, the described method by Jessome and Volmer [58] was implemented into the elution pathway of MudPIT-SRM and RP-SRM. Briefly, a continuous post-analytical column infusion (3 $\mu\text{L/h}$) into the flow path of an elution gradient (Figure 7.5a) was established for the three isotope labelled peptides used before (500 fmol/ μL). This allows for constant monitoring of ionization efficiency of infused peptides. Analysing the background without a complex solution, RP-SRM separation of human plasma, and MudPIT-SRM separation of human plasma in triplicates (figure 7.5b)



revealed improved ionization efficiencies using MudPIT-SRM. Reproducible ionization efficiency of infused peptides was demonstrated monitoring the background. Compared to the background, however, MudPIT-SRM and RP-SRM demonstrated increased ionization efficiencies of CRP and PON1 peptide 2 in the desalting step. Interestingly, changes in ionization efficiency were not seen when high amounts of peptides are co-eluting, but throughout the entire gradient. A significant reduction of targeted peptide ion counts by 70–80% was observed in the RP-SRM elution of the plasma sample, demonstrating a high impact of the complex background to the ionization efficiency. In contrast, the MudPIT-SRM strategy showed 10 – 20% increases for CRP and PON1 peptide 2 and 60% increase for PON1 peptide 1 in the 15 mM salt injection step and 50 – 60% increases for CRP and PON1 peptide 2 and 230% increase for PON1 peptide 1 in the 30 mM salt injection steps. In the 1.5 M salt elution the intensities decreased to comparable levels as in the RP-SRM elution step. The observed differing behaviour of PON1 peptide 1 in terms of intensity increases is most likely related to the 3+ charge state of this peptide. However, it still followed the overall trend of the other two standard peptides.

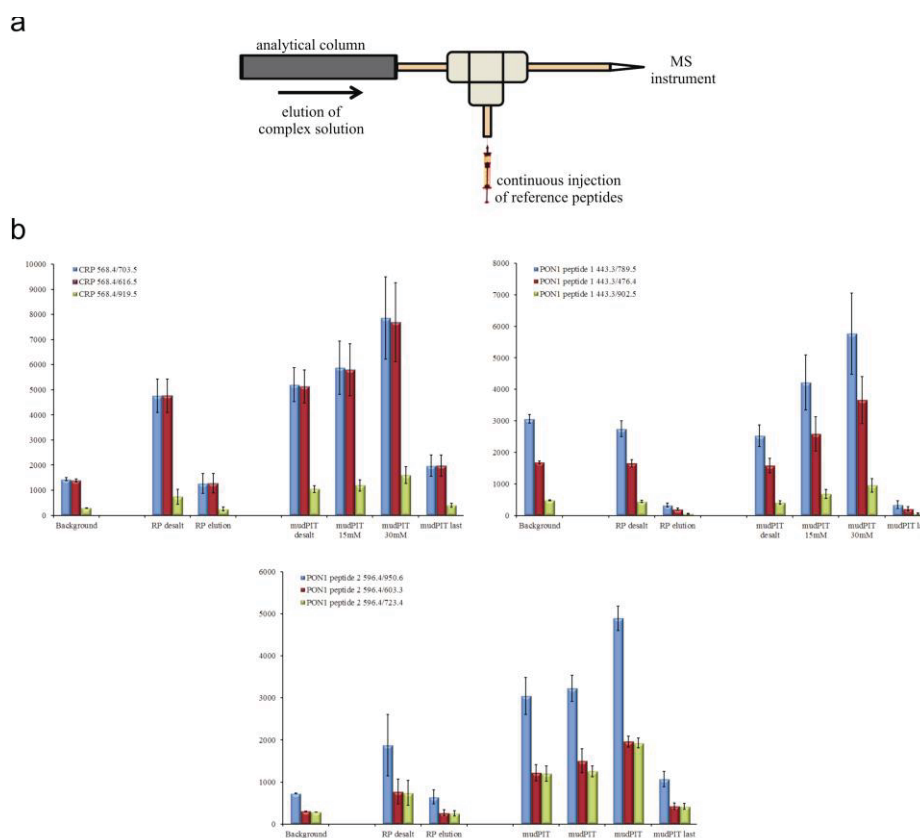
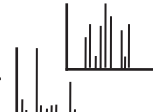
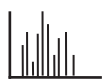


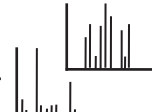
Figure 7.5: a) scheme of the setup to infuse reference peptides into the flow path of elution complex samples after separation on an analytical column; b) mean intensities of reference peptides continuously introduced into the flow path of an eluting complex sample using RP-SRM and MudPIT-SRM



7.1.2. MudPIT-SRM of target proteins in human wound fluids

MudPIT-SRM has been shown to significantly facilitate identification and quantitation of high abundant target proteins in a complex background. In a second step MudPIT-SRM advantages were applied to human wound fluids investigating proteins identified to be dysregulated in poor healing wounds. Sixteen proteins with 26 peptides were investigated with three transitions per peptide (table 7.3). In total 90 transitions (78 + 12 standard peptide transitions) were monitored. Targeting 90 transitions in a single run reach the limitations of conventional SRM approaches. Due to reliable quantitation requirements at least 6 data points acquired per eluting peptide are necessary. Increasing numbers of transitions lengthen the duty cycle of the instrument resulting in less data points acquired per target peptide in a certain amount of time. Conventionally, to overcome this limitation either the gradient time has to be increased which would lead to broader peaks with less intensity of eluting peptides or with short gradient times multiple analyses of the same sample with differing lists of targeted peptides has to be conducted. Both strategies would increase the instrument time needed for such experiments and the latter would dramatically increase the sample amount required for each investigation. In the MudPIT-SRM analysis peptides are already fractionated by their charge and elute in different fractions as shown in human plasma. Therefore, MudPIT-SRM enables specific peptide targeting in each elution fraction without multiple sample injection to be necessary. To generate elution fraction specific target lists preliminary experiments have to be conducted to identify in which salt step the target peptides elute. Generated lists for human wound fluids based on preliminary elution tests typically targeted 15 peptides per salt step. The preliminary tests were also used to optimise the RP gradient in terms of instrument time usage and quantitation requirements. Due to 20 ms dwell times required for reliable quantitation on 4000 QTrap instruments as demonstrated before the efficient gradient time was reduced to ten minutes. With sample injection and analytical column reequilibration, the total instrument usage for one sample was 2.5 h.

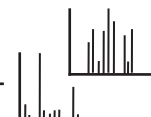
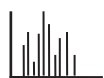
Elution fraction optimised MudPIT-SRM was compared to RP-SRM performing triplicate analyses of a human wound fluid sample using equal trapping condition. Similar to the plasma protein results, MudPIT-SRM showed advantages in peptide intensities and peak AUC. Figure 7.4 shows exemplarily the peak increases of targeted peptides from S100A8 and SAMP. Several target peptides detectable or quantifiable in MudPIT-SRM were unable to be detected (below LLOD) using RP-SRM (table 7.3). These results further proved the advantage of MudPIT-SRM applied to highly complex specimens common to



clinical applications with the possibility of simultaneous monitoring of numerous different target molecules specific to their behaviour on the SCX material.

Table 7.3: MudPIT-SRM and RP-SRM targeted peptides in human wound fluids including precursor and product ion masses, and peak AUC changes; used synonyms n/d: not detected (below LLOD), d: detectable (above LLOD), q: quantifiable (above LLOQ), n/a: ratio not able to be calculated

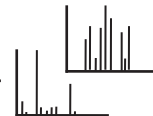
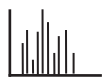
protein code	peptide sequence	precursor mass (m/z)	product ion mass (m/z)	RP-SRM	MudPIT-SRM	peak area changes (%)
ANXA1	GLGTDEDTLIEILASR	851.9	1015.614 688.399 801.482	n/d	d	n/a
ANXA2	SLYYIQQDTK	711.3	895.451 732.388 619.304	d	d	n/a
ANXA3	GAGTNEDALIEILTTR	837.4	732.430 845.510 958.590	d	q	n/a
	GIGTDEFTLNR	611.8	1052.501 894.431 995.479	d	q	n/a
GDIR1	AEEYEFLTPVEEAPK	876.4	769.410 870.460 1130.610	n/d	q	n/a
GDIR2	TLLGDGPVVTDPK	656.4	812.450 755.429 927.478	n/d	n/d	n/a
MMP2	AFQVWSDVTPLR	709.8	973.510 787.430 1200.637	q	q	-30.3
MMP8	YYAFDLIAQR	630.3	933.520 1096.578 862.480	q	q	24.5
	DAFELWSVASPLIFTR	926.5	1090.625 833.454 904.525	q	q	9.8
	ISQGEADINIAFYQR	862.9	911.473 1139.664 797.430	q	q	66.8
MMP9	QLSLPETGELDSATLK	851.4	1034.540 933.488 734.420	n/d	q	n/a
	AFALWSAVTPLTFTR	841.0	1092.568 934.540	q	q	28.3
	LGLGADVAQVTGALR	720.9	744.430 815.480 1029.568	d	d	n/a
PROF1	TFVNITPAEVGVLVGK	822.5	871.524 968.58 1069.625	q	q	60.5
	SSFYVNGTLGGQK	735.9	887.500 986.562 773.450	q	q	55.3
	STGGAPT FNVT VTK	690.4	1006.556 909.503 503.782	q	q	36.9



protein code	peptide sequence	precursor mass (m/z)	product ion mass (m/z)	RP-SRM	MudPIT-SRM	peak area changes (%)
SAMP	VGEYSLYIGR	578.8	708.404 057.530 871.467 1000.509	d	q	n/a
			825.384 972.452 738.357			
S100A4	ELPSFLGK	445.7	551.318 464.287 648.372	n/d	d	n/a
			849.430 948.497 718.390			
S100A7	GTNYLADVFEK	628.8	708.356 821.440 984.503	q	q	-21.2
			965.450 1066.498 1196.525			
S100A8	LLET*PQYIR	711.4	1034.588 818.510 905.550	q	q	49.7
			710.371 563.303 448.277			
S100A11	C*IESLIAVFQK	654.4	835.450 1108.540 964.500	n/d	q	n/a
			417.229 833.451 736.399			
S100A12	GHFDLSK	452.7	835.450 1108.540 964.500	q	d	n/a
			417.229 833.451 736.399			
S100P	YSGSEGSTQTLTK	679.8	835.450 1108.540 964.500	n/d	q	n/a
			417.229 833.451 736.399			
S100P	ELPGFLQSGK	538.3	835.450 1108.540 964.500	q	q	-63.2
			417.229 833.451 736.399			

7.2. Concluding aspects

The integration of a second chromatography interface into SRM investigations revealed prodigious advantages in peptide quantitation. Optimal positioning of the chromatography material allows an automatable strategy with 2-dimensional trapping system. Human plasma and human wound fluid submitted to MudPIT-SRM demonstrated significant increases in detection and quantitation of targeted peptides. SCX based fractionation enabled the generation of elution specific transition lists increasing the number of possible molecules of interest to be targeted in single injection experiments. This dramatically decreases instrument usage time what can benefit high throughput laboratories who commonly suffer from instrument time shortage. In addition to reduced instrument usage, application of MudPIT-SRM might make anti-peptide antibody based enrichment of middle concentrated proteins unnecessary, as MudPIT-SRM showed higher sensitivity and specificity investigating such peptides. Therefore, MudPIT-SRM can significantly improve the biomarker work flow currently used in proteomics.



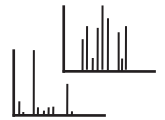
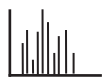
8. Membrane specific protein elimination in haemodialysis patients

Patients diagnosed with either type 1 or type 2 diabetes mellitus are not only at high risk to incur wound healing impairments but also commonly suffer from organ damage as a consequence of limited supply of glucose to organ cells or tissue, or protein damage by free glucose or its metabolites in the circulation generating severe changes to proteins and hormones with potential loss of their function [16, 192]. Organ damage in diabetics is most commonly derived by angiopathy. Angiopathy and impaired angiogenic stimulation, as shown in chapter 5 and chapter 6, is one of major factors in developing chronic ulcers in lower extremities of diabetes mellitus patients. Therefore, organ damage and chronic wound development have similar etiology. Diabetic retinopathy is described as diminished or complete loss of the visual function of the eye as a consequence of changes in blood vessel growth and a shortage in oxygen supply. Kidney capillary damage by angiopathy leads to diabetic nephropathy, the most prominent complication in patients with kidney failure.

DM patients who have incurred diabetic nephropathy highly depend on haemodialysis (HD). HD of patients with renal insufficiency is a method of artificial kidney functionality replacement in order to eliminate uremic toxins from the circulation. Substances classified as uremic toxins are metabolites, hormones, peptides, or proteins normally excreted by the kidney in healthy individuals that are accumulating in the blood and thereby cause damage to other macromolecules, blood vessels, or organs. Predominantly, oxidative stress in the circulating system derived from a variety of small molecules cause damage to proteins leading to chronic inflammation [192, 193]. Thus, these patients are prone to viral and bacterial infections derived by a compromised immune system

Studies revealed several macromolecules to have toxic potential in the circulation [194-196]. To the present day, 147 molecules are listed in the European Work Group of Uremic Toxins (EUTox) database [197] with known toxicity if accumulated. Forty of them are proteins or peptides (table 3.1). The development and the optimization of semi-permeable membranes with specific elimination properties for these substances is therefore a crucial process. Important for patient survival is the performance of the employed membrane in terms of permeability throughout dialysis session, clearance of uremic toxins, and depletion of essential macromolecules such as albumin and haemoglobin [198].

Common application in haemodialysis treatments are haemodiafiltration, low-flux HD, high-flux HD or high-flux haemodiafiltration (HDF). The differences of these techniques are depicted in figure 8.1. However, none of these treatments have been proven to



significantly contribute to overall survival or quality of live improvements. Several RCTs have been conducted [199-203] and frequently demonstrated beneficial survival outcomes only in subgroups of the investigated patient cohorts. The HEMO study group identified beneficial effects of high-flux HD on cardiovascular diseases (CVD) and cerebrovascular diseases (CBVD) in patients with no CVD or CBVD at the beginning of treatment [204, 205]. No effect in high dose versus normal dose high-flux HD was found [206]. The membrane permeability outcome (MPO) study group revealed better survival rates in patients with albumin level below 4g/dl (high-risk patients) and diabetics [207] leading to high-flux usage recommendation of the European Renal Best Practice Advisory Board for these patients [208].

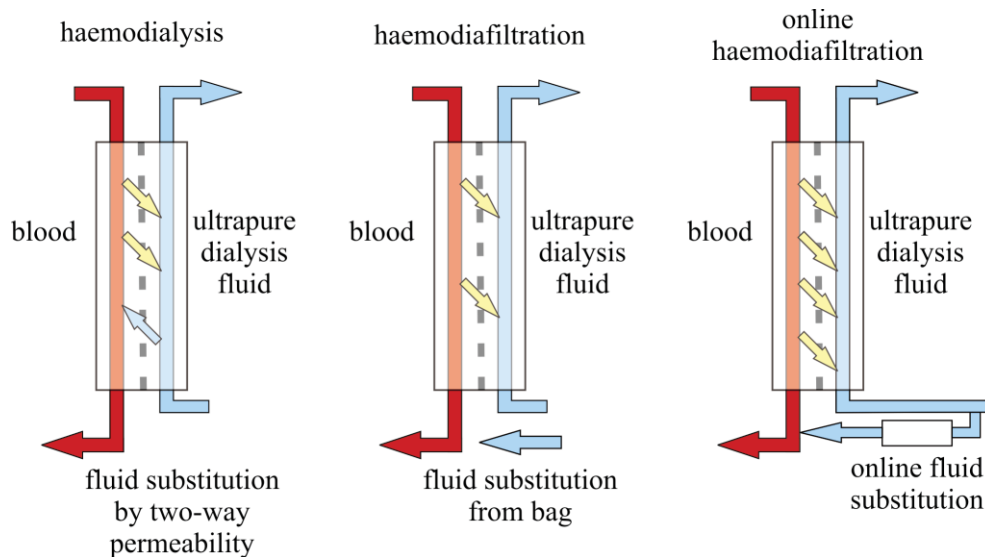
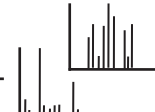


Figure 8.1: principles of commonly employed haemodialysis and haemodiafiltration devices

The CONTRAST group also stated no overall improvement in survival of patients either treated with online HDF or low-flux HD except for a subgroup of patients treated with high volume substitution HDF [209]. However, they found a positive long term effect of haemodialysis in terms of health-related quality of life compared to patients in previous haemodialysis assessments [210] but are influenced by the dialysis centre [211]. Similar results were observed from the TURKISH HDF group [203] and the ESHOL group comparing online HDF to high-flux HD. The TURKISH HDF group showed better CVD and overall survival in patients with high volume substitution HDF. All-cause mortality improvements were revealed by the ESHOL group in high-efficiency post dilution online HDF [212]. Taking these findings together, further optimization of haemodialysis membranes and a better understanding of molecule clearance from the circulation system is required.



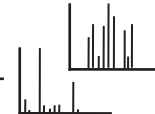
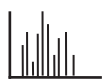
A challenging aspect in HD and HDF membrane development is the necessity to cover a broad mass range. Molecules classified as uremic toxins range from low mass molecules such as urea or creatinine to middle molecular weight proteins such as A1AG1/2 (23.5 kDa, 23.6 kDa), beta-2 microglobulin (B2MG, 13.7 kDa), RBP4 (23.0 kDa), complement factor D (CFAD, 27.0 kDa), cystatin C (CysC, 15.7 kDa), myoglobin (MYO, 17.2 kDa), the c-regions of immunoglobulin light chains kappa and lambda (IgKC, LAC), and proteins of the cytokine families. For other macromolecules, however, it is essential to remain undepleted like serum albumin, haemoglobin, or vitamin transporting proteins. Therefore, semi-permeable membranes with defined pore size and pore size distribution are required to allow sufficient uremic toxin elimination with low leakage of essential proteins.

uremic toxins			
adiponectin	fibrinblast growth factor 2	leptin	tumor necrosis factor α
adrenomedullin	fibroblast growth factor 23	melatonin	uroguanylin
angiogenin	guanylin	methionine-enkephalin	uteroglobin
atrial natriuretic peptide	insulin-like growth factor 1	motiline	vascular endothelial growth factor
calcitonin	interleukin 1- β	myoglobin	vasoactive intestinal polypeptide
calcitonin gene-related peptide	interleukin 6	neuropeptide Y	vasopressin
cholecystokinin	interleukin-10	osteocalcin	α 1-acid glycoprotein
complement factor D	interleukin-18	resistin	β -2-microglobulin
cystatin C	kappa-Ig light chain	retinol binding protein	β -endorphin
endothelin	lambda-Ig light chain	substance P	β -lipotropin

Table 8.1: list of known proteins, peptides and hormones with known toxic potential which are integrated into the EUTox Database [197]

Besides the need of membrane optimization, development of reliable analysis methods have to be developed in order to assess uremic toxin elimination efficiencies. A potential applicable strategy to address these needs is the MudPIT strategy.

Both diabetic and non-diabetic kidney replacement therapy dependent patients show oxidative stress in the circulating system. Therefore, further analysis of the protein content of spent dialysates from non-diabetic kidney replacement therapy dependent patients, as used in this study, might shed light on proteins involved in processes leading to arterial damage which might facilitate identification of similar processes in the development of chronic diabetic ulcers.



8.1. Protein clearance of high flux HD membranes

The impact of high flux membranes on protein elimination was investigated by comparing the protein composition of spent dialysates derived from Amembrix® (Xevonta Hi23) and Gambro Polyamix™ (Polyflux 210H) haemodialysis treated patients. A cohort of 9 patients who underwent dialysis treatments thrice a week were analyzed using the workflow depict in figure 8.2. Each patient was treated with both membranes in a crossover study. Five patients were treated with Xevonta Hi23 membranes in the first week of performance assessment and in the second week with Polyflux 210H, Xevonta Hi23/Polyflux 210H (X/P) crossover. The remaining 4 patients were treated vice versa within the Polyflux 210H/Xevonta Hi23 (P/X) crossover.

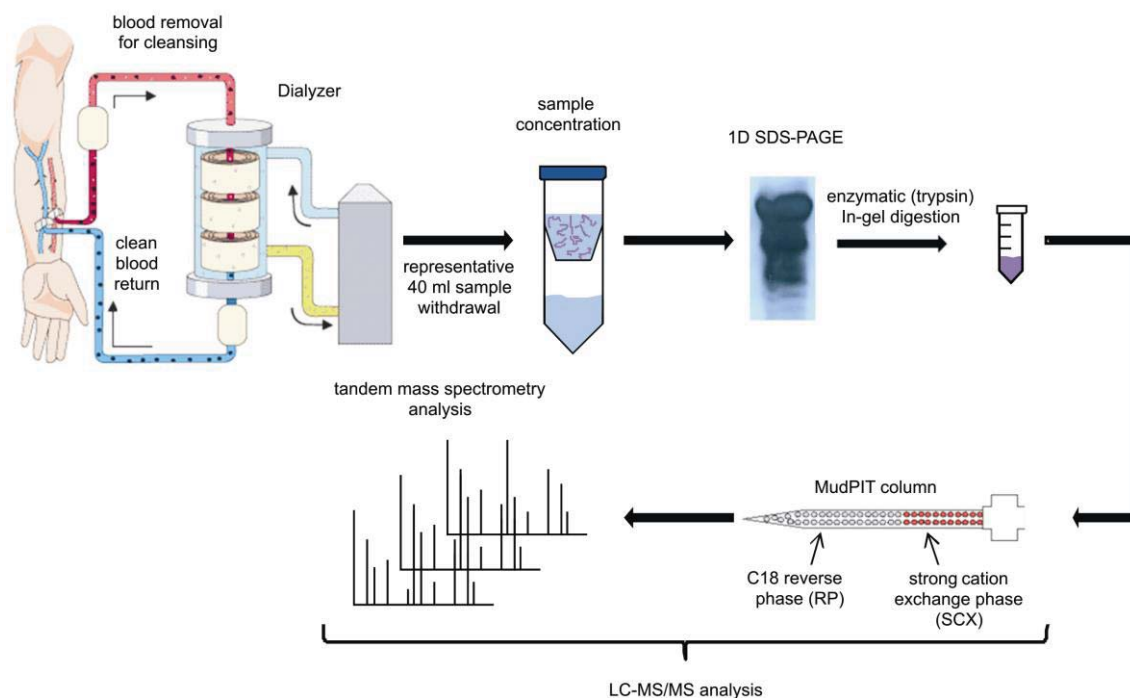


Figure 8.2: used workflow for analysis of proteins in spent dialysates of haemodialysis treated patients

The protein concentrations of selected individuals were estimated by BCA protein assays (figure 8.3). Dialysates derived from Xevonta Hi23 treatments demonstrated higher protein concentration if compared to Polyflux 210H treatments. Higher protein concentration implies higher rate of protein clearance by Xevonta Hi23. However, this might suggest elevated leakage of proteins with molecular weights above 60 kDa. Interestingly, Xevonta Hi23 membranes demonstrated excessive protein elimination in the P/X crossover, and only moderate increase in the X/P crossover, suggesting crossover related influences on the effectiveness of protein clearance.

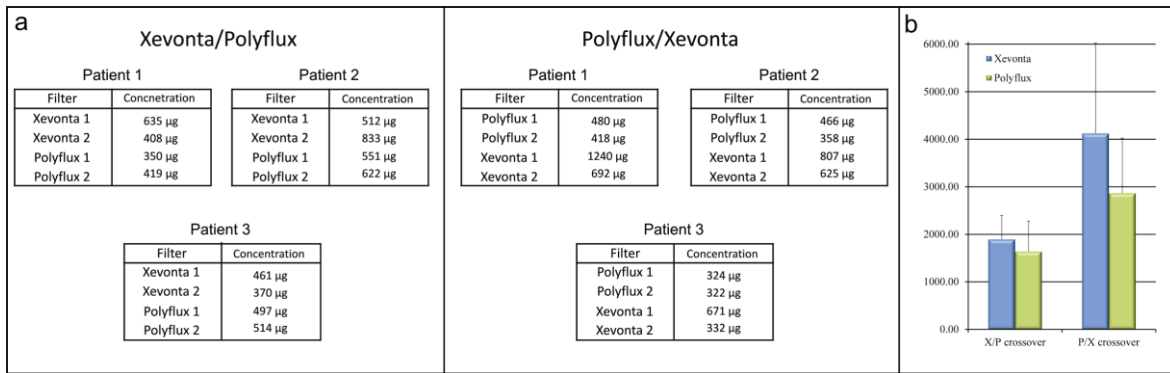
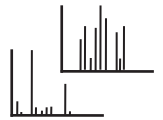
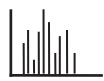


Figure 8.3: BCA assay analyses of 3 representatives of the X/P crossover (a) and 3 representatives of the P/X crossover (b); c) plot of mean total spectrum counts in the X/P and the P/X crossover

Spent dialysates were further investigated by mass spectrometry. Each patient sample set (two Xevonta Hi23 and two Polyflux 210H dialysate samples) were intra individually compared using label-free spectral counting. Therefore, the individual spectrum count per protein was normalized against the total spectrum count (TSC) of a sample to estimate the percentage of each protein on the TSC. In general, 120 proteins were identified in the dialysates. Both membranes supposed to have a molecular weight cut-off of 55 kDa. Therefore, most proteins were located in the 5 – 55 kDa mass range (60%). However, proteins with molecular weights above 55 kDa were also identified. Albumin was the most abundant protein in all samples with approximately 30% of the TSC. Proteins above 80 kDa made up 5%. Worth mentioning, several proteins identified in the dialysates undergo further proteolytic processing after secretion. Identification of the proteolysis generated products instead of the protein precursor was observed for some high molecular weight proteins, such as collagens and perlecan, explaining the detection of those proteins in the dialysates. Especially, perlecan was frequently detected in the dialysates. This 468 kDa protein can be enzymatically processed at the C-terminus to produce endorepellin (75.9 kDa), which can be further processed to the LG3 peptide (25 kDa). Figure 8.4 demonstrates that only the LG3 peptide from perlecan was identified and not its precursor.

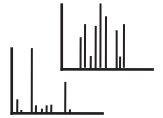
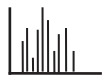


Figure 8.4: Perlecan sequence coverage of MS/MS identified peptides (green), sequence cover only represent parts of the amino acid sequence of the LG3 peptide region of perlecan (framed red)

Taking this effect into account, the high molecular weight protein percentage (> 80 kDa) is reduced to 2% and is therefore negligible in the assessment of membrane performance. Therefore, the elimination efficiencies were compared by the elimination of proteins below 55 kDa in an albumin dependency. The acquired data showed a decrease in TSC percentages of lower molecular weight proteins as albumin TSC percentage increased. Nonetheless, in both crossover studies Xevonta Hi23 membranes demonstrated higher elimination rates of proteins below 55 kDa in an albumin dependency (figure 8.5). Further, 7 of 9 individuals showed higher TSC values in Xevonta dialysate analysis. As protein specific spectrum counts correspond to protein abundance, higher TSC indicates a higher rate of peptide identification and thereby higher concentration of eliminated proteins in Xevonta Hi23 dialysates. Apparently, Xevonta Hi23 membranes showed higher excess rates in P/X than in X/P (figure 8.3b), which confirms the BCA assay results previously discussed.

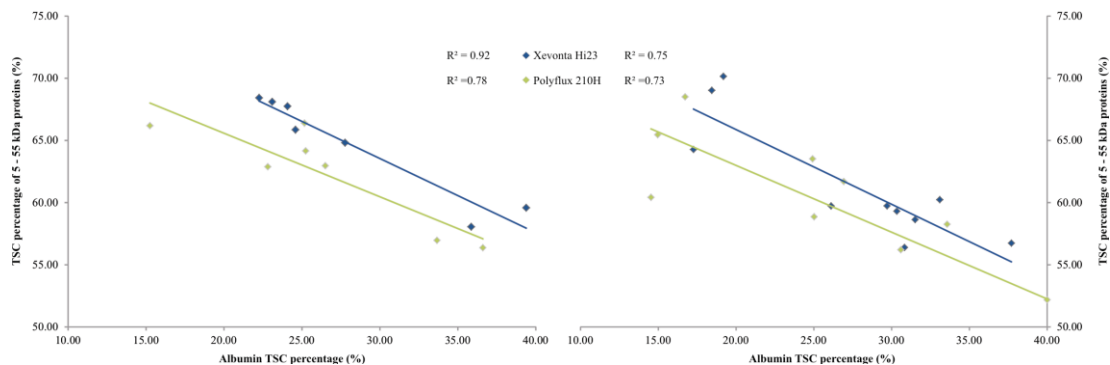
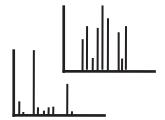
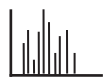


Figure 8.5: clearance percentage rate (based on the sum of TSC percentage) in dependence of albumin of proteins in the mass range from 5 – 55 kDa identified in spent dialysates of Xevonta Hi23 and Polyflux 210H crossover experiments



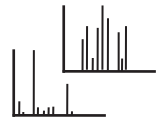
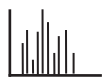
To investigate elimination efficiencies in specific mass ranges, the identified proteins were grouped by their molecular weight (table 8.2). The 10 – 18 kDa, 20 – 23 kDa and the 23 – 30 kDa mass ranges comprise the known uremic toxins A1AG1 and A1AG 2, B2MG, CysC, CFAD, IgKC, MYG, LAC; and RBP4. Comparably to the BCA results and the albumin dependency plots, crossover specific influences in membrane performance were also observed in the mass range comparison. In the X/P crossover, Xevonta Hi23 demonstrated advantages in elimination efficiencies in the 20 – 23 kDa, 23 – 30 kDa and 40 – 55 kDa mass ranges, but not in the 10 – 18 kDa and 30 – 40 kDa mass ranges, where higher protein elimination rates were observed in dialysates from Polyflux 210H membrane treatments. In the P/X crossover, Xevonta Hi23 membranes demonstrated higher clearance only in the 20 – 23 kDa and 20 – 30 kDa mass ranges, the other mass ranges revealed higher clearances in the Polyflux 201H treatment. These findings demonstrate a molecular mass range optimum for Xevonta Hi23 membranes in the mass range from 20 – 30 kDa.

A comparative study of elimination efficiencies of Xevonta Hi23, Xenium 210 and FX 100 dialysis membranes was conducted by Ficheux et al [213] using SDS-PAGE scanning methods. Consistent with the observations in the MS based comparison of Xevonta Hi23 to Polyflux 210H, they described advantages for Xevonta Hi23 in the elimination of middle molecular mass range proteins and identified an protein elimination optimum in the mass range from 20 – 30 kDa.

Table 8.2: mass range based assessment of elimination efficiencies in the employed high flux membranes; indicators used ↔: similarly eliminated; ↑: higher elimination rates in Xevonta Hi23; ↓: higher elimination rates in Polyflux 210H dialysates

mass range (kDa)	most abundant proteins	X/P crossover			P/X crossover		
		Xevonta	Polyflux		Polyflux	Xevonta	
10 – 18	B2MG, CysC, MYG	21.6	22.2	↓	17.4	15.9	↓
20 – 23	RBP4, LG3 peptide	9.1	8.3	↑	8.3	11.7	↑
23 – 30	CFAD, ILBPs A1AG1/2	8.3	6.0	↑	8.4	9.9	↑
30 – 40	ZA2G, A2GL, FETUA AMBP	9.7	10.9	↓	11.4	10.1	↓
40 – 55	A1AT, AACT, ANT3, VDBP	14.0	13.1	↓	12.1	9.9	↑
60 – 80	ALBU	29.4	27.4	↑	32.7	28.8	↓

Although the mass range assessment revealed a clearance optimum for Xevonta Hi23 membranes for proteins with molecular weights from 20 – 30 kDa, clearance of the uremic toxins A1AG1/2, B2MG, CFAD, CysC, MYO, and RBP4 were in general better in HD treatments with Xevonta Hi23 membranes (figure 8.6). A1AG1, RBP4 and CFAD were in



both P/X and X/P better eliminated using Xevonta Hi23. A1AB2 and B2MG were better eliminated by Xevonta Hi23 in the P/X crossover but revealed similar elimination rates in X/P. Contrary results were found for CysC. It was equally eliminated by both membranes in the P/X crossover and more efficiently by Xevonta Hi23 in the X/P crossover. Although MYO was identified in a relatively low abundance, it demonstrated more efficient elimination in the Xevonta Hi23 dialysates. Only IgKC and LAC demonstrated higher elimination rates by Polyflux 210H membranes in one crossover. IgKC was more efficiently eliminated by Polyflux 210H in the P/X crossover, LAC in the X/P crossover.

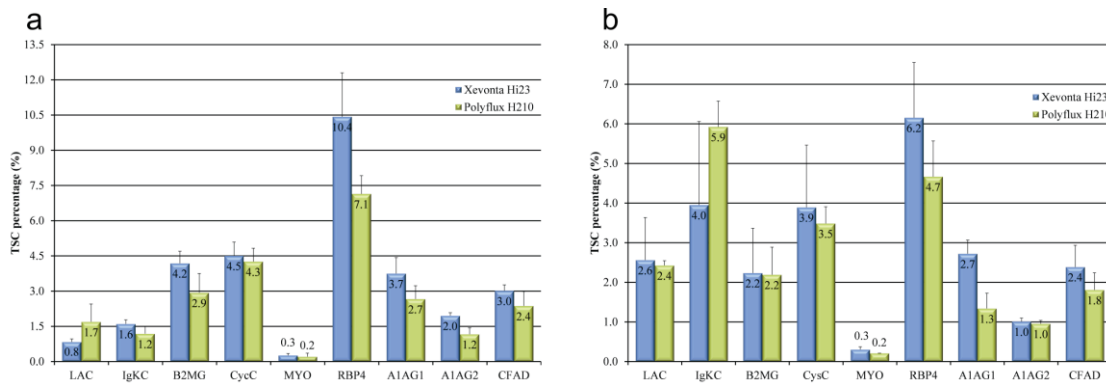
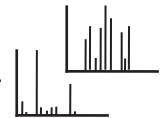
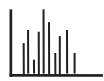


Figure 8.6: TSC percentage based uremic toxin elimination efficiencies in a) X/P crossover and in b) the P/X crossover

In conclusion, Xevonta Hi23 membranes demonstrated improved protein elimination efficiencies in the X/P and the P/X crossovers. However, the P/X crossover revealed more promising results for Xevonta Hi23 protein clearance than the X/P crossover. Therefore, a crossover related influence on the assessment was suggested. Differences in the elimination efficiency might arise from membrane saturation. The sooner a membrane is saturated the fewer proteins are eliminated. Since significant protein concentration increases from Polyflux 210H to Xevonta Hi23 in the P/X crossover was observed by BCA assays and by TSC comparison, a faster saturation of Polyflux 210H can be assumed. This effect was further observed comparing the elimination rates of the uremic toxins. Except for CysC the increase in the clearance of the assessed proteins was more dominant in the P/X crossover. Therefore, it can be assumed that Polyflux 210H membranes may tend to faster membrane saturations, leading to reduced protein clearance and therefore to higher accumulation rates of the toxins.

Beside the known uremic toxins A1AG1/2, B2MG, CysC, myoglobin, CFAD and RBP4, who were identified as one of the most abundant proteins in the investigated dialysates, the dataset comprised other proteins identified with high spectrum counts. The protein AMBP (alpha-1 microglobulin/bikunin precursor) was identified in comparable



abundance to RBP4 and CysC, who were two of the most abundant proteins identified in the analysed dialysates. This protein has not been described previously to be involved in renal failure or investigated for toxic potential. However, since it is a part of the major histocompatibility complex class I, consisting of alpha-1,-2,-3 and beta-2 microglobulin, it might be worth to be investigated.

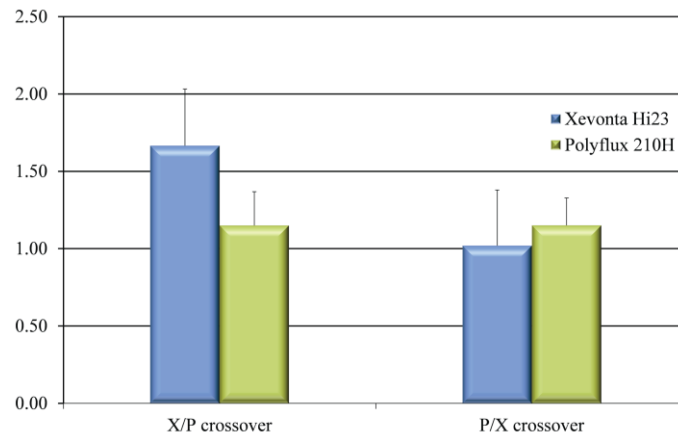
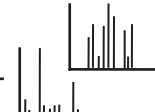
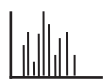


Figure 8.7: elimination of vitamin D binding protein based on TSC percentage in Xevonta Hi23 and Polyflux 210H dialysates

Another protein frequently identified is the vitamin D-binding protein (VDBP). It is one of the major vitamin D transporting proteins in the blood. In contrast to uremic toxins, VDBP should remain in the circulation [214]. However, the protein is with 52.9 kDa below the molecular weight cut-off. A frequent elimination of VDBP by dialysis reduces the vitamin D supply, a common complication in HD patients. Comparison of the TSC percentages (figure 8.7) of VDBP clearance revealed higher elimination by Xevonta Hi23 membranes. However, in haemodialysis compromises have to be made between the need of proteins required to be eliminated and proteins required to be remained in the blood.

In conclusion, mass spectrometry was successfully used to identify proteins present in spent dialysates from kidney replacement therapy dependent patients. This study demonstrated an approach to assess membrane permeability of employed dialysis devices and showed weaknesses in elimination efficiencies of specific proteins. Importantly, the approach highlighted additional proteins with potential uremic toxin capabilities. The MudPIT-MS/MS strategy could also be used in future studies to investigate the degree of plasma protein modification to assess the oxidative stress in the circulation. Therefore, employing this proteomic tool in the assessment of spent dialysates could add new knowledge to patient response of kidney replacement treatment and contribute towards improved treatments for HD patients, especially those whose disease has developed as a result of T2D.

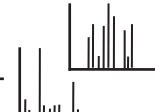
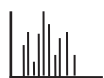


9. Conclusion

In this study the protein composition of human wound fluids from poor healing chronic wounds and normal healing acute wounds were investigated by proteomic tools to identify crucial processes in wound healing. The understanding of healing processes is of huge importance as the number of patients with diabetes mellitus is continuously increasing [25], thus increased occurrence of chronic wounds in these patients is to be expected. Besides the progress that has been made in the treatment of these wounds, amputations of extremities, especially in patients with diabetes mellitus, is still a common consequence as a last alternative to ensure patient survival. Therefore, the investigation and identification of specific markers for chronic wounds are needed to enable early diagnosis and initiate appropriate treatment more quickly. Some efforts have been done to investigate biological processes in chronic wounds, which led to the identification of dysregulation of matrix metalloproteinases [97-101], prolonged inflammation [95, 96], and reduced vascularisation in chronic wounds [119, 120].

Despite these findings, no study has been conducted showing wound healing in its complex proteomic background. Therefore, in this thesis, large scale mass spectrometry analyses of human wound fluids from diabetics with chronic wounds and patients with normal healing wounds were performed. Initial experiments were conducted to investigate strategies to enhance detection and quantification of proteins in human wound fluids with the aim to elucidate biological wound healing processes. Wound fluids are considered as highly complex protein mixtures and therefore challenging for MS identification, comparably to serum or plasma, which comprise dynamic protein ranges of 10-14 orders of magnitude [215]. In order to assess this large dynamic range, enrichment and fractionation strategies have been investigated towards applicability to human wound fluids.

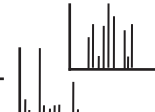
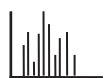
The development of an enrichment strategy of post-translational glycosylated proteins using a boronic acid gel resin affinity chromatography was demonstrated to be applicable to purified and complex samples with satisfying enrichment of 85% of identified glycoproteins in a human wound fluid sample (chapter 4). In terms of enrichment efficiency of glycosylated proteins, BAGAC demonstrated advantages when compared to the multi lectin affinity chromatography (MLAC), where the enrichment efficiency was stated to be 75% [81]. Further, it involved less complex sample handling reducing the sources of sample loss. However, BAGAC enrichment failed in the enrichment of glycosylated peptides. An explanation was proposed as the binding strength of glycans to the boronic acids. This binding of glycans is a reversible, non-covalent interaction and



therefore depends on the number of glycans per protein/peptide, the accessibility, steric hindrance and other interfering side groups of the protein/peptide. Results from the glycoprotein enrichment demonstrated more efficient enrichment of glycoproteins with more than one glycosylation site (e. g. fetuin A) than mono-glycosylated proteins (A1AG1). Therefore, multi-glycosylated proteins demonstrated higher affinity to the resin, which explains poor binding of glycopeptides, as almost all of them contain only a single glycosylation site.

Another enrichment strategy that was investigated was immunoaffinity chromatography to deplete the 20 most abundant plasma proteins (chapter 5). This strategy was proven to be incompatible to large scale analyses of human wound fluid. Comparison of depleted and non-depleted wound fluids demonstrated substantial co-depletion of less abundant proteins whilst highly concentrated proteins were still present in high quantities in the depleted samples, consistent with saturation. These results corroborate with findings from other groups investigating immunoaffinity depletion and a movement of the proteomic field away from extensive immunodepletion strategies towards less complex ones, or even to avoid immunodepletion altogether [216, 217].

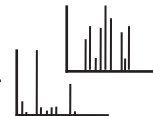
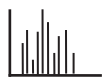
Since enrichment or depletion strategies in general suffer from extensive protein losses, online LC enrichment methods were investigated. This led to the development of a 2D LC-SRM-MS application based on the MudPIT technology (chapter 7) [31, 189]. The so call MudPIT-SRM strategy demonstrated in comparison to conventional RP-SRM significant increases in peak areas of monitored transitions and a reduced lower detection limit. The integration of a second injection loop, which was continuously filled with isotope labelled reference peptides, enabled a novel strategy to introduce reference peptides into the flow path of MudPIT experiments after fractionation on the SCX resin. This strategy is essential for intra and inter-fraction normalisation. The benefits of MudPIT-SRM were demonstrated on proteins in albumin and IgG depleted human plasma and non-depleted human wound fluids. Especially the analysis strategy showed the advantages of MudPIT-SRM over RP-SRM. As almost all peptides eluted in one fraction only, MudPIT-SRM allows for increased multiplexing since different peptides can be targeted in each fraction analysis. This means from a single sample injection numerous target peptides can be quantitated, where on the other hand several injections of the same sample are necessary for conventional RP-SRM. Therefore, MudPIT-SRM-MS has been proven to enhance detection and quantitation of targeted peptides in SRM approaches and



reduces the amount of sample needed for quantitation, which is essential for SRM-MS integration into clinical analysis routines.

Since offline based fractionation of human wound fluids was considered inappropriate due to the risk of significant protein losses during sample handling, the samples were analysed by label-free large scale MudPIT-MS/MS (chapter 5). This analysis revealed 714 proteins to be common amongst the exudates, with reproducible normalised spectral counting percentages of housekeeping proteins. Proteins demonstrating spectral counting differences ≥ 2 -fold and p-values ≤ 0.05 were considered as significantly differentially expressed. Therefore, 151 proteins were identified in significantly higher expression levels and 37 proteins were at significantly lower expression levels in the fluids of chronic wounds. The investigation of protein expression in exudates of acute and chronic wounds demonstrated dramatic differences in essential wound healing phases including inflammation, and revascularisation. The chronic wounds demonstrated excessive inflammation with S100A8 and A9 almost 10-fold elevated, which was validated by western blot analyses. This correlates well with previous studies, which also demonstrated excessive inflammation in chronic wounds [53, 95, 96]. These and other studies further described increased ECM protease activity and reduced vascularisation derived from over-responsive inflammatory regulation [18, 99, 100]. The investigation of fluids from chronic wounds demonstrated excessive degradation of the ECM structure proteins (collagens) and revealed elevated expression of MMP 1, 2 and 8. Additionally, these fluids showed diminished revascularisation, since important pro-angiogenic mediators were identified at lower expression levels in the fluids of chronic wounds and anti-angiogenic mediators were elevated. Elevated inflammatory signalling, mediating cell growth, cell division or cell migration, paired with diminished vascularisation, a shortage in oxygen and nutrition supply, should lead to dramatically increased cell death either by controlled cell death, which was demonstrated by elevation of the late apoptotic cell marker ANXA5 in the chronic wounds. Elevated cell death and reduced supply of tissue in wounds are most common complications leading to the development of chronic wounds [218]. This is exemplified in poor or non-treated chronic ulcers in diabetics which are dominated by necrotic tissue [219], creating wound bed conditions incapable of regaining and maintaining structural integrity and unable to heal.

Selected proteins that were found to be at differing expression levels in the fluids of chronic wounds were further investigated by SRM-MS to validate the MudPIT-MS/MS results (chapter 6). Here it was shown in the fluids from chronic and acute wounds, the

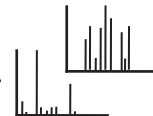
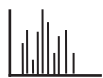


presence of the inflammation mediating S100 proteins A8, A9, A11 and A12 at higher levels in the fluids of chronic wounds. Further, the expression level of the ECM degrading proteases MMP2 and MMP9 were confirmed by SRM. However, the SRM targeted MMP8 peptides did not correlate with the MudPIT-MS/MS finding. This might be explained by the characteristics of the selected peptides. Both peptides were highly hydrophobic and therefore eluted late from the column compared to the other targeted peptides. The elution profiles of these peptides were broader and thus more susceptible for misinterpretation due to interferences. Further, MMP8 has a probable disulphide bond between cysteine 279 and cysteine 464. Interestingly, in the MudPIT-MS/MS study the MMP8 peptide YYAFDLIAQR was infrequently identified in the acute wound fluids but was present in all chronic wound fluids. The MudPIT-MS/MS study was performed under non-reducing conditions, whereas the SRM-MS study involved reduction and alkylation of cysteine residues. Since the YYAFDLIAQR peptide is located in the proximity of the later cysteine (464), trypsin cleavage of this site might be reduced. These results could indicate differences in the folding of MMP8 in the chronic wound fluids, which has to be validated in future studies. Nonetheless, except for the MMP8 peptides, the SRM-MS results correlated very well with the findings in the MudPIT-MS/MS study.

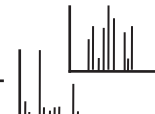
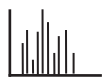
The conclusions drawn from the protein composition investigation of exudates from chronic and acute wounds is coherent with the current understanding of wound healing complications and may give new insights into processes potentially involved in the development of poor healing wounds.

Worth mentioning, the comparison of wounds was carried out on samples derived from different areas of the skin, acute wound fluids from skin-grafts taken from thighs and chronic wound fluids from foot or lower leg ulcers. However, these depicted the well-known differences between normal healing wounds and poor healing wounds making it a valuable model system to investigate and contrast healing processes. For future investigations it could be interesting to compare wound fluids derived from a more closely related patient cohort. For example, comparing normal healing wounds from diabetes mellitus patients to poor healing chronic wounds from diabetics might add additional information to understand the processes leading to chronic wounds.

In a study closely related to diabetes mellitus complication that lead to kidney failure and the need of kidney replacement therapy, the performance of two online haemodiafiltration membranes were assessed in terms of protein elimination efficiencies during a two week cross over treatment course (chapter 8). Label-free MudPIT-MS/MS

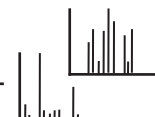


analyses was applied and revealed protein elimination advantages of Xevonta Hi23 membrane when compared to Polyflux 210H membranes. An elimination optimum was observed for Xevonta Hi23 membranes for proteins in the mass range from 20 – 30 kDa. The advantage of Xevonta Hi23 in this area has also been demonstrated by an SDS-PAGE scanning method established by Ficheux et al. [213]. Further examination focused on specific elimination of proteins known as uremic toxins and listed in the EUTox database [197], demonstrated that, except for Ig lambda and kappa, all identified uremic toxins with molecular weights above 10 kDa were more efficiently eliminated using Xevonta Hi23 membranes. Therefore, this study shows advantages of Xevonta Hi23 over Polyflux 210H in terms of proteins present in spent dialysates. Besides the performance assessment of the haemodialysis membranes, the acquired data revealed a deeper insight into composition of spent dialysates. Thus, proteomic profiling of spent dialysates might help to understand current complications that arise in patients undergoing kidney replacement therapy. It was shown in previous studies that online HDF benefit patients and increases the overall survival rate, if compared to conventional high-flux haemodialysis [203, 209, 212]. It was beyond the scope of this study to investigate the effect on the overall survival and the long term effect in Xevonta Hi23 membrane treated patients, but might be an interesting subject for future studies. Further, comparison of the spent dialysates of online HDF to high-flux HD applying LC-MS/MS might give interesting insight into protein elimination differences and might identify drawbacks in kidney replacement therapy that could lead to further optimised dialysis membranes and ultimately to treatments adjusted to the needs of each individual patient.

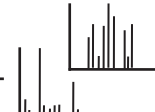


10. References

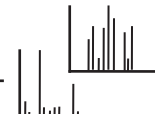
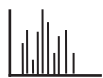
- [1] Proksch, E., Brandner, J. M., Jensen, J.-M., The skin: an indispensable barrier. *Exp. Dermatol.* 2008, 17, (12), 1063-1072.
- [2] Habif, T. P., *Principles of Diagnosis and Anatomy*, in: Habif, T. P. (Ed.), *Clinical Dermatology*, 5th edition, Mosby, Edingburgh 2010, pp. 1-5.
- [3] MacNeil, S., Progress and opportunities for tissue-engineered skin. *Nature* 2007, 445, (7130), 874-880.
- [4] Simpson, C. L., Patel, D. M., Green, K. J., Deconstructing the skin: cytoarchitectural determinants of epidermal morphogenesis. *Nat. Rev. Mol. Cell Biol.* 2011, 12, (9), 565-580.
- [5] Paulsson, M., Mats Basement Membrane Proteins: Structure, Assembly, and Cellular Interactions. *Crit. Rev. Biochem. Mol. Biol.* 1992, 27, (1-2), 93-127.
- [6] Soller, E. C., Yannas, I. V., *Induced Regeneration of Skin and Peripheral Nerves*, in: Veves, A., Giurini, J., Logerfo, F. (Eds.), *The Diabetic Foot*, Humana Press, Boston 2006, pp. 83-103.
- [7] Davidson, J., DiPietro, L., *The Wound-Healing Process*, in: Veves, A., Giurini, J., Logerfo, F. (Eds.), *The Diabetic Foot*, Humana Press, Boston 2006, pp. 59-82.
- [8] Harding, K. G., Morris, H. L., Patel, G. K., Science, medicine, and the future - Healing chronic wounds. *Br. Med. J.* 2002, 324, (7330), 160-163.
- [9] Artuc, M., Hermes, B., Steckelings, U. M., Grutzkau, A., Henz, B. M., Mast cells and their mediators in cutaneous wound healing--active participants or innocent bystanders? *Exp. Dermatol.* 1999, 8, (1), 1-16.
- [10] Leibovich, S. J., Ross, R., The role of the macrophage in wound repair. A study with hydrocortisone and antimacrophage serum. *Am. J. Pathol.* 1975, 78, (1), 71-100.
- [11] Shai, A., Maibach, H. I., *Natural Course of Wound Repair Versus Impaired Healing in Chronic Skin Ulcers*, in: Shai, A., Maibach, H. I. (Eds.), *Wound Healing and Ulcers of the Skin*, Springer, Heidelberg 2005, pp. 7-17.
- [12] Bennett, N. T., Schultz, G. S., Growth factors and wound healing: biochemical properties of growth factors and their receptors. *Am. J. Surg.* 1993, 165, (6), 728-737.
- [13] Akira, S., Takeda, K., Toll-like receptor signalling. *Nat. Rev. Immunol.* 2004, 4, (7), 499-511.
- [14] Bierhaus, A., Humpert, P., Morcos, M., Wendt, T., *et al.*, Understanding RAGE, the receptor for advanced glycation end products. *J. Mol. Med.* 2005, 83, (11), 876-886.



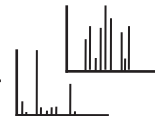
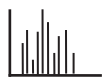
- [15] Ramasamy, R., Vannucci, S. J., Yan, S. S. D., Herold, K., *et al.*, Advanced glycation end products and RAGE: a common thread in aging, diabetes, neurodegeneration, and inflammation. *Glycobiology* 2005, 15, (7), 16R-28R.
- [16] Ahmed, N., Advanced glycation endproducts--role in pathology of diabetic complications. *Diabetes Res. Clin. Pract.* 2005, 67, (1), 3-21.
- [17] Dinh, T., *Microvascular Changes in the Diabetic Foot*, in: Veves, A., Giurini, J., Logerfo, F. (Eds.), *The Diabetic Foot*, Humana Press, Boston 2006, pp. 131-145.
- [18] Hunt, T. K., Knighton, D. R., Thakral, K. K., Goodson, W. H., 3rd, Andrews, W. S., Studies on inflammation and wound healing: angiogenesis and collagen synthesis stimulated in vivo by resident and activated wound macrophages. *Surgery* 1984, 96, (1), 48-54.
- [19] Iruela-Arispe, M. L., Dvorak, H. F., Angiogenesis: a dynamic balance of stimulators and inhibitors. *Thromb. Haemostasis* 1997, 78, (1), 672-677.
- [20] Brown, N. J., Smyth, E. A., Cross, S. S., Reed, M. W., Angiogenesis induction and regression in human surgical wounds. *Wound Repair Regen.* 2002, 10, (4), 245-251.
- [21] Shai, A., Maibach, H. I., *Basic Definitions and Introduction*, in: Shai, A., Maibach, H. I. (Eds.), *Wound Healing and Ulcers of the Skin*, Springer, Heidelberg 2005, pp. 1-5.
- [22] Shai, A., Maibach, H. I., *Debridement*, in: Shai, A., Maibach, H. I. (Eds.), *Wound Healing and Ulcers of the Skin*, Springer, Heidelberg 2005, pp. 119-134.
- [23] Eisenbarth, G. S., Type I diabetes mellitus. A chronic autoimmune disease. *N. Engl. J. Med.* 1986, 314, (21), 1360-1368.
- [24] Thévenod, F., *Pathophysiology of Diabetes Mellitus Type 2: Roles of Obesity, Insulin Resistance and beta-Cell Dysfunction*, in: Masur, K., Thévenod, F., Zänker, K. S. (Eds.), *Diabetes and Cancer*, Karger, Basel 2008.
- [25] Shaw, J. E., Sicree, R. A., Zimmet, P. Z., Global estimates of the prevalence of diabetes for 2010 and 2030. *Diabetes Res. Clin. Pract.* 2010, 87, (1), 4-14.
- [26] Rosenbloom, A. L., Joe, J. R., Young, R. S., Winter, W. E., Emerging epidemic of type 2 diabetes in youth. *Diabetes Care* 1999, 22, (2), 345-354.
- [27] Steen, H., Mann, M., The ABC's (and XYZ's) of peptide sequencing. *Nat. Rev. Mol. Cell Biol.* 2004, 5, (9), 699-711.
- [28] Makarov, A., Scigelova, M., Coupling liquid chromatography to Orbitrap mass spectrometry. *J. Chromatogr. A* 2010, 1217, (25), 3938-3945.



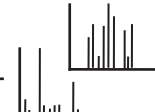
- [29] Olsen, J. V., Schwartz, J. C., Griep-Raming, J., Nielsen, M. L., *et al.*, A Dual Pressure Linear Ion Trap Orbitrap Instrument with Very High Sequencing Speed. *Mol. Cell. Proteomics* 2009, 8, (12), 2759-2769.
- [30] Tabb, D. L., Eng, J. K., Yates, J. R., *Protein Identification by Sequest*, Springer, New York 2001.
- [31] Washburn, M., Wolters, D., Yates, J., Large-scale analysis of the yeast proteome by multidimensional protein identification technology. *Nat. Biotechnol.* 2001, 19, (3), 242 - 247.
- [32] Ong, S.-E., Mann, M., Mass spectrometry-based proteomics turns quantitative. *Nat. Chem. Biol.* 2005, 1, (5), 252-262.
- [33] Liu, H., Sadygov, R. G., Yates, J. R., A Model for Random Sampling and Estimation of Relative Protein Abundance in Shotgun Proteomics. *Anal. Chem.* 2004, 76, (14), 4193-4201.
- [34] Han, B., Higgs, R. E., Proteomics: from hypothesis to quantitative assay on a single platform. Guidelines for developing MRM assays using ion trap mass spectrometers. *Brief. Funct. Genomics Proteomics* 2008, 7, (5), 340-354.
- [35] Prakash, A., Tomazela, D. M., Frewen, B., MacLean, B., *et al.*, Expediting the Development of Targeted SRM Assays: Using Data from Shotgun Proteomics to Automate Method Development. *J. Proteome Res.* 2009, 8, (6), 2733-2739.
- [36] Chiu, C.-L., Randall, S., Molloy, M. P., Recent progress in selected reaction monitoring MS-driven plasma protein biomarker analysis. *Bioanalysis* 2009, 1, (4), 847-855.
- [37] Krisp, C., Randall, S. A., McKay, M. J., Molloy, M. P., Towards clinical applications of selected reaction monitoring for plasma protein biomarker studies. *Proteomics Clin. Appl.* 2011, 6, (1-2), 42-59.
- [38] Lehmann, S., Poinot, P., Tiers, L., Junot, C., *et al.*, From "Clinical Proteomics" to "Clinical Chemistry Proteomics": considerations using quantitative mass-spectrometry as a model approach. *Clin. Chem. Lab. Med.* 2012, 50, (2), 235-242.
- [39] Mikami, T., Aoki, M., Kimura, T., The application of mass spectrometry to proteomics and metabolomics in biomarker discovery and drug development. *Curr. Mol. Pharm.* 2012, 5, (2), 301-316.
- [40] Rauh, M., LC-MS/MS for protein and peptide quantification in clinical chemistry. *J. Chromatogr. B* 2012, 883, (S1), 59-67.



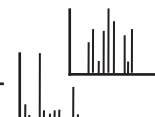
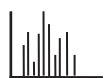
- [41] Broadbent, J., Walsh, T., Upton, Z., Proteomics in chronic wound research: potentials in healing and health. *Proteomics Clin. Appl.* 2010, 4, (2), 204-214.
- [42] Hermes, O., Schlage, P., auf dem Keller, U., Wound degradomics - current status and future perspectives. *Biol. Chem.* 2011, 392, (11), 949-954.
- [43] Sweitzer, S. M., Fann, S. A., Borg, T. K., Baynes, J. W., Yost, M. J., What is the future of diabetic wound care? *Diabetes Educ.* 2006, 32, (2), 197-210.
- [44] Cecchi, R., Estimating wound age: looking into the future. *Int. J. Leg. Med.* 2010, 124, (6), 523-536.
- [45] Groessl, M., Luksch, H., Rosen-Wolff, A., Shevchenko, A., Gentzel, M., Profiling of the human monocytic cell secretome by quantitative label-free mass spectrometry identifies stimulus-specific cytokines and proinflammatory proteins. *Proteomics* 2012, 12, (18), 2833-2842.
- [46] Muller, S. A., van der Smissen, A., von Feilitzsch, M., Anderegg, U., *et al.*, Quantitative proteomics reveals altered expression of extracellular matrix related proteins of human primary dermal fibroblasts in response to sulfated hyaluronan and collagen applied as artificial extracellular matrix. *J. Mater. Sci. Mater. Med.* 2012, 23, (12), 3053-3065.
- [47] Boraldi, F., Annovi, G., Carraro, F., Naldini, A., *et al.*, Hypoxia influences the cellular cross-talk of human dermal fibroblasts. A proteomic approach. *Biochim. Biophys. Acta* 2007, 1774, (11), 1402-1413.
- [48] Cipriani, V., Ranzato, E., Balbo, V., Mazzucco, L., *et al.*, Long-term effect of platelet lysate on primary fibroblasts highlighted with a proteomic approach. *J. Tissue Eng. Regen. Med.* 2009, 3, (7), 531-538.
- [49] Garcia, A., Prabhakar, S., Brock, C. J., Pearce, A. C., *et al.*, Extensive analysis of the human platelet proteome by two-dimensional gel electrophoresis and mass spectrometry. *Proteomics* 2004, 4, (3), 656-668.
- [50] Sharma, N., Medikayala, S., Defour, A., Rayavarapu, S., *et al.*, Use of quantitative membrane proteomics identifies a novel role of mitochondria in healing injured muscles. *J. Biol. Chem.* 2012, 287, (36), 30455-30467.
- [51] Edsberg, L. E., Wyffels, J. T., Brogan, M. S., Fries, K. M., Analysis of the proteomic profile of chronic pressure ulcers. *Wound Repair Regen.* 2012, 20, (3), 378-401.
- [52] Wyffels, J. T., Fries, K. M., Randall, J. S., Ha, D. S., *et al.*, Analysis of pressure ulcer wound fluid using two-dimensional electrophoresis. *Int. Wound J.* 2010, 7, (4), 236-248.



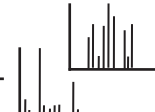
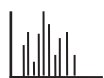
- [53] Eming, S. A., Koch, M., Krieger, A., Brachvogel, B., *et al.*, Differential Proteomic Analysis Distinguishes Tissue Repair Biomarker Signatures in Wound Exudates Obtained from Normal Healing and Chronic Wounds. *J. Proteome Res.* 2010, 9, (9), 4758-4766.
- [54] Fernandez, M., Broadbent, J., Shooter, G., Malda, J., Upton, Z., Development of an enhanced proteomic method to detect prognostic and diagnostic markers of healing in chronic wound fluid. *Br. J. Dermatol.* 2008, 158, (2), 281 - 290.
- [55] Taverna, D., Nanney, L. B., Pollins, A. C., Sindona, G., Caprioli, R., Multiplexed molecular descriptors of pressure ulcers defined by imaging mass spectrometry. *Wound Repair Regen.* 2011, 19, (6), 734-744.
- [56] Pollins, A. C., Friedman, D. B., Nanney, L. B., Proteomic investigation of human burn wounds by 2D-difference gel electrophoresis and mass spectrometry. *J. Sur. Res.* 2007, 142, (1), 143-152.
- [57] Annesley, T. M., Ion Suppression in Mass Spectrometry. *Clin. Chem.* 2003, 49, (7), 1041-1044.
- [58] Jessome, L. L., Volmer, D. A., Ion Suppression: A Major Concern in Mass Spectrometry. *LCGC North America* 2006, 24, (5), 498-510.
- [59] Müller, C., Schäfer, P., Stärtzel, M., Vogt, S., Weinmann, W., Ion suppression effects in liquid chromatography-electrospray-ionisation transport-region collision induced dissociation mass spectrometry with different serum extraction methods for systematic toxicological analysis with mass spectra libraries. *J. Chromatogr. B* 2002, 773, (1), 47-52.
- [60] Varki, A., Lowe, J. B., *Biological Roles of Glycans*, in: Varki, A., Cummings, R. D., Esko, J. D., Freeze, H. H., *et al.* (Eds.), *Essentials of Glycobiology. 2nd edition.*, Cold Spring Harbor Laboratory Press, Cold Spring Harbor 2009.
- [61] Stanley, P., Schachter, H., Taniguchi, N., *N-Glycans*, in: Varki, A., Cummings, R. D., Esko, J. D., Freeze, H. H., *et al.* (Eds.), *Essentials of Glycobiology. 2nd edition.*, Cold Spring Harbor Laboratory Press, Cold Spring Harbor 2009.
- [62] Brockhausen, I., Schachter, H., Stanley, P., *O-GalNAc Glycans*, in: Varki, A., Cummings, R. D., Esko, J. D., Freeze, H. H., *et al.* (Eds.), *Essentials of Glycobiology. 2nd edition.*, Cold Spring Harbor Laboratory Press, Cold Spring Harbor 2009.
- [63] Dai, Z., Zhou, J., Qiu, S. J., Liu, Y. K., Fan, J., Lectin-based glycoproteomics to explore and analyze hepatocellular carcinoma-related glycoprotein markers. *Electrophoresis* 2009, 30, (17), 2957-2966.



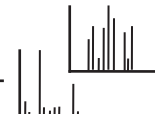
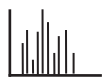
- [64] Ahn, Y. H., Lee, J. Y., Lee, J. Y., Kim, Y. S., *et al.*, Quantitative Analysis of an Aberrant Glycoform of TIMP1 from Colon Cancer Serum by L-PHA-Enrichment and SISCAPA with MRM Mass Spectrometry. *J. Proteome Res.* 2009, 8, (9), 4216-4224.
- [65] Dayarathna, M., Hancock, W. S., Hincapie, M., A two step fractionation approach for plasma proteomics using immunodepletion of abundant proteins and multi-lectin affinity chromatography: Application to the analysis of obesity, diabetes, and hypertension diseases. *J. Sep. Sci.* 2008, 31, (6-7), 1156-1166.
- [66] Plavina, T., Wakshull, E., Hancock, W. S., Hincapie, M., Combination of abundant protein depletion and multi-lectin affinity chromatography (M-LAC) for plasma protein biomarker discovery. *J. Proteome Res.* 2007, 6, (2), 662-671.
- [67] Wang, Y. H., Wu, S. L., Hancock, W. S., Approaches to the study of N-linked glycoproteins in human plasma using lectin affinity chromatography and nano-HPLC coupled to electrospray linear ion trap-Fourier transform mass spectrometry. *Glycobiology* 2006, 16, (6), 514-523.
- [68] Wang, Y. H., Wu, S. L., Hancock, W. S., Monitoring of glycoprotein products in cell culture lysates using lectin affinity chromatography and capillary HPLC coupled to electrospray linear ion trap-Fourier transform mass spectrometry (LTQ/FTMS). *Biotechnol. Progr.* 2006, 22, (3), 873-880.
- [69] Yang, Z. P., Hancock, W. S., Chew, T. R., Bonilla, L., A study of glycoproteins in human serum and plasma reference standards (HUPO) using multilectin affinity chromatography coupled with RPLC-MS/MS. *Proteomics* 2005, 5, (13), 3353-3366.
- [70] Patel, T., Bruce, J., Merry, A., Bigge, C., *et al.*, Use of hydrazine to release in intact and unreduced form both N- and O-linked oligosaccharides from glycoproteins. *Biochemistry* 1993, 32, (2), 679-693.
- [71] Zhang, H., Li, X.-j., Martin, D. B., Aebersold, R., Identification and quantification of N-linked glycoproteins using hydrazide chemistry, stable isotope labeling and mass spectrometry. *Nat. Biotechnol.* 2003, 21, (6), 660-666.
- [72] Liu, T., Qian, W.-J., Gritsenko, M. A., Camp, D. G., *et al.*, Human Plasma N-Glycoproteome Analysis by Immunoaffinity Subtraction, Hydrazide Chemistry, and Mass Spectrometry. *J. Proteome Res.* 2005, 4, (6), 2070-2080.
- [73] Monzo, A., Olajos, M., De Benedictis, L., Rivera, Z., *et al.*, Boronic acid lectin affinity chromatography (BLAC). 2. Affinity micropartitioning-mediated comparative glycosylation profiling. *Anal. Bioanal. Chem.* 2008, 392, (1-2), 195-201.



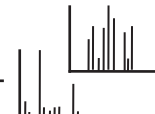
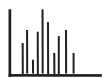
- [74] Kuroda, N., Determination of glycated hemoglobins of cadaveric blood: a study involving the use of affinity chromatography with m-amino phenyl boronic acid. *Nihon Hoigaku Zasshi* 1990, 44, (2), 115-125.
- [75] Kullolli, M., Hancock, W. S., Hincapie, M., Automated Platform for Fractionation of Human Plasma Glycoproteome in Clinical Proteomics. *Anal. Chem.* 2009, 82, (1), 115-120.
- [76] Cao, Z., Partyka, K., McDonald, M., Brouhard, E., *et al.*, Modulation of Glycan Detection on Specific Glycoproteins by Lectin Multimerization. *Anal. Chem.* 2013, 85, (3), 1689-1698.
- [77] Lee, L. Y., Hincapie, M., Packer, N., Baker, M. S., *et al.*, An optimized approach for enrichment of glycoproteins from cell culture lysates using native multi-lectin affinity chromatography. *J. Sep. Sci.* 2013, 35, (18), 2445-2452.
- [78] Orazine, C. L., Hincapie, M., Hancock, W. S., Hattersley, M., Hanke, J. H., A proteomic analysis of the plasma glycoproteins of a MCF-7 mouse xenograft: A model system for the detection of tumor markers. *J. Proteome Res.* 2008, 7, (4), 1542-1554.
- [79] Xu, Y., Zhang, L., Lu, H., Yang, P., On-plate enrichment of glycopeptides by using boronic acid functionalized gold-coated Si wafer. *Proteomics* 2010, 10, (5), 1079-1086.
- [80] Bañó-Polo, M., Baldin, F., Tamborero, S., Marti-Renom, M. A., Mingarro, I., N-glycosylation efficiency is determined by the distance to the C-terminus and the amino acid preceding an Asn-Ser-Thr sequon. *Protein Sci.* 2000, 20, (1), 179-186.
- [81] Yang, Z., Hancock, W. S., Approach to the comprehensive analysis of glycoproteins isolated from human serum using a multi-lectin affinity column. *J. Chromatogr. A* 2004, 1053, (1-2), 79-88.
- [82] Baussant, T., Bougueleret, L., Johnson, A., Rogers, J., *et al.*, Effective depletion of albumin using a new peptide-based affinity medium. *Proteomics* 2005, 5, (4), 973-977.
- [83] Björhall, K., Miliotis, T., Davidsson, P., Comparison of different depletion strategies for improved resolution in proteomic analysis of human serum samples. *Proteomics* 2005, 5, (1), 307-317.
- [84] Brand, J., Haslberger, T., Zolg, W., Pestlin, G., Palme, S., Depletion efficiency and recovery of trace markers from a multiparameter immunodepletion column. *Proteomics* 2006, 6, (11), 3236-3242.
- [85] Fountoulakis, M., Juranville, J. F., Jiang, L., Avila, D., *et al.*, Depletion of the high-abundance plasma proteins. *Amino Acids* 2004, 27, (3-4), 249-259.



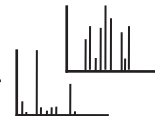
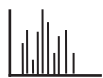
- [86] Fu, Q., Garnham, C. P., Elliott, S. T., Bovenkamp, D. E., Van Eyk, J. E., A robust, streamlined, and reproducible method for proteomic analysis of serum by delipidation, albumin and IgG depletion, and two-dimensional gel electrophoresis. *Proteomics* 2005, 5, (10), 2656-2664.
- [87] Govorukhina, N. I., Keizer-Gunnink, A., van der Zee, A. G. J., de Jong, S., *et al.*, Sample preparation of human serum for the analysis of tumor markers: Comparison of different approaches for albumin and $\hat{\Gamma}^3$ -globulin depletion. *J. Chromatogr. A* 2003, 1009, (1â€“2), 171-178.
- [88] Greenough, C., Jenkins, R. E., Kitteringham, N. R., Pirmohamed, M., *et al.*, A method for the rapid depletion of albumin and immunoglobulin from human plasma. *Proteomics* 2004, 4, (10), 3107-3111.
- [89] Huang, H.-L., Stasyk, T., Morandell, S., Mogg, M., *et al.*, Enrichment of low-abundant serum proteins by albumin/immunoglobulin G immunoaffinity depletion under partly denaturing conditions. *Electrophoresis* 2005, 26, (14), 2843-2849.
- [90] Ramstrom, M., Hagman, C., Mitchell, J. K., Derrick, P. J., *et al.*, Depletion of High-Abundant Proteins in Body Fluids Prior to Liquid Chromatography Fourier Transform Ion Cyclotron Resonance Mass Spectrometry. *J. Proteome Res.* 2005, 4, (2), 410-416.
- [91] Steinstraesser, L., Jacobsen, F., Hirsch, T., Kesting, M., *et al.*, Immunodepletion of high-abundant proteins from acute and chronic wound fluids to elucidate low-abundant regulators in wound healing. *BMC Res. Notes* 2010, 3, (1), 335.
- [92] Yocum, A. K., Yu, K., Oe, T., Blair, I. A., Effect of Immunoaffinity Depletion of Human Serum during Proteomic Investigations. *J. Proteome Res.* 2005, 4, (5), 1722-1731.
- [93] Zolotarjova, N., Martosella, J., Nicol, G., Bailey, J., *et al.*, Differences among techniques for high-abundant protein depletion. *Proteomics* 2005, 5, (13), 3304-3313.
- [94] Anderson, N., Anderson, N., The human plasma proteome: history, character, and diagnostic prospects. *Mol. Cell. Proteomics* 2002, 1, (11), 845 - 867.
- [95] Wetzler, C., Kampfer, H., Stallmeyer, B., Pfeilschifter, J., Frank, S., Large and Sustained Induction of Chemokines during Impaired Wound Healing in the Genetically Diabetic Mouse: Prolonged Persistence of Neutrophils and Macrophages during the Late Phase of Repair. *J Investig Dermatol* 2000, 115, (2), 245-253.
- [96] Angele, M. K., Knoferl, M. W., Ayala, A., Albina, J. E., *et al.*, Trauma-hemorrhage delays wound healing potentially by increasing pro-inflammatory cytokines at the wound site. *Surgery* 1999, 126, (2), 279-285.



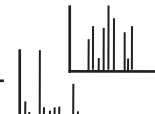
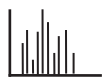
- [97] Briggaman, R. A., Schechter, N. M., Fraki, J., Lazarus, G. S., Degradation of the epidermal-dermal junction by proteolytic enzymes from human skin and human polymorphonuclear leukocytes. *J. Exp. Med.* 1984, *160*, (4), 1027-1042.
- [98] Dovi, J. V., Szpaderska, A. M., DiPietro, L. A., Neutrophil function in the healing wound: adding insult to injury? *Thromb. Haemostasis* 2004, *92*, (2), 275-280.
- [99] Grinnell, F., Zhu, M., Fibronectin degradation in chronic wounds depends on the relative levels of elastase, alpha1-proteinase inhibitor, and alpha2-macroglobulin. *J. Invest. Dermatol.* 1996, *106*, (2), 335-341.
- [100] Herrick, S., Ashcroft, G., Ireland, G., Horan, M., *et al.*, Up-regulation of elastase in acute wounds of healthy aged humans and chronic venous leg ulcers are associated with matrix degradation. *Lab. Invest.* 1997, *77*, (3), 281-288.
- [101] Palolahti, M., Lauharanta, J., Stephens, R. W., Kuusela, P., Vaheri, A., Proteolytic activity in leg ulcer exudate. *Exp. Dermatol.* 1993, *2*, (1), 29-37.
- [102] Dovi, J. V., He, L. K., DiPietro, L. A., Accelerated wound closure in neutrophil-depleted mice. *J. Leukoc. Biol.* 2003, *73*, (4), 448-455.
- [103] Stechmiller, J., Cowan, L., Schultz, G., The role of doxycycline as a matrix metalloproteinase inhibitor for the treatment of chronic wounds. *Biol. Res. Nurs.* 2010, *11*, (4), 336-344.
- [104] Ramamurthy, N. S., Kucine, A. J., McClain, S. A., McNamara, T. F., Golub, L. M., Topically applied CMT-2 enhances wound healing in streptozotocin diabetic rat skin. *Adv. Dent. Res.* 1998, *12*, (2), 144-148.
- [105] Siemonsma, M. A., de Hingh, I. H. J. T., de Man, B. M., Lomme, R. M. L. M., *et al.*, Doxycycline improves wound strength after intestinal anastomosis in the rat. *Surgery* 2003, *133*, (3), 268-276.
- [106] Seedor, J. A., Perry, H. D., McNamara, T. F., Golub, L. M., *et al.*, Systemic tetracycline treatment of alkali-induced corneal ulceration in rabbits. *Arch. Ophthalmol.* 1987, *105*, (2), 268-271.
- [107] Smith Jr, G. N., Mickler, E. A., Hasty, K. A., Brandt, K. D., Specificity of inhibition of matrix metalloproteinase activity by doxycycline: Relationship to structure of the enzyme. *Arthritis Rheum.* 1999, *42*, (6), 1140-1146.
- [108] Weckroth, M., Vaheri, A., Lauharanta, J., Sorsa, T., Kontinen, Y. T., Matrix Metalloproteinases, Gelatinase and Collagenase, in Chronic Leg Ulcers. *J. Invest. Dermatol.* 1996, *106*, (5), 1119-1124.



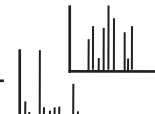
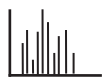
- [109] Nwomeh, B. C., Liang, H.-X., Cohen, I. K., Yager, D. R., MMP-8 Is the Predominant Collagenase in Healing Wounds and Nonhealing Ulcers. *J. Sur. Res.* 1999, 81, (2), 189-195.
- [110] Liu, Y., Min, D., Bolton, T., Nubé, V., *et al.*, Increased Matrix Metalloproteinase-9 Predicts Poor Wound Healing in Diabetic Foot Ulcers. *Diabetes Care* 2009, 32, (1), 117-119.
- [111] Muller, M., Trocme, C., Lardy, B., Morel, F., *et al.*, Matrix metalloproteinases and diabetic foot ulcers: the ratio of MMP-1 to TIMP-1 is a predictor of wound healing. *Diabetic Med.* 2008, 25, (4), 419 - 426.
- [112] Trengove, N. J., Stacey, M. C., MacAuley, S., Bennett, N., *et al.*, Analysis of the acute and chronic wound environments: the role of proteases and their inhibitors. *Wound Repair Regen.* 1999, 7, (6), 442-452.
- [113] Madlener, M., Parks, W. C., Werner, S., Matrix Metalloproteinases (MMPs) and Their Physiological Inhibitors (TIMPs) Are Differentially Expressed during Excisional Skin Wound Repair. *Exp. Cell Res.* 1998, 242, (1), 201-210.
- [114] Bullen, E. C., Longaker, M. T., Updike, D. L., Benton, R., *et al.*, Tissue inhibitor of metalloproteinases-1 is decreased and activated gelatinases are increased in chronic wounds. *J. Invest. Dermatol.* 1995, 104, (2), 236-240.
- [115] Jeffcoate, W. J., Price, P., Harding, K. G., Wound healing and treatments for people with diabetic foot ulcers. *Diabetes Metab. Res. Rev.* 2004, 20 Suppl 1, S78-89.
- [116] Kilpadi, D. V., Stechmiller, J. K., Childress, B., Cowan, L., *et al.*, Composition of wound fluid from pressure ulcers treated with negative pressure wound therapy using VAC (R) therapy in home health or extended care patients: A pilot study. *Wounds-Compend. Clin. Res. Pract.* 2006, 18, (5), 119-128.
- [117] Chan, J. C. Y., Duszczyszyn, D. A., Castellino, F. J., Ploplis, V. A., Accelerated Skin Wound Healing in Plasminogen Activator Inhibitor-1-Deficient Mice. *Am. J. Pathol.* 2001, 159, (5), 1681-1688.
- [118] Katz, M. H., Alvarez, A. F., Kirsner, R. S., Eaglstein, W. H., Falanga, V., Human wound fluid from acute wounds stimulates fibroblast and endothelial cell growth. *J. Am. Acad. Dermatol.* 1991, 25, (6, Part 1), 1054-1058.
- [119] Drinkwater, S. L., Smith, A., Sawyer, B. M., Burnand, K. G., Effect of venous ulcer exudates on angiogenesis in vitro. *Br. J. Sur.* 2002, 89, (6), 709-713.
- [120] Bategay, E. J., Angiogenesis: mechanistic insights, neovascular diseases, and therapeutic prospects. *J. Mol. Med. (Berl.)* 1995, 73, (7), 333-346.



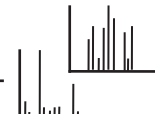
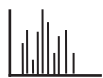
- [121] Jacobi, J., Tam, B. Y., Sundram, U., von Degenfeld, G., *et al.*, Discordant effects of a soluble VEGF receptor on wound healing and angiogenesis. *Gene Ther.* 2004, *11*, (3), 302-309.
- [122] Cowin, A. J., Hatzirodos, N., Holding, C. A., Dunaiski, V., *et al.*, Effect of healing on the expression of transforming growth factor beta(s) and their receptors in chronic venous leg ulcers. *J. Invest. Dermatol.* 2001, *117*, (5), 1282-1289.
- [123] Jude, E. B., Blakytyn, R., Bulmer, J., Boulton, A. J., Ferguson, M. W., Transforming growth factor-beta 1, 2, 3 and receptor type I and II in diabetic foot ulcers. *Diabetic Med.* 2002, *19*, (6), 440-447.
- [124] Blakytyn, R., Jude, E. B., Martin Gibson, J., Boulton, A. J., Ferguson, M. W., Lack of insulin-like growth factor 1 (IGF1) in the basal keratinocyte layer of diabetic skin and diabetic foot ulcers. *J. Pathol.* 2000, *190*, (5), 589-594.
- [125] Carmeliet, P., Collen, D., Molecular analysis of blood vessel formation and disease. *Am. J. Physiol.* 1997, *273*, (5 Pt 2), H2091-2104.
- [126] Lauer, G., Sollberg, S., Cole, M., Flamme, I., *et al.*, Expression and proteolysis of vascular endothelial growth factor is increased in chronic wounds. *J. Invest. Dermatol.* 2000, *115*, (1), 12-18.
- [127] Ferrara, N., Vascular endothelial growth factor and the regulation of angiogenesis. *Recent Prog. Horm. Res.* 2000, *55*, 15-35; discussion 35-16.
- [128] Galiano, R. D., Tepper, O. M., Pelo, C. R., Bhatt, K. A., *et al.*, Topical vascular endothelial growth factor accelerates diabetic wound healing through increased angiogenesis and by mobilizing and recruiting bone marrow-derived cells. *Am. J. Pathol.* 2004, *164*, (6), 1935-1947.
- [129] Kirchner, L. M., Meerbaum, S. O., Gruber, B. S., Knoll, A. K., *et al.*, Effects of vascular endothelial growth factor on wound closure rates in the genetically diabetic mouse model. *Wound Repair Regen.* 2003, *11*, (2), 127-131.
- [130] Kiritsy, C. P., Lynch, A. B., Lynch, S. E., Role of growth factors in cutaneous wound healing: a review. *Crit. Rev. Oral Biol. Med.* 1993, *4*, (5), 729-760.
- [131] Bevan, D., Gherardi, E., Fan, T. P., Edwards, D., Warn, R., Diverse and potent activities of HGF/SF in skin wound repair. *J. Pathol.* 2004, *203*, (3), 831-838.
- [132] Steed, D. L., Clinical evaluation of recombinant human platelet-derived growth factor for the treatment of lower extremity diabetic ulcers. Diabetic Ulcer Study Group. *J. Vasc. Sur.* 1995, *21*, (1), 71-78; discussion 79-81.



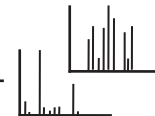
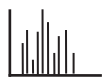
- [133] Smiell, J. M., Wieman, T. J., Steed, D. L., Perry, B. H., *et al.*, Efficacy and safety of becaplermin (recombinant human platelet-derived growth factor-BB) in patients with nonhealing, lower extremity diabetic ulcers: a combined analysis of four randomized studies. *Wound Repair Regen.* 1999, 7, (5), 335-346.
- [134] Falanga, V., Eaglstein, W. H., Bucalo, B., Katz, M. H., *et al.*, Topical use of human recombinant epidermal growth factor (h-EGF) in venous ulcers. *J. Dermatol. Sur. Oncol.* 1992, 18, (7), 604-606.
- [135] Robson, M. C., Phillips, L. G., Lawrence, W. T., Bishop, J. B., *et al.*, The safety and effect of topically applied recombinant basic fibroblast growth factor on the healing of chronic pressure sores. *Ann. Sur.* 1992, 216, (4), 401-406; discussion 406-408.
- [136] Knighton, D. R., Ciresi, K. F., Fiegel, V. D., Austin, L. L., Butler, E. L., Classification and treatment of chronic nonhealing wounds. Successful treatment with autologous platelet-derived wound healing factors (PDWHF). *Ann Sur.* 1986, 204, (3), 322-330.
- [137] Yoshida, S., Matsumoto, K., Tomioka, D., Bessho, K., *et al.*, Recombinant hepatocyte growth factor accelerates cutaneous wound healing in a diabetic mouse model. *Growth Factors* 2004, 22, (2), 111-119.
- [138] Comerota, A. J., Thom, R. C., Miller, K. A., Henry, T., *et al.*, Naked plasmid DNA encoding fibroblast growth factor type 1 for the treatment of end-stage unreconstructible lower extremity ischemia: preliminary results of a phase I trial. *J. Vasc. Sur.* 2002, 35, (5), 930-936.
- [139] Badiavas, E., Falanga, V., Treatment of chronic wounds with bone marrow-derived cells. *Arch. Dermatol.* 2003, 139, (4), 510-516.
- [140] Saap, L. J., Falanga, V., Debridement performance index and its correlation with complete closure of diabetic foot ulcers. *Wound Repair Regen.* 2002, 10, (6), 354-359.
- [141] Brummel-Ziedins, K., Orfeo, T., Jenny, N. S., Everse, S. J., Mann, K. G., *Blood Coagulation and Fibrinolysis*, in: Greer, J. P., Foerster, J., Rodgers, G. M., Paraskevas, F., *et al.* (Eds.), *Wintrobe's Clinical Hematology*, Lippincott Williams & Wilkins, Philadelphia 2009, pp. 528-619.
- [142] Moss, S. E., Morgan, R. O., The annexins. *Genome Biol.* 2004, 5, (4), 219.
- [143] Goyette, J., Yan, W. X., Yamen, E., Chung, Y. M., *et al.*, Pleiotropic Roles of S100A12 in Coronary Atherosclerotic Plaque Formation and Rupture. *J. Immunol.* 2009, 183, (1), 593-603.



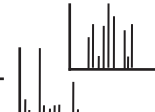
- [144] Zhang, Z., Huang, L., Zhao, W., Rigas, B., Annexin 1 Induced by Anti-Inflammatory Drugs Binds to NF-kappaB and Inhibits Its Activation: Anticancer Effects In vitro and In vivo. *Cancer Research* 2010, 70, (6), 2379-2388.
- [145] Hoffmann, D. C., Textoris, C., Oehme, F., Klaassen, T., *et al.*, Pivotal Role for α 1-Antichymotrypsin in Skin Repair. *J. Biol. Chem.* 2011, 286, (33), 28889-28901.
- [146] Brownlee, M., The Pathobiology of Diabetic Complications. *Diabetes* 2005, 54, (6), 1615-1625.
- [147] Vlassara, H., Palace, M. R., Diabetes and advanced glycation endproducts. *J. Intern. Med.* 2002, 251, (2), 87-101.
- [148] Kokkola, R., Andersson, Å., Mullins, G., Östberg, T., *et al.*, RAGE is the Major Receptor for the Proinflammatory Activity of HMGB1 in Rodent Macrophages. *Scand. J. Immunol.* 2005, 61, (1), 1-9.
- [149] Whitelock, J. M., Murdoch, A. D., Iozzo, R. V., Underwood, P. A., The Degradation of Human Endothelial Cell-derived Perlecan and Release of Bound Basic Fibroblast Growth Factor by Stromelysin, Collagenase, Plasmin, and Heparanases. *J. Biol. Chem.* 1996, 271, (17), 10079-10086.
- [150] Brooks, P. C., Silletti, S., von Schalscha, T. L., Friedlander, M., Cheresh, D. A., Disruption of Angiogenesis by PEX, a Noncatalytic Metalloproteinase Fragment with Integrin Binding Activity. *Cell* 1998, 92, (3), 391-400.
- [151] Nedeau, A. E., Gallagher, K. A., Liu, Z.-J., Velazquez, O. C., Elevation of hemopexin-like fragment of matrix metalloproteinase-2 tissue levels inhibits ischemic wound healing and angiogenesis. *J. Vasc. Sur.* 2011, 54, (5), 1430-1438.
- [152] Ikari, Y., Fujikawa, K., Yee, K. O., Schwartz, S. M., α 1-Proteinase Inhibitor, α 1-Antichymotrypsin, or α 2-Macroglobulin Is Required for Vascular Smooth Muscle Cell Spreading in Three-dimensional Fibrin Gel. *J. Biol. Chem.* 2000, 275, (17), 12799-12805.
- [153] Zou, Z., Anisowicz, A., Hendrix, M., Thor, A., *et al.*, Maspin, a serpin with tumor-suppressing activity in human mammary epithelial cells. *Science* 1994, 263, (5146), 526-529.
- [154] López-Casillas, F., Payne, H., Andres, J., Massagué, J., Betaglycan can act as a dual modulator of TGF-beta access to signaling receptors: mapping of ligand binding and GAG attachment sites. *J. Cell Biol.* 1994, 124, (4), 557-568.
- [155] Faler, B. J., Macsata, R. A., Plummer, D., Mishra, L., Sidawy, A. N., Transforming Growth Factor- β and Wound Healing. *Persp. Vasc. Sur. Endovasc. Therapy* 2006, 18, (1), 55-62.



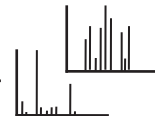
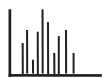
- [156] Hocevar, B. A., Howe, P. H., Mechanisms of TGF-beta-induced cell cycle arrest. *Miner Electrolyte Metab.* 1998, 24, (2-3), 131-135.
- [157] Schuster, N., Kriegstein, K., Mechanisms of TGF-beta-mediated apoptosis. *Cell Tissue Res.* 2002, 307, (1), 1-14.
- [158] Matsumura, T., Wolff, K., Petzelbauer, P., Endothelial cell tube formation depends on cadherin 5 and CD31 interactions with filamentous actin. *J. Immunol.* 1997, 158, (7), 3408-3416.
- [159] Maretzky, T., Reiss, K., Ludwig, A., Buchholz, J., *et al.*, ADAM10 mediates E-cadherin shedding and regulates epithelial cell-cell adhesion, migration, and β -catenin translocation. *Proc. Natl. Acad. Sci. U. S. A.* 2005, 102, (26), 9182-9187.
- [160] Di Colandrea, T., Wang, L., Wille, J., D'Armiento, J., Chada, K. K., Epidermal Expression of Collagenase Delays Wound-Healing in Transgenic Mice. *J. Invest. Dermatol.* 1998, 111, (6), 1029-1033.
- [161] Rossignol, P., Ho-Tin-No \AA , B. t., Vranckx, R., Bouton, M.-C., *et al.*, Protease Nexin-1 Inhibits Plasminogen Activation-induced Apoptosis of Adherent Cells. *J. Biol. Chem.* 2004, 279, (11), 10346-10356.
- [162] Mogues, T., Etzerodt, M., Hall, C., Engelich, G., *et al.*, Tetranectin Binds to the Kringle 1-4 Form of Angiostatin and Modifies Its Functional Activity. *Journal of Biomedicine and Biotechnology* 2004, 2004, (2), 73-78.
- [163] Sreenivasan, A., Anti-angiogenesis is anti-actin. *J. Cell Biol.* 2004, 166, (1), 6-7.
- [164] Leffers, H., Nielsen, M. S., Andersen, A. H., Honore, B., *et al.*, Identification of 2 Human Rho GDP-dissociation Inhibitor Proteins whose overexpression leads to Disruption of the Actin Cytoskeleton. *Exp. Cell Res.* 1993, 209, (2), 165-174.
- [165] Bauer, S. M., Bauer, R. J., Velazquez, O. C., Angiogenesis, Vasculogenesis, and Induction of Healing in Chronic Wounds. *Vasc. Endovascular Surg.* 2005, 39, (4), 293-306.
- [166] Latijnhouwers, M. A., Bergers, M., Van Bergen, B. H., Spruijt, K. I., *et al.*, Tenascin Expression during Wound Healing in Human Skin. *J. Pathol.* 1996, 178, (1), 30-35.
- [167] Anderson, K. S., Wong, J., Polyak, K., Aronzon, D., Enerbäck, C., Detection of psoriasin/S100A7 in the sera of patients with psoriasis. *Br. J. Dermatol.* 2009, 160, (2), 325-332.
- [168] El-Rachkidy, R. G., Young, H. S., Griffiths, C. E. M., Camp, R. D. R., Humoral Autoimmune Responses to the Squamous Cell Carcinoma Antigen Protein Family in Psoriasis. *J. Invest. Dermatol.* 2008, 128, (9), 2219-2224.



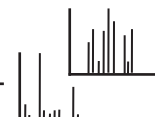
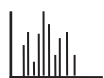
- [169] Quarta, S., Vidalino, L., Turato, C., Ruvoletto, M., *et al.*, SERPINB3 induces epithelial–mesenchymal transition. *J. Pathol.* 2010, 221, (3), 343-356.
- [170] Xu, J., Zhang, X., Pelayo, R., Monestier, M., *et al.*, Extracellular histones are major mediators of death in sepsis. *Nat. Med.* 2009, 15, (11), 1318-1321.
- [171] Lopez, M. F., Kuppusamy, R., Sarracino, D. A., Prakash, A., *et al.*, Mass Spectrometric Discovery and Selective Reaction Monitoring (SRM) of Putative Protein Biomarker Candidates in First Trimester Trisomy 21 Maternal Serum. *J. Proteome Res.* 2010, 10, (1), 133-142.
- [172] Schiess, R., Wollscheid, B., Aebersold, R., Targeted proteomic strategy for clinical biomarker discovery. *Mol. Oncol.* 2009, 3, (1), 33-44.
- [173] Hoofnagle, A. N., Wu, M., Gosmanova, A. K., Becker, J. O., *et al.*, Low Clusterin Levels in High-Density Lipoprotein Associate With Insulin Resistance, Obesity, and Dyslipoproteinemia. *Arterioscler. Thromb. Vasc. Biol.* 2010, 30, (12), 2528-2534.
- [174] Keshishian, H., Addona, T., Burgess, M., Mani, D. R., *et al.*, Quantification of Cardiovascular Biomarkers in Patient Plasma by Targeted Mass Spectrometry and Stable Isotope Dilution. *Mol. Cell. Proteomics* 2009, 8, (10), 2339-2349.
- [175] Anderson, N. L., Jackson, A., Smith, D., Hardie, D., *et al.*, SISCAPA Peptide Enrichment on Magnetic Beads Using an In-line Bead Trap Device. *Mol. Cell. Proteomics* 2009, 8, (5), 995-1005.
- [176] Addona, T. A., Shi, X., Keshishian, H., Mani, D. R., *et al.*, A pipeline that integrates the discovery and verification of plasma protein biomarkers reveals candidate markers for cardiovascular disease. *Nat. Biotechnol.* 2011, 29, (7), 635-643.
- [177] Izrael-Tomasevic, A., Phu, L., Phung, Q. T., Lill, J. R., Arnott, D., Targeting Interferon Alpha Subtypes in Serum: A Comparison of Analytical Approaches to the Detection and Quantitation of Proteins in Complex Biological Matrices. *J. Proteome Res.* 2009, 8, (6), 3132-3140.
- [178] Sherman, J., McKay, M. J., Ashman, K., Molloy, M. P., How specific is my SRM?: The issue of precursor and product ion redundancy. *Proteomics* 2009, 9, (5), 1120-1123.
- [179] *SRM Atlas*, Institute for Systems Biology, <http://www.srmatlas.org/>, June 2010
- [180] Addona, T. A., Abbatiello, S. E., Schilling, B., Skates, S. J., *et al.*, Multi-site assessment of the precision and reproducibility of multiple reaction monitoring-based measurements of proteins in plasma. *Nat. Biotechnol.* 2009, 27, (7), 633-641.
- [181] Anderson, N. L., Anderson, N. G., Pearson, T. W., Borchers, C. H., *et al.*, A Human Proteome Detection and Quantitation Project. *Mol. Cell. Proteomics* 2009, 8, (5), 883-886.



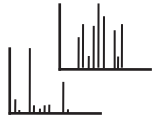
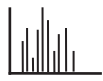
- [182] Fortin, T., Salvador, A., Charrier, J. P., Lenz, C., *et al.*, Multiple Reaction Monitoring Cubed for Protein Quantification at the Low Nanogram/Milliliter Level in Nondepleted Human Serum. *Anal. Chem.* 2009, 81, (22), 9343-9352.
- [183] Gallien, S., Duriez, E., Domon, B., Selected reaction monitoring applied to proteomics. *J. Mass Spectrom.* 2011, 46, (3), 298-312.
- [184] Lange, V., Picotti, P., Domon, B., Aebersold, R., Selected reaction monitoring for quantitative proteomics: a tutorial. *Mol. Syst. Biol.* 2008, 4.
- [185] McIntosh, M., Fitzgibbon, M., Biomarker validation by targeted mass spectrometry. *Nat. Biotechnol.* 2009, 27, (7), 622-623.
- [186] Rodriguez, H., Rivers, R., Kinsinger, C., Mesri, M., *et al.*, Reconstructing the pipeline by introducing multiplexed multiple reaction monitoring mass spectrometry for cancer biomarker verification: An NCI-CPTC initiative perspective. *Proteomics Clin. Appl.* 2010, 4, (12), 904-914.
- [187] Wang, P., Whiteaker, J. R., Paulovich, A. G., The evolving role of mass spectrometry in cancer biomarker discovery. *Cancer Biology & Therapy* 2009, 8, (12), 1083-1094.
- [188] Washburn, M. P., Ulaszek, R. R., Yates, J. R., Reproducibility of Quantitative Proteomic Analyses of Complex Biological Mixtures by Multidimensional Protein Identification Technology. *Anal. Chem.* 2003, 75, (19), 5054-5061.
- [189] Wolters, D. A., Washburn, M. P., Yates, J. R., 3rd, An automated multidimensional protein identification technology for shotgun proteomics. *Anal. Chem.* 2001, 73, (23), 5683-5690.
- [190] Randall, S. A., McKay, M. J., Molloy, M. P., Evaluation of blood collection tubes using selected reaction monitoring MS: Implications for proteomic biomarker studies. *Proteomics* 2010, 10, (10), 2050-2056.
- [191] Prakash, A., Rezai, T., Krastins, B., Sarracino, D., *et al.*, Platform for Establishing Interlaboratory Reproducibility of Selected Reaction Monitoring-Based Mass Spectrometry Peptide Assays. *J. Proteome Res.* 2010, 9, (12), 6678-6688.
- [192] Galli, F., Protein damage and inflammation in uraemia and dialysis patients. *Nephrol. Dial. Transplant.* 2007, 22, (suppl 5), 20-36.
- [193] Morena, M., Delbosc, S., Dupuy, A.-M., Canaud, B., Cristol, J.-P., Overproduction of reactive oxygen species in end-stage renal disease patients: A potential component of hemodialysis-associated inflammation. *Hemodialysis Int.* 2005, 9, (1), 37-46.



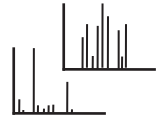
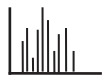
- [194] Duranton, F., Cohen, G., De Smet, R., Rodriguez, M., *et al.*, Normal and Pathologic Concentrations of Uremic Toxins. *J. Am. Soc. Nephrol.* 2012, 23, (7), 1258-1270.
- [195] Meert, N., Schepers, E., De Smet, R., Argiles, A., *et al.*, Inconsistency of Reported Uremic Toxin Concentrations. *Artif. Organs* 2007, 31, (8), 600-611.
- [196] Vanholder, R., De Smet, R., Glorieux, G., Argiles, A., *et al.*, Review on uremic toxins: Classification, concentration, and interindividual variability. *Kidney Int.* 2003, 63, (5), 1934-1943.
- [197] Vanholder, R., *EUTOX Uremic Solutes Database*, European Work Group of Uremic Toxins (EUTox) on behalf of the European Society for Artificial Organs (ESAO), <http://eutodb.odeesoft.com/index.php>, March 2013
- [198] Vanholder, R., Smet, R. D., Glorieux, G., Dhondt, A., Survival of Hemodialysis Patients and Uremic Toxin Removal. *Artif. Organs* 2003, 27, (3), 218-223.
- [199] Greene, T., Beck, G. J., Gassman, J. J., Gotch, F. A., *et al.*, Design and statistical issues of the hemodialysis (HEMO) study. *Control. Clin. Trials* 2000, 21, (5), 502-525.
- [200] Locatelli, F., Gauly, A., Czekalski, S., Hannedouche, T., *et al.*, The MPO Study: just a European HEMO Study or something very different? *Blood Purif.* 2008, 26, (1), 100-104.
- [201] Penne, E. L., Blankestijn, P. J., Bots, M. L., van den Dorpel, M. A., *et al.*, Effect of increased convective clearance by on-line hemodiafiltration on all cause and cardiovascular mortality in chronic hemodialysis patients - the Dutch CONvective TRANsport STudy (CONTRAST): rationale and design of a randomised controlled trial [ISRCTN38365125]. *Curr. Control. Trials Cardiovasc. Med.* 2005, 6, (1), 8.
- [202] Maduell, F., Moreso, F., Pons, M., Ramos, R., *et al.*, Design and patient characteristics of ESHOL study, a Catalanian prospective randomized study. *J. Nephrol.* 2011, 24, (2), 196-202.
- [203] Ok, E., Asci, G., Toz, H., Ok, E. S., *et al.*, Mortality and cardiovascular events in online haemodiafiltration (OL-HDF) compared with high-flux dialysis: results from the Turkish OL-HDF Study. *Nephrol. Dial. Transplant.* 2013, 28, (1), 192-202.
- [204] Cheung, A. K., Levin, N. W., Greene, T., Agodoa, L., *et al.*, Effects of High-Flux Hemodialysis on Clinical Outcomes: Results of the HEMO Study. *J. Am. Soc. Nephrol.* 2003, 14, (12), 3251-3263.
- [205] Delmez, J. A., Yan, G., Bailey, J., Beck, G. J., *et al.*, Cerebrovascular Disease in Maintenance Hemodialysis Patients: Results of the HEMO Study. *Am. J. Kidney Dis.* 2006, 47, (1), 131-138.



- [206] Eknoyan, G., Beck, G. J., Cheung, A. K., Daugirdas, J. T., *et al.*, Effect of Dialysis Dose and Membrane Flux in Maintenance Hemodialysis. *N. Engl. J. Med.* 2002, 347, (25), 2010-2019.
- [207] Locatelli, F., Martin-Malo, A., Hannedouche, T., Loureiro, A., *et al.*, Effect of Membrane Permeability on Survival of Hemodialysis Patients. *J. Am. Soc. Nephrol.* 2009, 20, (3), 645-654.
- [208] Locatelli, F., Cavalli, A., Manzoni, C., Pontoriero, G., The Membrane Permeability Outcome study. *Contrib. Nephrol.* 2011, 175, 81-92.
- [209] Grooteman, M. P., van den Dorpel, M. A., Bots, M. L., Penne, E. L., *et al.*, Effect of online hemodiafiltration on all-cause mortality and cardiovascular outcomes. *J. Am. Soc. Nephrol.* 2012, 23, (6), 1087-1096.
- [210] Mazairac, A. H., de Wit, G. A., Penne, E. L., van der Weerd, N. C., *et al.*, Changes in quality of life over time--Dutch haemodialysis patients and general population compared. *Nephrol. Dial. Transplant.* 2011, 26, (6), 1984-1989.
- [211] Mazairac, A. H., de Wit, G. A., Grooteman, M. P., Penne, E. L., *et al.*, Effect of hemodiafiltration on quality of life over time. *Clin. J. Am. Soc. Nephrol.* 2013, 8, (1), 82-89.
- [212] Maduell, F., Moreso, F., Pons, M., Ramos, R., *et al.*, High-Efficiency Postdilution Online Hemodiafiltration Reduces All-Cause Mortality in Hemodialysis Patients. *J. Am. Soc. Nephrol.* 2013.
- [213] Ficheux, A., Gayraud, N., Szwarc, I., Andress, D., *et al.*, The use of SDS-PAGE scanning of spent dialysate to assess uraemic toxin removal by dialysis. *Nephrol. Dial. Transplant.* 2010, 26, (7), 2281-2289.
- [214] Speeckaert, M. M., Glorieux, G. L., Vanholder, R., Van Biesen, W., *et al.*, Vitamin D Binding Protein and the Need for Vitamin D in Hemodialysis Patients. *J. Renal Nutr.* 2008, 18, (5), 400-407.
- [215] Anderson, N. L., Anderson, N. G., The human plasma proteome. History, character, and diagnostic prospects. *Mol. Cell. Proteomics* 2002, 1, (11), 845-867.
- [216] Percy, A. J., Chambers, A. G., Yang, J., Borchers, C. H., Multiplexed MRM-based quantitation of candidate cancer biomarker proteins in undepleted and non-enriched human plasma. *Proteomics* 2013, 13, (14), 2202-2215.
- [217] Shi, T., Fillmore, T. L., Sun, X., Zhao, R., *et al.*, Antibody-free, targeted mass-spectrometric approach for quantification of proteins at low picogram per milliliter levels in human plasma/serum. *Proc. Natl. Acad. Sci. U. S. A.* 2012, 109, (38), 15395-15400.



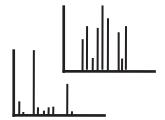
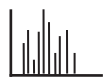
- [218] Darby, I. A., Bisucci, T., Hewitson, T. D., MacLellan, D. G., Apoptosis is increased in a model of diabetes-impaired wound healing in genetically diabetic mice. *Int. J. Biochem. Cell Biol.* 1997, 29, (1), 191-200.
- [219] Falanga, V., *Preparation of the Wound Bed of the Diabetic Foot Ulcer*, in: Veves, A., Giurini, J., Logerfo, F. (Eds.), *The Diabetic Foot*, Humana Press, Boston 2006, pp. 299-310.



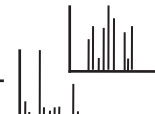
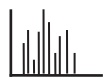
11. Appendix 1: Supporting tables

Table 11.1: Protein concentration in investigated chronic and acute wound fluids estimated by BCA assay analysis

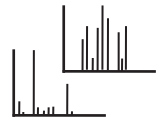
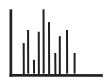
acute wounds		chronic wounds	
patient No.	protein concentration in wound fluids (mg/mL)	patient No.	protein concentration in wound fluids (mg/mL)
1	44.9	1	9.5
2	20.7	2	22.0
3	55.3	3	30.1
4	67.7	4	6.9
5	14.0	5	12.3
6	45.2	6	8.9
7	14.6	7	23.5
8	49.2	8	41.0
9	26.6	9	76.7
10	35.3	10	67.2
11	47.6	11	50.0
		12	16.7
		13	30.5
		14	56.2
		15	16.6
mean	38.3	mean	31.2

**Table 11.2: list of proteins identified in the MudPIT-MS/MS study as higher or exclusively expressed in the fluids of chronic wounds**

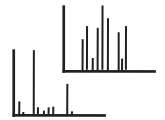
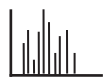
accession number (SwissProt)	protein	mean expression chronic	SD chronic	mean expression acute	SD acute	expression difference (chronic vs. acute)	p-value
P31947	14-3-3 protein sigma	0.072	0.032	n/a	n/a	n/a	n/a
P05387	60S acidic ribosomal protein P2	0.010	0.008	n/a	n/a	n/a	n/a
P17858	6-phosphofructokinase, liver type	0.025	0.006	0.008	0.011	2.966	0.030
P08253	72 kDa type IV collagenase (MMP2)	0.061	0.031	0.026	0.020	2.335	0.033
P11021	78 kDa glucose-regulated protein	0.076	0.042	0.038	0.034	2.002	0.033
P07108	Acyl-CoA-binding protein	0.041	0.026	n/a	0.014	n/a	n/a
Q10588	ADP-ribosyl cyclase 2	0.023	0.009	0.009	0.007	2.748	0.005
P14550	Alcohol dehydrogenase [NADP+]	0.012	0.004	0.004	0.004	3.203	0.027
Q8IZ83	Aldehyde dehydrogenase family 16 member A1	0.017	0.009	n/a	0.006	n/a	n/a
P06733	Alpha-enolase	0.992	0.594	0.449	0.367	2.208	0.049
Q01432	AMP deaminase 3	0.006	0.005	n/a	0.007	n/a	n/a
P04083	Annexin A1	0.240	0.121	0.046	0.079	5.219	0.005
P50995	Annexin A11	0.041	0.024	n/a	n/a	n/a	n/a
P07355	Annexin A2	0.076	0.037	0.022	0.029	3.462	0.049
P12429	Annexin A3	0.095	0.073	0.014	0.045	7.011	0.046
P09525	Annexin A4	0.026	0.041	n/a	n/a	n/a	n/a
P08758	Annexin A5	0.064	0.041	n/a	n/a	n/a	n/a
P08133	Annexin A6	0.051	0.092	n/a	n/a	n/a	n/a
P05089	Arginase-1	0.063	0.037	0.021	0.022	2.954	0.050
P04424	Argininosuccinate lyase	0.004	0.003	n/a	n/a	n/a	n/a
P53396	ATP-citrate synthase	0.032	0.018	0.013	0.011	2.533	0.028
P98160	Basement membrane-specific heparan sulfate proteoglycan core protein (perlecan)	0.126	0.054	0.047	0.030	2.714	0.006
P08236	Beta-glucuronidase	0.009	0.010	n/a	n/a	n/a	n/a
Q9Y376	Calcium-binding protein 39	0.010	0.011	n/a	n/a	n/a	n/a
P62158	Calmodulin	0.014	0.011	n/a	n/a	n/a	n/a
Q9NZT1	Calmodulin-like protein 5	0.009	0.073	n/a	n/a	n/a	n/a
P04632	Calpain small subunit 1	0.016	0.007	n/a	n/a	n/a	n/a
P49747	Cartilage oligomeric matrix protein	0.011	0.015	n/a	n/a	n/a	n/a
P31944	Caspase-14	0.063	0.038	n/a	n/a	n/a	n/a
Q6YHK3	CD109 antigen	0.014	0.008	n/a	n/a	n/a	n/a



accession number (SwissProt)	protein	mean expression chronic	SD chronic	mean expression acute	SD acute	expression difference (chronic vs. acute)	p-value
P43121	Cell surface glycoprotein MUC18	0.006	0.002	n/a	n/a	n/a	n/a
Q14019	Coactosin-like protein	0.034	0.021	0.013	0.018	2.568	0.049
P00748	Coagulation factor XII	0.049	0.027	0.015	0.008	3.190	0.015
P02452	Collagen alpha-1(I) chain	0.041	0.033	n/a	n/a	n/a	n/a
P02461	Collagen alpha-1(III) chain	0.039	0.030	0.005	0.005	7.618	0.016
P20908	Collagen alpha-1(V) chain	0.053	0.053	0.007	0.019	7.633	0.033
P12109	Collagen alpha-1(VI) chain	0.093	0.027	n/a	n/a	n/a	n/a
Q99715	Collagen alpha-1(XII) chain	0.113	0.069	n/a	n/a	n/a	n/a
P39059	Collagen alpha-1(XV) chain	0.026	0.017	n/a	n/a	n/a	n/a
P39060	Collagen alpha-1(XVIII) chain	0.017	0.009	0.004	0.005	4.419	0.019
P08123	Collagen alpha-2(I) chain	0.033	0.025	n/a	n/a	n/a	n/a
P05997	Collagen alpha-2(V) chain	0.010	0.011	n/a	n/a	n/a	n/a
P12111	Collagen alpha-3(VI) chain	0.355	0.133	0.054	0.115	6.562	0.003
O75131	Copine-3	0.012	0.018	n/a	n/a	n/a	n/a
P04080	Cystatin-B	0.036	0.008	0.016	0.016	2.212	0.043
P99999	Cytochrome c	0.022	0.012	n/a	n/a	n/a	n/a
P28838	Cytosol aminopeptidase	0.019	0.011	n/a	n/a	n/a	n/a
Q96KP4	Cytosolic non-specific dipeptidase	0.013	0.011	n/a	n/a	n/a	n/a
Q02487	Desmocollin-2	0.014	0.021	n/a	n/a	n/a	n/a
Q02413	Desmoglein-1	0.020	0.017	n/a	n/a	n/a	n/a
P09172	Dopamine beta-hydroxylase	0.011	0.010	n/a	n/a	n/a	n/a
P50570	Dynamin-2	0.008	0.010	n/a	n/a	n/a	n/a
O75923	Dysferlin	0.015	0.008	n/a	n/a	n/a	n/a
Q96C19	EF-hand domain-containing protein D2	0.046	0.032	0.017	0.011	2.717	0.032
P29692	Elongation factor 1-delta	0.010	0.007	n/a	n/a	n/a	n/a
P26641	Elongation factor 1-gamma	0.024	0.007	0.008	0.008	2.902	0.016
P13639	Elongation factor 2	0.061	0.025	0.022	0.022	2.733	0.014
P58107	Epiplakin	0.010	0.014	n/a	n/a	n/a	n/a
Q01469	Fatty acid-binding protein, epidermal	0.016	0.092	n/a	n/a	n/a	n/a
P02675	Fibrinogen beta chain	1.711	0.497	0.841	0.432	2.035	0.000
P02679	Fibrinogen gamma chain	0.772	0.193	0.377	0.230	2.048	0.001
O75369	Filamin-B	0.047	0.025	n/a	n/a	n/a	n/a

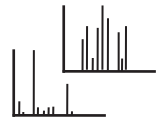
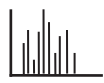


accession number (SwissProt)	protein	mean expression chronic	SD chronic	mean expression acute	SD acute	expression difference (chronic vs. acute)	p-value
P62826	GTP-binding nuclear protein Ran	0.025	0.014	0.011	0.008	2.238	0.047
P04792	Heat shock protein beta-1	0.009	0.005	n/a	n/a	n/a	n/a
Q14103	Heterogeneous nuclear ribonucleoprotein D0	0.026	0.013	0.008	0.007	3.385	0.032
P49773	Histidine triad nucleotide-binding protein 1	0.019	0.011	0.007	0.001	2.595	0.043
Q96KK5	Histone H2A type 1-H	0.053	0.021	n/a	n/a	n/a	n/a
P62805	Histone H4	0.294	0.066	0.151	0.101	1.939	0.019
P23083	Ig heavy chain V-I region V35	0.012	0.004	n/a	n/a	n/a	n/a
P01598	Ig kappa chain V-I region EU	0.046	0.039	n/a	n/a	n/a	n/a
P01610	Ig kappa chain V-I region WEA	0.076	0.030	0.038	0.027	2.021	0.013
P18135	Ig kappa chain V-III region HAH	0.145	0.048	n/a	n/a	n/a	n/a
P01622	Ig kappa chain V-III region Ti	0.117	0.049	n/a	n/a	n/a	n/a
P01714	Ig lambda chain V-III region SH	0.008	0.006	n/a	n/a	n/a	n/a
Q12906	Interleukin enhancer-binding factor 3	0.008	0.014	n/a	n/a	n/a	n/a
P18510	Interleukin-1 receptor antagonist protein	0.004	0.006	n/a	n/a	n/a	n/a
P03956	Interstitial collagenase	0.055	0.021	0.025	0.013	2.175	0.041
P02533	Keratin, type I cytoskeletal 14	0.124	0.106	0.010	0.033	12.307	0.037
P08779	Keratin, type I cytoskeletal 16	0.185	0.137	n/a	n/a	n/a	n/a
Q04695	Keratin, type I cytoskeletal 17	0.089	0.071	n/a	n/a	n/a	n/a
P02538	Keratin, type II cytoskeletal 6A	0.130	0.123	n/a	n/a	n/a	n/a
P60985	Keratinocyte differentiation-associated protein	0.017	0.020	0.006	0.002	2.773	0.034
P02788	Lactotransferrin	0.348	0.301	0.136	0.041	2.558	0.016
P08575	Leukocyte common antigen	0.011	0.010	n/a	n/a	n/a	n/a
P61626	Lysozyme C	0.069	0.056	0.023	0.017	3.027	0.033
P40121	Macrophage-capping protein	0.056	0.017	0.018	0.018	3.107	0.008
P40926	Malate dehydrogenase, mitochondrial	0.030	0.012	0.012	0.007	2.546	0.030
Q15691	Microtubule-associated protein RP/EB family member 1	0.019	0.016	n/a	n/a	n/a	n/a
P28482	Mitogen-activated protein kinase 1	0.031	0.009	n/a	n/a	n/a	n/a
Q16539	Mitogen-activated protein kinase 14	0.015	0.017	n/a	n/a	n/a	n/a
P24158	Myeloblastin	0.203	0.142	0.098	0.055	2.077	0.032

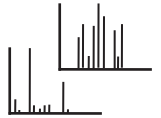
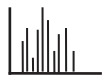


accession number (SwissProt)	protein	mean expression chronic	SD chronic	mean expression acute	SD acute	expression difference (chronic vs. acute)	p-value
P05164	Myeloperoxidase	0.290	0.109	0.114	0.128	2.549	0.044
P15586	N-acetylglucosamine-6-sulfatase	0.010	0.004	n/a	n/a	n/a	n/a
Q14697	Neutral alpha-glucosidase AB	0.018	0.013	0.007	0.003	2.622	0.038
P22894	Neutrophil collagenase	0.178	0.072	0.049	0.043	3.668	0.002
Q6XQN6	Nicotinate phosphoribosyltransferase	0.029	0.020	0.013	0.007	2.293	0.034
P19338	Nucleolin	0.008	0.017	n/a	n/a	n/a	n/a
P06748	Nucleophosmin	0.022	0.016	0.007	0.004	3.119	0.036
Q9NTK5	Obg-like ATPase 1	0.013	0.009	n/a	n/a	n/a	n/a
P23284	Peptidyl-prolyl cis-trans isomerase B	0.022	0.012	0.006	0.008	3.597	0.044
Q15063	Periostin	0.266	0.184	0.073	0.138	3.647	0.031
P05120	Plasminogen activator inhibitor 2	0.005	0.007	n/a	n/a	n/a	n/a
P13797	Plastin-3	0.044	0.053	n/a	n/a	n/a	n/a
P08567	Pleckstrin	0.009	0.027	n/a	n/a	n/a	n/a
P11940	Polyadenylate-binding protein 1	0.006	0.004	n/a	n/a	n/a	n/a
P26599	Polypyrimidine tract-binding protein 1	0.018	0.016	n/a	n/a	n/a	n/a
P07737	Profilin-1	0.234	0.106	0.100	0.069	2.351	0.011
P48147	Prolyl endopeptidase	0.009	0.009	n/a	n/a	n/a	n/a
P48147	Prolyl endopeptidase	0.009	0.009	n/a	n/a	n/a	n/a
P28070	Proteasome subunit beta type-4	0.018	0.017	n/a	n/a	n/a	n/a
P30101	Protein disulfide-isomerase A3	0.026	0.013	n/a	n/a	n/a	n/a
Q15084	Protein disulfide-isomerase A6	0.011	0.006	n/a	n/a	n/a	n/a
Q13045	Protein flightless-1 homolog	0.009	0.009	n/a	n/a	n/a	n/a
Q92597	Protein NDRG1	0.010	0.009	n/a	n/a	n/a	n/a
P31949	Protein S100A11	0.083	0.054	0.023	0.020	3.603	0.037
P80511	Protein S100A12	0.142	0.061	0.075	0.046	1.902	0.035
P26447	Protein S100A4	0.028	0.019	0.007	0.002	4.261	0.012
P05109	Protein S100A8	0.540	0.347	0.068	0.019	7.916	0.011
P06702	Protein S100A9	1.064	0.610	0.111	0.047	9.549	0.007
P25815	Protein S100P	0.229	0.124	0.051	0.022	4.478	0.012
P22061	Protein-L-isoaspartate(D-aspartate) O-methyltransferase	0.040	0.017	0.018	0.010	2.272	0.025
Q6P4A8	Putative phospholipase B-like 1	0.103	0.046	0.019	0.018	5.285	0.014
O00764	Pyridoxal kinase	0.028	0.017	0.005	0.012	6.206	0.012
P46940	Ras GTPase-activating-like protein IQGAP1	0.209	0.077	0.063	0.064	3.305	0.007

accession number (SwissProt)	protein	mean expression chronic	SD chronic	mean expression acute	SD acute	expression difference (chronic vs. acute)	p-value
Q9H0U4	Ras-related protein Rab-1B	0.015	0.017	n/a	n/a	n/a	n/a
P51148	Ras-related protein Rab-5C	0.014	0.009	n/a	n/a	n/a	n/a
P52565	Rho GDP-dissociation inhibitor 1	0.026	0.018	n/a	n/a	n/a	n/a
P52566	Rho GDP-dissociation inhibitor 2	0.101	0.038	0.039	0.027	2.619	0.006
P34096	Ribonuclease 4	0.011	0.005	n/a	n/a	n/a	n/a
Q13177	Serine/threonine-protein kinase PAK 2	0.009	0.008	n/a	n/a	n/a	n/a
P29508	Serpin B3	0.098	0.113	n/a	n/a	n/a	n/a
P36952	Serpin B5	0.009	0.016	n/a	n/a	n/a	n/a
P02743	Serum amyloid P-component	0.089	0.045	0.023	0.009	3.911	0.003
Q9H299	SH3 domain-binding glutamic acid-rich-like protein 3	0.013	0.004	n/a	n/a	n/a	n/a
P62314	Small nuclear ribonucleoprotein Sm D1	0.019	0.018	n/a	n/a	n/a	n/a
Q13126	S-methyl-5'-thioadenosine phosphorylase	0.004	0.005	n/a	n/a	n/a	n/a
O75563	Src kinase-associated phosphoprotein 2	0.007	0.009	n/a	n/a	n/a	n/a
P04179	Superoxide dismutase [Mn], mitochondrial	0.050	0.033	0.025	0.019	2.012	0.033
P40227	T-complex protein 1 subunit zeta	0.015	0.009	0.007	0.002	2.048	0.041
P24821	Tenascin	0.209	0.080	0.015	0.098	14.358	0.020
P19971	Thymidine phosphorylase	0.045	0.020	0.012	0.016	3.826	0.016
A8MW06	Thymosin beta-4-like protein 3	0.030	0.025	0.013	0.006	2.299	0.016
P37837	Transaldolase	0.105	0.029	0.045	0.024	2.313	0.019
Q15582	Transforming growth factor-beta-induced protein ig-h3	0.190	0.100	0.092	0.025	2.068	0.007
P02766	Transthyretin	1.532	0.550	0.635	0.362	2.413	0.015
P07437	Tubulin beta chain	0.087	0.027	0.034	0.026	2.567	0.008
Q6IBS0	Twinfilin-2	0.021	0.016	0.008	0.005	2.702	0.044
Q9NYU2	UDP-glucose:glycoprotein glucosyltransferase 1	0.009	0.009	n/a	n/a	n/a	n/a
Q969H8	UPF0556 protein C19orf10	0.006	0.004	n/a	n/a	n/a	n/a
Q12907	Vesicular integral-membrane protein VIP36	0.008	0.008	n/a	n/a	n/a	n/a
O75083	WD repeat-containing protein 1	0.061	0.035	0.029	0.028	2.090	0.042

**Table 11.3: list of proteins identified in the MudPIT-MS/MS study as higher or exclusively expressed in the fluids of acute wounds**

accession number (SwissProt)	protein	mean expression chronic	SD chronic	mean expression acute	SD acute	expression difference (acute vs. chronic)	p-value
Q99798	Aconitate hydratase, mitochondrial	n/a	n/a	0.021	0.003	n/a	n/a
P02763	Alpha-1-acid glycoprotein 1	0.424	0.287	1.009	0.246	2.381	0.004
P01011	Alpha-1-antichymotrypsin	0.316	0.387	1.095	0.568	3.459	0.023
P37840	Alpha-synuclein	n/a	n/a	0.015	0.007	n/a	n/a
P55056	Apolipoprotein C-IV	n/a	n/a	0.014	0.005	n/a	n/a
Q13790	Apolipoprotein F	n/a	n/a	0.008	0.005	n/a	n/a
P07738	Bisphosphoglycerate mutase	n/a	n/a	0.021	0.009	n/a	n/a
P20851	C4b-binding protein beta chain	n/a	n/a	0.004	0.002	n/a	n/a
P55290	Cadherin-13	n/a	n/a	0.002	0.000	n/a	n/a
P33151	Cadherin-5	0.007	0.003	0.015	0.005	2.041	0.003
P07451	Carbonic anhydrase 3	n/a	n/a	0.013	0.006	n/a	n/a
P11597	Cholesteryl ester transfer protein	n/a	n/a	0.016	0.026	n/a	n/a
Q00610	Clathrin heavy chain 1	0.022	0.017	0.051	0.030	2.304	0.049
P00740	Coagulation factor IX	0.016	0.006	0.028	0.006	1.820	0.000
P00742	Coagulation factor X	0.008	0.010	0.025	0.010	3.027	0.021
P03951	Coagulation factor XI	0.010	0.008	0.019	0.008	1.913	0.016
Q02985	Complement factor H-related protein 3	n/a	n/a	0.012	0.009	n/a	n/a
P81605	Dermcidin	n/a	n/a	0.006	0.007	n/a	n/a
P08294	Extracellular superoxide dismutase [Cu-Zn]	0.006	0.003	0.018	0.012	3.257	0.020
P35555	Fibrillin-1	n/a	n/a	0.004	0.001	n/a	n/a
P10412	Histone H1.4	n/a	n/a	0.015	0.004	n/a	n/a
P58876	Histone H2B type 1-D	n/a	n/a	0.057	0.161	n/a	n/a
P01880	Ig delta chain C region	0.017	0.015	0.048	0.029	2.732	0.020
P01743	Ig heavy chain V-I region HG3	n/a	n/a	0.007	0.003	n/a	n/a
P01700	Ig lambda chain V-I region HA	0.013	0.010	0.035	0.036	2.771	0.049
P05362	Intercellular adhesion molecule 1	n/a	n/a	0.008	0.003	n/a	n/a
P14151	L-selectin	n/a	n/a	0.011	0.004	n/a	n/a
P33908	Mannosyl-oligosaccharide 1,2-alpha-mannosidase IA	0.003	0.002	0.012	0.007	4.170	0.041



accession number (SwissProt)	protein	mean expression chronic	SD chronic	mean expression acute	SD acute	expression difference (acute vs. chronic)	p-value
O00533	Neural cell adhesion molecule L1-like protein	n/a	n/a	0.007	0.004	n/a	n/a
Q09666	Neuroblast differentiation-associated protein AHNAK	n/a	n/a	0.024	0.016	n/a	n/a
P26022	Pentraxin-related protein PTX3	0.008	0.007	0.037	0.016	4.514	0.003
P12273	Prolactin-inducible protein	n/a	n/a	0.008	0.003	n/a	n/a
P02760	Protein AMBP	0.160	0.085	0.354	0.136	2.213	0.013
P02753	Retinol-binding protein 4	0.026	0.077	0.101	0.251	3.803	0.039
P13489	Ribonuclease inhibitor	n/a	n/a	0.004	0.002	n/a	n/a
P02735	Serum amyloid A protein	0.045	0.071	0.225	0.133	5.054	0.012
P05452	Tetranectin	0.017	0.008	0.047	0.023	2.690	0.002

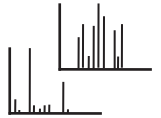
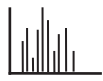


Table 11.4: individual peak areas of SRM targeted peptides normalised against the CRP peptide

protein	peptide	1	2	3	4	5	6	7	8	9	1	2	3	4	5	6	7	8	9
ANXA1	GLGTDEDTLEILASR	1.13e ⁺⁰⁶	-	-	-	9.03e ⁺⁰⁴	7.03e ⁺⁰⁵	-	-	2.22e ⁺⁰⁵	3.11e ⁺⁰⁶	1.68e ⁺⁰⁶	3.32e ⁺⁰⁵	3.11e ⁺⁰⁵	1.10e ⁺⁰⁵	6.51e ⁺⁰⁶	5.94e ⁺⁰⁶	1.71e ⁺⁰⁵	2.14e ⁺⁰⁵
ANXA3	GAGTNEDALIEILTR	5.70e ⁺⁰⁵	-	-	-	-	4.85e ⁺⁰⁵	-	-	-	1.64e ⁺⁰⁶	2.04e ⁺⁰⁶	5.37e ⁺⁰⁵	3.07e ⁺⁰⁵	1.99e ⁺⁰⁵	3.84e ⁺⁰⁶	2.94e ⁺⁰⁶	9.08e ⁺⁰⁵	2.36e ⁺⁰⁵
	GIGTDEFTLNR	5.49e ⁺⁰⁵	-	-	-	-	7.36e ⁺⁰⁵	-	-	-	1.93e ⁺⁰⁵	1.95e ⁺⁰⁶	4.96e ⁺⁰⁵	5.39e ⁺⁰⁵	3.01e ⁺⁰⁵	5.40e ⁺⁰⁵	2.71e ⁺⁰⁵	1.31e ⁺⁰⁶	3.89e ⁺⁰⁵
GD1R1	ABEYFLTPVEEAPK	7.15e ⁺⁰⁵	-	3.95e ⁺⁰⁵	9.44e ⁺⁰⁴	4.70e ⁺⁰⁵	8.15e ⁺⁰⁵	9.88e ⁺⁰⁴	1.55e ⁺⁰⁵	7.22e ⁺⁰⁴	2.39e ⁺⁰⁶	3.27e ⁺⁰⁶	5.90e ⁺⁰⁵	4.22e ⁺⁰⁵	2.58e ⁺⁰⁵	3.87e ⁺⁰⁶	3.83e ⁺⁰⁶	1.27e ⁺⁰⁶	2.79e ⁺⁰⁵
GD1R2	TLLGDGPVTDPK	-	-	1.67e ⁺⁰⁵	5.06e ⁺⁰⁴	-	-	5.55e ⁺⁰⁴	2.32e ⁺⁰⁵	5.86e ⁺⁰⁴	2.30e ⁺⁰⁵	3.51e ⁺⁰⁵	4.76e ⁺⁰⁵	3.31e ⁺⁰⁵	1.12e ⁺⁰⁵	2.81e ⁺⁰⁵	3.79e ⁺⁰⁵	5.43e ⁺⁰⁵	3.50e ⁺⁰⁴
MMP2	AFQVWSVDVPLR	-	-	4.81e ⁺⁰⁴	1.20e ⁺⁰⁵	2.35e ⁺⁰⁵	4.50e ⁺⁰⁴	7.13e ⁺⁰⁴	7.49e ⁺⁰⁵	-	5.79e ⁺⁰⁵	7.31e ⁺⁰⁵	2.03e ⁺⁰⁶	4.03e ⁺⁰⁵	1.53e ⁺⁰⁵	4.22e ⁺⁰⁵	1.50e ⁺⁰⁶	7.24e ⁺⁰⁵	1.45e ⁺⁰⁵
MMP8	DAFELWSVASPLIFTR	2.51e ⁺⁰⁵	1.98e ⁺⁰⁶	3.03e ⁺⁰⁵	4.20e ⁺⁰⁴	5.36e ⁺⁰⁶	4.05e ⁺⁰⁷	1.26e ⁺⁰⁶	6.15e ⁺⁰⁶	7.12e ⁺⁰⁵	1.26e ⁺⁰⁶	4.87e ⁺⁰⁵	4.93e ⁺⁰⁷	1.80e ⁺⁰⁶	5.57e ⁺⁰⁴	1.38e ⁺⁰⁶	1.10e ⁺⁰⁸	1.08e ⁺⁰⁵	1.05e ⁺⁰⁶
	YYAFDLIAQR	1.04e ⁺⁰⁶	-	3.16e ⁺⁰⁵	1.23e ⁺⁰⁵	9.95e ⁺⁰⁴	6.41e ⁺⁰⁵	1.18e ⁺⁰⁵	1.73e ⁺⁰⁵	4.68e ⁺⁰⁵	2.70e ⁺⁰⁵	2.76e ⁺⁰⁶	2.03e ⁺⁰⁵	2.24e ⁺⁰⁵	2.35e ⁺⁰⁵	1.14e ⁺⁰⁶	4.01e ⁺⁰⁵	2.53e ⁺⁰⁵	2.16e ⁺⁰⁵
MMP9	AFALWSAVTPLTFR	1.17e ⁺⁰⁶	5.77e ⁺⁰⁵	3.09e ⁺⁰⁵	5.01e ⁺⁰⁵	1.34e ⁺⁰⁶	9.10e ⁺⁰⁵	5.16e ⁺⁰⁵	1.50e ⁺⁰⁶	4.16e ⁺⁰⁶	6.15e ⁺⁰⁶	5.60e ⁺⁰⁶	1.15e ⁺⁰⁶	6.85e ⁺⁰⁵	2.48e ⁺⁰⁵	6.04e ⁺⁰⁶	7.21e ⁺⁰⁶	2.95e ⁺⁰⁵	6.75e ⁺⁰⁵
	LGLGADVAVQVTGALR	-	-	1.64e ⁺⁰⁵	1.30e ⁺⁰⁵	5.16e ⁺⁰⁵	-	1.73e ⁺⁰⁵	6.25e ⁺⁰⁵	2.68e ⁺⁰⁶	-	-	3.01e ⁺⁰⁵	2.51e ⁺⁰⁵	2.16e ⁺⁰⁵	5.66e ⁺⁰⁶	2.91e ⁺⁰⁶	2.19e ⁺⁰⁵	2.37e ⁺⁰⁵
	QLSLPETGELDSATLK	7.14e ⁺⁰⁴	-	-	-	7.62e ⁺⁰⁴	5.27e ⁺⁰⁴	-	1.27e ⁺⁰⁵	-	7.38e ⁺⁰⁵	1.89e ⁺⁰⁵	5.35e ⁺⁰⁵	2.73e ⁺⁰⁵	3.65e ⁺⁰⁵	2.30e ⁺⁰⁶	6.57e ⁺⁰⁶	9.05e ⁺⁰⁴	1.08e ⁺⁰⁵
MMP19	AFQEASELPVSGQLDDATR	-	1.09e ⁺⁰⁵	1.06e ⁺⁰⁶	3.85e ⁺⁰⁵	2.17e ⁺⁰⁵	-	8.75e ⁺⁰⁴	8.74e ⁺⁰⁵	4.61e ⁺⁰⁶	9.62e ⁺⁰⁶	3.64e ⁺⁰⁵	-	3.75e ⁺⁰⁵	5.27e ⁺⁰⁴	3.06e ⁺⁰⁶	1.30e ⁺⁰⁶	2.29e ⁺⁰⁵	-
PROF1	SSFYYNGLTLGGQK	9.00e ⁺⁰⁵	5.25e ⁺⁰⁴	8.09e ⁺⁰⁵	4.44e ⁺⁰⁴	2.13e ⁺⁰⁵	1.29e ⁺⁰⁶	2.01e ⁺⁰⁵	2.26e ⁺⁰⁵	4.20e ⁺⁰⁵	-	4.65e ⁺⁰⁶	4.23e ⁺⁰⁶	8.33e ⁺⁰⁵	1.49e ⁺⁰⁵	1.38e ⁺⁰⁶	3.20e ⁺⁰⁶	6.67e ⁺⁰⁵	6.93e ⁺⁰⁵
	TFVNITPAEYGVLVGK	2.18e ⁺⁰⁶	1.58e ⁺⁰⁵	6.00e ⁺⁰⁶	5.42e ⁺⁰⁵	1.31e ⁺⁰⁶	2.02e ⁺⁰⁶	5.93e ⁺⁰⁵	2.26e ⁺⁰⁶	6.93e ⁺⁰⁶	8.56e ⁺⁰⁶	1.64e ⁺⁰⁷	1.14e ⁺⁰⁶	2.19e ⁺⁰⁶	1.10e ⁺⁰⁶	2.83e ⁺⁰⁷	2.26e ⁺⁰⁷	5.32e ⁺⁰⁶	1.07e ⁺⁰⁶
S100A4	ALDVMVSTFHK	-	-	5.55e ⁺⁰⁵	-	-	1.21e ⁺⁰⁵	-	-	-	-	-	3.84e ⁺⁰⁵	7.00e ⁺⁰⁵	3.13e ⁺⁰⁵	3.83e ⁺⁰⁵	3.13e ⁺⁰⁵	1.89e ⁺⁰⁶	9.29e ⁺⁰⁴
	ELPSFLGK	1.35e ⁺⁰⁶	4.01e ⁺⁰⁵	7.25e ⁺⁰⁵	2.01e ⁺⁰⁵	9.47e ⁺⁰⁵	1.67e ⁺⁰⁶	3.92e ⁺⁰⁵	2.36e ⁺⁰⁶	1.50e ⁺⁰⁶	6.22e ⁺⁰⁶	7.48e ⁺⁰⁶	1.18e ⁺⁰⁶	1.64e ⁺⁰⁶	6.62e ⁺⁰⁵	1.28e ⁺⁰⁷	1.07e ⁺⁰⁷	3.12e ⁺⁰⁶	1.27e ⁺⁰⁶
S100A8	ALNSIIDVYHK	3.99e ⁺⁰⁶	-	8.00e ⁺⁰⁴	2.13e ⁺⁰⁴	-	2.56e ⁺⁰⁶	-	1.87e ⁺⁰⁵	-	2.14e ⁺⁰⁶	5.72e ⁺⁰⁶	-	4.89e ⁺⁰⁶	7.05e ⁺⁰⁵	9.17e ⁺⁰⁶	1.57e ⁺⁰⁷	1.16e ⁺⁰⁶	2.28e ⁺⁰⁶
	LLETTC*POYIR	1.65e ⁺⁰⁷	7.43e ⁺⁰⁵	6.40e ⁺⁰⁵	8.10e ⁺⁰⁵	5.80e ⁺⁰⁵	1.99e ⁺⁰⁷	7.01e ⁺⁰⁵	3.18e ⁺⁰⁶	1.10e ⁺⁰⁶	2.47e ⁺⁰⁷	5.44e ⁺⁰⁷	6.84e ⁺⁰⁶	3.65e ⁺⁰⁷	1.29e ⁺⁰⁷	1.51e ⁺⁰⁷	2.09e ⁺⁰⁷	5.98e ⁺⁰⁷	3.45e ⁺⁰⁷
S100A9	LGHPTLNOGEFK	-	-	1.56e ⁺⁰⁵	3.49e ⁺⁰⁴	-	2.65e ⁺⁰⁶	3.10e ⁺⁰⁴	3.98e ⁺⁰⁵	1.58e ⁺⁰⁶	2.13e ⁺⁰⁷	4.88e ⁺⁰⁶	7.21e ⁺⁰⁴	5.62e ⁺⁰⁶	1.09e ⁺⁰⁶	6.35e ⁺⁰⁷	7.60e ⁺⁰⁷	2.40e ⁺⁰⁶	4.05e ⁺⁰⁶
	NIETINTFHQYSVK	4.05e ⁺⁰⁵	-	1.07e ⁺⁰⁴	-	-	3.79e ⁺⁰⁵	-	-	1.34e ⁺⁰⁵	1.15e ⁺⁰⁶	7.66e ⁺⁰⁵	-	4.54e ⁺⁰⁵	9.25e ⁺⁰⁵	3.64e ⁺⁰⁶	7.07e ⁺⁰⁶	3.34e ⁺⁰⁵	4.29e ⁺⁰⁵
	VIEHIMEDLDTNADK	3.51e ⁺⁰⁵	-	5.05e ⁺⁰⁴	-	-	3.00e ⁺⁰⁵	-	-	2.22e ⁺⁰⁵	3.64e ⁺⁰⁶	8.18e ⁺⁰⁵	-	5.49e ⁺⁰⁵	3.74e ⁺⁰⁵	6.36e ⁺⁰⁶	4.13e ⁺⁰⁶	8.14e ⁺⁰⁵	9.13e ⁺⁰⁵
S100A11	C*IESLIAVFQK	5.12e ⁺⁰⁵	5.23e ⁺⁰⁴	3.02e ⁺⁰⁵	4.36e ⁺⁰⁴	5.72e ⁺⁰⁴	3.40e ⁺⁰⁵	-	2.03e ⁺⁰⁵	4.87e ⁺⁰⁵	4.45e ⁺⁰⁵	4.90e ⁺⁰⁶	-	3.15e ⁺⁰⁵	4.21e ⁺⁰⁵	1.21e ⁺⁰⁶	1.01e ⁺⁰⁶	2.70e ⁺⁰⁵	2.44e ⁺⁰⁵
S100A12	GHFDTLISK	1.58e ⁺⁰⁶	-	-	-	-	1.15e ⁺⁰⁶	-	4.75e ⁺⁰⁵	5.49e ⁺⁰⁵	2.78e ⁺⁰⁶	2.19e ⁺⁰⁶	9.67e ⁺⁰⁵	1.00e ⁺⁰⁶	7.01e ⁺⁰⁵	1.36e ⁺⁰⁷	2.38e ⁺⁰⁷	7.89e ⁺⁰⁵	2.67e ⁺⁰⁶
S100P	ELPGFLQSGK	3.01e ⁺⁰⁶	4.77e ⁺⁰⁵	5.33e ⁺⁰⁶	5.79e ⁺⁰⁵	3.34e ⁺⁰⁵	3.32e ⁺⁰⁶	8.93e ⁺⁰⁵	7.97e ⁺⁰⁵	3.19e ⁺⁰⁶	1.26e ⁺⁰⁷	2.02e ⁺⁰⁷	6.12e ⁺⁰⁵	3.51e ⁺⁰⁶	4.38e ⁺⁰⁶	2.34e ⁺⁰⁷	3.25e ⁺⁰⁶	2.06e ⁺⁰⁷	9.54e ⁺⁰⁵
	YSGSEGSTQLTK	1.54e ⁺⁰⁵	1.40e ⁺⁰⁴	4.41e ⁺⁰⁵	5.75e ⁺⁰⁴	7.60e ⁺⁰⁴	1.52e ⁺⁰⁵	2.18e ⁺⁰⁴	4.23e ⁺⁰⁵	7.04e ⁺⁰⁵	2.83e ⁺⁰⁶	1.14e ⁺⁰⁶	-	3.69e ⁺⁰⁵	4.03e ⁺⁰⁵	5.33e ⁺⁰⁶	1.16e ⁺⁰⁶	1.93e ⁺⁰⁶	4.25e ⁺⁰⁴
SAMP	AYSLSFSYNTQGR	1.29e ⁺⁰⁵	-	-	1.24e ⁺⁰⁵	-	1.88e ⁺⁰⁵	-	-	-	3.74e ⁺⁰⁶	1.89e ⁺⁰⁶	-	8.32e ⁺⁰⁵	1.15e ⁺⁰⁵	2.55e ⁺⁰⁶	-	5.39e ⁺⁰⁵	5.64e ⁺⁰⁴
	VGEYSLYIGR	2.44e ⁺⁰⁵	-	-	1.21e ⁺⁰⁵	-	3.00e ⁺⁰⁵	-	-	-	9.99e ⁺⁰⁵	3.19e ⁺⁰⁶	1.65e ⁺⁰⁵	1.65e ⁺⁰⁶	7.61e ⁺⁰⁴	1.31e ⁺⁰⁶	-	2.88e ⁺⁰⁵	1.43e ⁺⁰⁵
TIMP1	EPGLCTWQSLR	1.24e ⁺⁰⁵	-	9.97e ⁺⁰⁴	9.00e ⁺⁰⁴	-	1.56e ⁺⁰⁵	1.25e ⁺⁰⁵	4.42e ⁺⁰⁵	2.64e ⁺⁰⁵	2.38e ⁺⁰⁵	1.96e ⁺⁰⁵	2.38e ⁺⁰⁵	3.20e ⁺⁰⁵	5.22e ⁺⁰⁴	1.72e ⁺⁰⁵	-	2.81e ⁺⁰⁵	8.32e ⁺⁰⁴

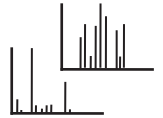
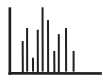
Due to copyright restrictions, the following articles have been omitted from Appendix 2 of the thesis. Please refer to the following citations for details.

Christoph Krisp; Caroline Kubutat; Andreas Kyas; Lars Steinsträßer; Frank Jacobsen; Dirk A. Wolters, Boric acid gel enrichment of glycosylated proteins in human wound fluids. *Journal of Proteomics* 2010, 74, (4), 502-509.

Christoph Krisp; Matthew J McKay; Dirk A. Wolters; Mark P. Molloy, Multidimensional protein identification technology-selected reaction monitoring improving detection and quantification for protein biomarker studies. *Analytical Chemistry* 2012, 84, (3), 1592-1600.

Christoph Krisp; Frank Jacobsen; Lars Steinsträßer; Matthew J McKay; Mark P Molloy; and Dirk A. Wolters, Proteome analysis reveals anti-angiogenic environments in chronic wounds of diabetes mellitus type 2 patients, *Proteomics* 2013, 13, (17), 2670-2681.

Christoph Krisp; Sarah A. Randall; Matthew J. McKay; Mark P. Molloy, Towards clinical applications of selected reaction monitoring for plasma protein biomarker studies. *Proteomics – Clinical Applications* 2011, 6, (1-2), 42-59.



13. Appendix 3: Ethics approval



RUHR-UNIVERSITÄT
BOCHUM
Medizinische Fakultät

ETHIK - KOMMISSION
Der Vorsitzende

Telefon: 0234/302-6421/6825
Telefax: 0234/302-6834
Bürkle-de-la-Camp-Platz1

44789 Bochum

Antrag vom 27.01.2003 **eingegangen** am 27.01.2003

Registrier - Nr.: **2028**

Bei Schriftwechsel bitte immer Registrier-Nr. angeben!

Thema: Studie zur Analyse von Expressionsprofilen aus Exsudaten
 von humanen chronischen Wunden

Untersucher: Dr. med. Lars Steinsträßer

Abteilung: Klinik für Plastische Chirurgie und Schwerbrandverletzte

Klinik: BG-Kliniken Bergmannsheil – Universitätsklinik –
 Bürkle-de-la-Camp-Platz 1, 44789 Bochum

Die Ethikkommission hat hinsichtlich des beantragten Untersuchungsvorhabens im Rahmen der Forschung am Menschen aufgrund des vorgelegten Materials

keine Bedenken

XX

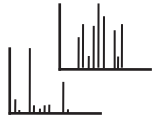
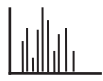
folgende Bedenken

folgende Auflagen

Bochum, den 21.02.2003

Professor Dr. med. Michael Zenz
Vorsitzender der Ethik-Kommission
der Medizinischen Fakultät
der Ruhr-Universität Bochum

Hinweis: Klinische Prüfungen gemäß § 67 AMG sind beim zuständigen Regierungspräsidenten und beim Bundesinstitut für Arzneimittel und Medizinprodukte / Berlin anzuzeigen.



**RUHR-UNIVERSITY
Bochum
Medical Facility**

**ETHIC – COMMITTEE
The president**

Telephone: 0234/302-6421/6825
Facsimile: 0234/302-6834
Bürkle-de-la-Camp-Platz 1

44789 Bochum

Application from 27.01.2003

received on 27.01.2003

Registration – no.: **2028**

Please quote registration-no. with any correspondence

Topic: Analysis of expression profiles in exudates
from human chronic wounds

Chief investigator: Dr. med. Lars Steinsträßer

Department: Clinic for Plastic Surgery and serious burn victims
BG-Hospitals Bergmannsheil – University hospital –
Bürkle-de-la-Camp-Platz 1

The ethic committee has regarding the Investigation application based on the provided material towards the research on human

no concerns

[XXX]

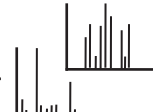
following concerns

following requirements

Bochum, 21.02.2003

Signature and stamp see original

Note: According to § 67 AMG, clinical approval must be reported to the relevant district president and to the federal institute for pharmaceuticals and medical products / Berlin.



14. Appendix 4: Curriculum Vitae

Personal details

Name	Christoph Krisp
Date of Birth	26.02.1984
Place of Birth	Essen, Germany
Citizenship	German

Education

Primary school

Sep. 1990 – June 1994	Bonifacius Primary School
-----------------------	---------------------------

High school

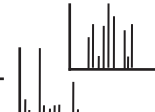
Sep. 1994 – June 2003	Gustav Heinemann Comprehensive School
Graduation	Abitur (German University-entrance diploma)

University

Sep. 2004 – Nov. 2007	Bachelor of Science in Chemistry, Ruhr University Bochum Thesis title: “Massenspektrometrische Analyse chronischer Wundflüssigkeiten” - “mass spectrometric analyses of chronic wound fluids”
Nov. 2007 – May 2009	Master of Science in Chemistry, Ruhr University Bochum Thesis title: ”Anreicherung niedrig abundanter Proteine zur Proteomanalyse humaner Wundexudate mittels MudPIT” - “Enrichment of low abundant proteins for proteome analyses of human wound exudates by MudPIT”
Oct. 2009 – April 2013	doctorate studies at Ruhr University Bochum, Germany, and Macquarie University, Sydney, Australia under a Cotutelle agreement

Employment History

May 2009 – Aug. 2009	practical training at Macquarie University, Sydney, Australia, with the focus on targeted mass spectrometry on human colon tissue from colorectal cancer patients, supported by a German Academic Exchange Service (DAAD) travel grant
----------------------	--



Awards

Macquarie University Research Scholarship (MQRES)

Macquarie University Postgraduate Research Fund (PGRF), June 2011

Macquarie University Faculty of Science Biomolecular Frontiers Research Postgraduate Prize

Awarded for the best internationally peer-reviewed paper by a postgraduate student as first author accepted for publication

Publications

[1] Lars Steinsträßer; Frank Jacobsen; Tobias Hirsch; Marco Kesting; Caroline Chojnacki; Christoph Krisp; Dirk A. Wolters, Immunodepletion of high-abundant proteins from acute and chronic wound fluids to elucidate low-abundant regulators in wound healing. *BMC Research Notes* 2010, 3, (1), 335.

[2] Christoph Krisp; Caroline Kubutat; Andreas Kyas; Lars Steinsträßer; Frank Jacobsen; Dirk A. Wolters, Boric acid gel enrichment of glycosylated proteins in human wound fluids. *Journal of Proteomics* 2010, 74, (4), 502-509.

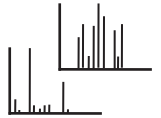
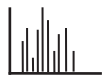
[3] Christoph Krisp; Sarah A. Randall; Matthew J. McKay; Mark P. Molloy, Towards clinical applications of selected reaction monitoring for plasma protein biomarker studies. *Proteomics – Clinical Applications* 2011, 6, (1-2), 42-59.

[4] Christoph Krisp; Matthew J McKay; Dirk A. Wolters; Mark P. Molloy, Multidimensional protein identification technology-selected reaction monitoring improving detection and quantification for protein biomarker studies. *Analytical Chemistry* 2012, 84, (3), 1592-1600.

This manuscript was selected by the faculty of thousand as one of the top 2% of published articles in biology and medicine

[5] Peter Lüdi; Ulrike B. Hendgen-Cotta; Julia Sobierajski; Matthias Totzeck; Marcel Reeh; Manfred Dewor; Hongqi Lue; Christoph Krisp; Dirk A. Wolters; Malte Kelm; Jürgen Bernhagen, Tienush Rassaf, Cardioprotection Through S-Nitros(yl)ation of Macrophage Migration Inhibitory Factor. *Circulation* 2012, 125, (15), 1880-1889.

[6] Miriam M. Cortese-Krott; Ana Rodriguez-Mateos; Roberto Sansone; Gunter G. C. Kuhnle; Sivatharsini Thasian-Sivarajah; Thomas Krenz; Patrik Horn; Christoph Krisp; Dirk A. Wolters; Christian Heiß; Klaus-Dietrich Kröncke; Neil Hogg; Martin Feelisch; Malte Kelm, Human red blood cells at work: identification and visualization of erythrocytic eNOS activity in health and disease, *Blood* 2012, 120, (20), 4229-4237.



[7] Jessica Jacob; Christina Marx; Vera Kock; Olga Reifschneider; Benjamin Fränzel; Christoph Krisp; Dirk A. Wolters; Ulrich Kück, Identification of a Chloroplast Ribonucleoprotein Complex Containing Trans-splicing Factors, Intron RNA and Novel Components, *Molecular and Cellular Proteomics* in press

[8] Christoph Krisp; Frank Jacobsen; Lars Steinsträßer; Matthew J McKay; Mark P Molloy; and Dirk A. Wolters, Proteome analysis reveals anti-angiogenic environments in chronic wounds of diabetes mellitus type 2 patients, *Proteomics* 2013, 13, (17), 2670-2681